Universidade de Aveiro Departamento de Química

2018/2019

Rui Filipe Neves Freitas

Desenvolvimento de vacinas contra o cancro baseadas em glico-neoantigénios

Development of cancer vaccines based on glyco-neoantigens

Universidade de Aveiro Departamento de Química

2018/2019

Rui Filipe Neves Freitas

Desenvolvimento de nanovacinas contra o cancro baseadas em glico-neoantigénios

Development of cancer nanovaccines based on glyco-neoantigens

Dissertação apresentada à Universidade de Aveiro para cumprimento dos requisitos necessários à obtenção do grau de Mestre em Bioquímica, realizada sob a orientação científica do Doutor José Alexandre Ferreira, Investigador Auxiliar do grupo de Patologia e Terapêutica Experimental do Instituto Português de Oncologia do Porto (IPO), do Doutor Bruno Sarmento, Investigador Principal do Instituto de Investigação e Inovação em Saúde e sob a orientação institucional do Professor Doutor Francisco Manuel Lemos Amado, Professor Associado com agregação do Departamento de Química da Universidade de Aveiro.

A Albino Carvalho de Freitas,

Maria Flor de Oliveira e Silva Freitas,

Domingos Ferreira de Sousa e Hermínia das Neves.

o júri

presidente

Professora Doutora Maria do Amparo Ferreira Faustino
Professora Auxiliar da Universidade de Aveiro

Doutor José Alexandre Ribeiro de Castro Ferreira
Investigador Auxiliar do Instituto Português de Oncologia do Porto

Doutora Maria José Cardoso de Oliveira
Investigadora Principal do Instituto de Investigação e Inovação em Saúde da Universidade do Porto

Contribution in the concept and accomplishment of the following research work during the year of development of Master degree's Thesis:

Scientific Papers

Fernandes E, Ferreira D, Peixoto A, **Freitas R**, Relvas-Santos M, Palmeira C, Martins G, Barros A, Santos LL, Sarmento B, Ferreira JA. Glycoengineered nanoparticles enhance the delivery of 5-fluoroucil and paclitaxel to gastric cancer cells of high metastatic potential. Int J Pharm. 2019 570:118646. doi: 10.1016/j.ijpharm.2019.118646. IF: 4.2 (original paper)

Fernandes E, Sores J, Cotton S, Peixoto A, Ferreira D, **Freitas R**, Reis CA, Santos LL and Ferreira JA. Esophageal, gastric and colorectal cancers: Looking beyond classical serological biomarkers towards glycoproteomics-assisted precision oncology. Theranostics (under review) IF: 8.5 (review paper)

Fernandes E, Ferreira D, Soares J, Azevedo R, Gaiteiro C, Peixoto A, Cotton S, **Freitas R**, Relvas-Santos M, Afonso LP, Palmeira C, Silva AMN, Santos LL, Ferreira JA. Nucleolin-SLeA glycoforms as E-selectin ligands and potentially targetable biomarkers at the cell surface of gastric cancer cells. Theranostics IF: 8.5 (submitted)

Scientific meetings

Freitas R and Relvas-Santos M, Fernandes E, Azevedo R, Silva AMN, Santos LL, Ferreira JA. Single-pot enzymatic synthesis of short-chain MUC16 O-sialoglycopeptides and protein glycoconjugates for bioanalytical and biomedical applications. Conference: GLUPOR 13: 13th International Meeting of the Portuguese Carbohydrate Group

agradecimentos

Ao Dr. José Alexandre Ferreira, por me ter dado a oportunidade de fazer parte da sua equipa, por ter acreditado em mim, pela orientação no trabalho e por todos os conhecimentos que me passou e ainda passa. É um prazer falar consigo e debater os mais diversos temas.
Ao Dr. Bruno Sarmento, por ter aceitado ser o coorientador deste trabalho e por toda a disponibilidade que demonstrou na concretização do mesmo.
À Professora Rita Ferreira, que me deu a oportunidade de fazer esta dissertação no IPO e por toda a disponibilidade que demonstrou em esclarecer todas as dúvidas que surgissem. Ao Professor Francisco Amado, por ter aceitado ser o meu orientador institucional e também pela sua disponibilidade e cuidado sempre que precisei.
A todos os meus colegas do Grupo de Patologia e Terapêutica Experimental, por me terem recebido e integrado na equipa de uma forma fantástica, pelos ensinamentos que me passaram, pela paciência, por todo o apoio e companheirismo que tiveram ao longo do tempo que estive convosco. É um prazer fazer parte da equipa. Muito obrigado a todos.
Aos meus colegas da Universidade de Aveiro, Catarina Almeida, João, Nuno, Filipe, Gabriela, Antunes e em especial à Catarina Cardoso que sempre se mostrou com grande amizade.
Aos meus amigos de longa data, Simão, João, Tiago, Rafaela pela amizade, e em especial ao Diogo Costa, que sempre me acompanhou de perto e não hesitou em apoiar-me sempre que precisei com grande amizade e companheirismo, obrigado meu irmão.
Aos meus avós, Flor e Albino, por todo o apoio e esforço que fizeram sempre para nos ajudarem, é um grande orgulho ser um "Freitas". Esta tese é dedicada a vocês.
À minha família: ao meu irmão e em especial aos meus pais, que sempre me apoiaram, incentivaram e fizeram muitos sacrifícios para que eu e o meu irmão pudéssemos ter uma vida melhor. Tudo o que sou é mérito vosso, esta tese é tão vossa quanto minha. Teria sido impossível sem vocês. Obrigado pelo vosso amor, tenho muito orgulho em ser vosso filho.
À minha namorada, Janine, por todo o apoio que me dá, pelo amor incondicional, companheirismo, preocupação, pela paciência e por me fazer acreditar, todos os dias, que sou especial e que sou capaz.
A todos, o meu sincero obrigado!

palavras-chave glicosilação, nanovacinas contra o cancro, neoantigénios

resumo As vacinas contra o cancro que exploram neoantigénios são capazes de provocar respostas imunes contra células tumorais com poucos efeitos adversos, sendo assim promissoras para o tratamento do cancro. Estas vacinas são capazes também de induzir memória imunológica contra recidivas, o que é essencial para a terapia. Os epítopos mais promissores são os péptidos derivados de mutações genéticas. No entanto, muitos tumores sólidos apresentam baixa carga mutacional, dificultando a generalização dessas abordagens e exigindo a exploração de outras classes de biomoléculas. Alterações na glicosilação de proteínas, traduzidas pela expressão de *O*-glicanos de cadeia curta na superfície das células tumorais oferecem um tremendo potencial para esse objetivo. Apesar da sua natureza associada ao cancro e papel relevante no desenvolvimento do mesmo, estes glicanos também contribuem para a imunossupressão, impedindo assim de se desenvolver vacinas à base de glicanos. Com vista a este objetivo, este trabalho descreve um método quimioenzimático para sintetizar glicoepítopos derivados de mucina 16 associada ao cancro (MUC16) que expressa diferentes classes de *O*-glicanos de cadeia curta neutros e sialilados. Paralelamente, os glicopéptidos MUC16-Tn foram conjugados com hemocianina linfocitária (KLH), prevendo o desenvolvimento de formulações vacinais convencionais glicano-proteína. A segunda parte do trabalho explora o potencial dos nanoveículos para melhorar as formulações de vacinas. Resumidamente, as nanopartículas de PLGA foram funcionalizadas ou adsorvidas com MUC16-Tn e caracterizadas por TEM e ^{1}H RMN. As nanopartículas apresentaram natureza esférica e homogénea, baixo índice de polidispersão, dimensões abaixo de 200 nm e alta estabilidade ao pH fisiológico. Os limiares de toxicidade e capacidade de internalização por células apresentadoras de antígeno foram determinados usando macrófagos. A terceira parte do trabalho diz respeito ao desenvolvimento de um modelo celular que expressa o antígeno Tn, que foi utilizado para inferir as implicações funcionais desse antígeno, com ênfase na evasão imunológica. Resumidamente, o genoma das células uroteliais T24 foi alterado através da tecnologia CRISPR / Cas9 para produzir um knock-out estável de C1GALT1. Essa linha celular expressa níveis significativamente altos de Tn à superfície e obliterou completamente a expressão de glicoformas estendidas, traduzidas por citometria de fluxo, microscopia de imunofluorescência e análise glicómica. Além disso, os estudos de glicoproteómica confirmaram a expressão de MUC16-Tn, apoiando a utilidade do modelo no contexto das construções de vacinas. Curiosamente, a expressão do antígeno Tn não teve impacto na proliferação, migração e invasão celular, bem como na expressão de moléculas importantes para a imunossupressão. No entanto, ensaios de co-cultura com células dendríticas sugeriram que as células tumorais que expressam Tn podem influenciar negativamente sua diferenciação e regulação de moléculas relevantes envolvidas na apresentação do antígeno.
Em resumo, foi criada uma base para apoiar o desenvolvimento e a melhoria de vacinas à base de glicano para o cancro, prevendo estudos in vivo.

keywords glycosylation, cancer nanovaccines, neoantigens

abstract Cancer vaccines exploiting cancer neoantigens have been proven capable of eliciting powerful immune responses against cancer cells with limited off-target effects, constituting the next cornerstone in cancer treatment. Cancer vaccines are also capable of inducing immunological memory against recurrences, which is key for cancer management. The most promising epitopes remain peptides derived from genomic mutations. However, many solid tumours present a low mutational burden, hampering the generalization of these approaches and demanding the exploitation of other classes of biomolecules. Alterations in protein glycosylation translated by the expression of short-chain *O*-glycans at the surface of cancer cells offers tremendous potential towards this objective. Despite their cancer-associated nature and relevant role in cancer development, these glycans also contribute to immunosuppression, frustrating attempts to develop glycan-based vaccines. Envisaging this goal, this work describes a single-pot chemoenzymatic method for synthesizing glycoepitopes derived from cancer-associated Mucin-16 (MUC16) expressing different classes of neutral and sialylated short-chain *O*-glycans in mimicry of cancer cells. In parallel, MUC16-Tn glycopeptides wereconjugated with immunogenic protein key lymphocyte hemocyanin (KLH), foreseeing the development of conventional glycan-protein vaccine constructs. The second part of the work exploits the potential of nanoconstructs for improved vaccine formulations. Briefly, PLGA nanoparticles were functionalized or adsorbed with MUC16-Tn and characterized by TEM and ^{1}H NMR. Nanoparticles showed a spherical and homogenous nature, low polydispersion index, dimensions bellow 200nm and high stability at physiological pH. Toxicity thresholds and internalization capacity by antigen presenting cells was determined using macrophages. The third part of the work concerned the development of a cell model expressing the Tn antigen which was used to infer the functional implications of this antigen, with emphasis on immune evasion. Briefly, the genome of T24 urothelial cells was edited through CRISPR/Cas9 technology to produce a stable *C1GALT1* knock-out. This cell line expressed significantly high levels of the Tn antigen at the cell surface and completely obliterated the expression of extended glycoforms, as translated by flow cytometry, immunofluorescence microscopy and glycomics analysis by mass spectrometry. Moreover, glycoproteomics studies confirmed MUC16-Tn expression, supporting the utility of the model in the context of the developed vaccine constructs. Interestingly, Tn antigen expression did not impact on cell proliferation, migration and invasion as well as in the expression of important molecules for cancer immune escape. Nevertheless, co-culture assays with dendritic cells suggested that Tn expressing cancer cells may negatively influence their differentiation and downregulate relevant molecules involved in antigen presentation.

In summary, a rationale has been created to support the development and improvement of glycan-based vaccines for cancer foreseeing *in vivo* studies. Given the pancarcinomic nature of these glycoepitopes, the generalization of more efficient vaccines to different cell models may be envisaged.

Table of Contents

List of figures

CHAPTER I – General Introduction

List of tables

Abbreviations

APC - Allophycocyanin

APCs – antigen presenting cells

Asn – asparagine

BSA – bovine serum albumin

CDGs – congenital disorders of glycosylation

CE – conjugation efficiency

CMP – cytidine monophosphate

CTLs – cytotoxic T cells

DCs – dendritic cells

DCM – dichloromethane

DLS - dynamic light scattering

DMSO – dimethyl sulfoxide

EGFR – epidermal growth factor receptor

ER – endoplasmic reticulum

FDA – U. S. Food and Drug Administration

FGF-2 – fibroblast growth factor 2

GA – Golgi apparatus

Glc – glucose

GalNAc – *N*-acetygalactosamine

GlcNAc – *N*-acetylglucosamine

GM-CSF - Granulocyte-macrophage colony-stimulating factor

HCl – chloridric acid

HER2 – human epidermal growth factor receptor 2

HGF – hepatocyte growth factor

IFN-γ – interferon gamma

IgG – immunoglobulin G

IL-23 – interleukin 23

IL-4 – interleukin 4

IL-10 – interleukin 10

IL-12 – interleukin 12

KLH – keyhole limpet hemocyanin

LPS - lipopolysaccharide

mAb – monoclonal antibody

MAL – maleimide

MHCs – major histocompatibility complexes

MMPs – matrix metalloproteinases

MPLA – monophosphoryl lipid A

MTT - 3-(4,5-dimethylthiazol-2-yl)-2,5-diphenyltetrazolium bromide

MUCs – mucins

MUC1 – mucin 1

MUC16 – mucin 16

NK – natural killer

NMR – nuclear magnetic resonance

NPs – nanoparticles

PdI – polydispersion index

PD-L1 - programmed death-ligand 1

PE – phosphatidylethanolamine

PEG – polyethylene glycol

PLGA – Poly (D, L-lactic-co-glycolic acid)

PMA - phorbol 12-myristate 13-acetate

ppGalNAcT – UDP-GalNacpolypeptide GalNAc-transferase

Ser – serine

SIGLECs - sialic acid-binding immunoglobulin-like lectins

S3T - sialyl-3-T

S6T - sialyl-6-T

STn – sialyl- Tn

ST6GalNAc-I – α2,6-sialyltransferase

TCEP - tris(2-carboxyethyl) phosphine hydrochloride

TEM – transmission electron microscopy

Th1 – T helper cells 1

Thr – threonine

TLRs – toll-like receptors

TNF-α – tumour necrosis factor alpha

TSA – total sialic acid

T-synthase – Core 1 β3-galactosyltransferase

CHAPTER I

General Introduction

1. Introduction

Cancer is a multifaceted disease originated from most cell types, being characterized by uncontrolled cell proliferation, healthy tissue invasion and metastasis to other organs[1]. Classically, cancer is discerned as a result of alterations in proto-oncogenes governing cell growth, division and survival[2,3]. Furthermore, lifestyle and environmental exposure to cigarette smoke, radiation and oncogenic viruses can contribute to neoplastic processes[3-5].

Despite its high mortality rates at advanced stages, cancer management has improved over the years due to a more profound understanding of the disease at the molecular level. This has led to the development of targeted therapeutics, including humanized monoclonal antibodies against many relevant cancer-associated proteins[6,7] and immune check point inhibitors[8]. In fact, immunotherapy is the next cornerstone towards innovative, more effective and safer cancer therapeutics. In particular, the vaccination of cancer patients with tumour neoantigens is an established concept that recently gained ground with the introduction of high-throughput genome sequencing technologies. These powerful analytical tools enable the large screening of patient genome for unique cancer fingerprints (neoantigens) that have been successfully incorporated into vaccines capable of eliciting powerful and highly-specific anti-tumour responses. The strategy has been effective for both tumour eradication and long-lasting protective effects against recurrence and metastasis. Moreover, it is well tolerated by patients in comparison to other therapies[9]. However, neoantigen discovery is significantly challenged by the low mutational burden exhibited by many primary lesions and metastasis[10]. This poses a significant limitation for the generalization and clinical success of anti-cancer vaccines.

Targeting glycoproteins at the cancer cell surface may present the necessary means to identify cancer-specific molecular signatures, thus overcoming limitations associated with low mutation frequency. In fact, oncogenic transformation, disease progression and dissemination are accompanied by profound alterations in protein glycosylation pathways[11]. Amongst the most common differentiating patterns in cancer are changes in glycan branching, length and terminal epitopes, as well as glycosylation sites distribution and density on a given protein[12]. These molecular features contribute to alter protein function, playing a key role in disease progression[13]. Moreover, they are often amplified by upregulation of certain membrane glycoproteins, creating cancer-unique molecular signatures at the cell surface that may be used to selectively target cancer cells[14,15].

Supporting the existence of cancer-specific glycan-associated molecular studies, many studies report autoantibodies against abnormally glycosylated proteins produced by cancer cells in the serum of cancer patients[16]. Therefore, aberrant glycosylation of cancer cells is being exploited in the context of immunotherapies and cancer vaccines, with some glycoprotein-based cancer vaccines being tested in clinical trials[17,18]. However, many glycophenotypes presented by cancer cells exert a cancer immunosuppressive function, which has challenged the generalization of cancer glycoimmunotherapy[16]. In this context, recent studies support that nanodelivery vehicles may be tailored to override immunotolerance, providing the necessary biotechnology solutions for exploiting cancer-associated glycoepitopes as cancer vaccines. Based on these considerations, the present document aims to set the molecular bases and cell models for the future development of innovative glycan-based cancer nanovaccines. This includes the establishment of easy methods for glycoepitope synthesis, the development of immunogenic protein glycoconjugates and glyconanoconstructs for potential vaccine applications. Envisaging these goals, cancer associated MUC16 glycoforms, expressed by many solid tumours and associated with cancer malignancy, are exploited as model glycoepitopes. Lastly, a glycoengineered cell model expressing the cancer-associated Tn glycan at the cell-surface, thus mimicking more aggressive tumours, was developed. This work also devotes to exploiting the functional implications of this antigen in relevant cancer cell features (proliferation, migration, invasion) as well as immune modulation. The goal is to provide a well characterized model capable of supporting the development of innovative cancer therapies, with emphasis on cancer vaccines. Facing this objective, we have elected the T24 urothelial cell line isolated from a solid tumour typically expressing the Tn antigen at advanced stages.

1.1. Protein Glycosylation in Cancer

Glycosylation is the enzymatic process responsible for the glyosidic linkage of saccharides to proteins and lipids[12], being the most common post transcriptional modification (PTM) [19]. This post transcriptional process occurs in the endoplasmic reticulum (ER) and Golgi apparatus (GA) through the coordinated activity of nucleotide sugar transporters, glycosyltransferases and glycosidases[20]. The two main classes of glycans found in membrane glycoproteins are *N*-glycans and *O*-glycans. Briefly, *N*-glycosylation starts with the covalent attachment of a 14-sugar glycan from the lipid precursor

Glc3Man9GlcNAc2-P-P-Dol to Asparagine (Asn) residues in Asn-X-Ser/Thr sequons (X denotes any amino acid except proline) of newly synthetized peptides[21]. Previously N-glycosylated glycoproteins are subsequently *O*-glycosylated through the action of polypeptide GalNAc-transferases (ppGalNAcT) which α-link GalNAc moieties to serine (Ser) or threonine (Thr) residues, forming the simplest *O*-glycan Tn antigen. Subsequently, the attachment of Gal to Tn by C1GALT-1 (T synthase) originates the core 1 T antigen in a chaperone COSMC-dependent manner[22]. *O*-glycan extension beyond the Tn or T antigens can be blocked by sialyltransferases, giving rise to sialyl-Tn (STn), sialyl-T (ST) or di-sialyl-T (dST) antigens (**Figure 1**). Furthermore, *O*-GalNAc glycans can be extended to form core 1 to 4, which are the most common in humans.

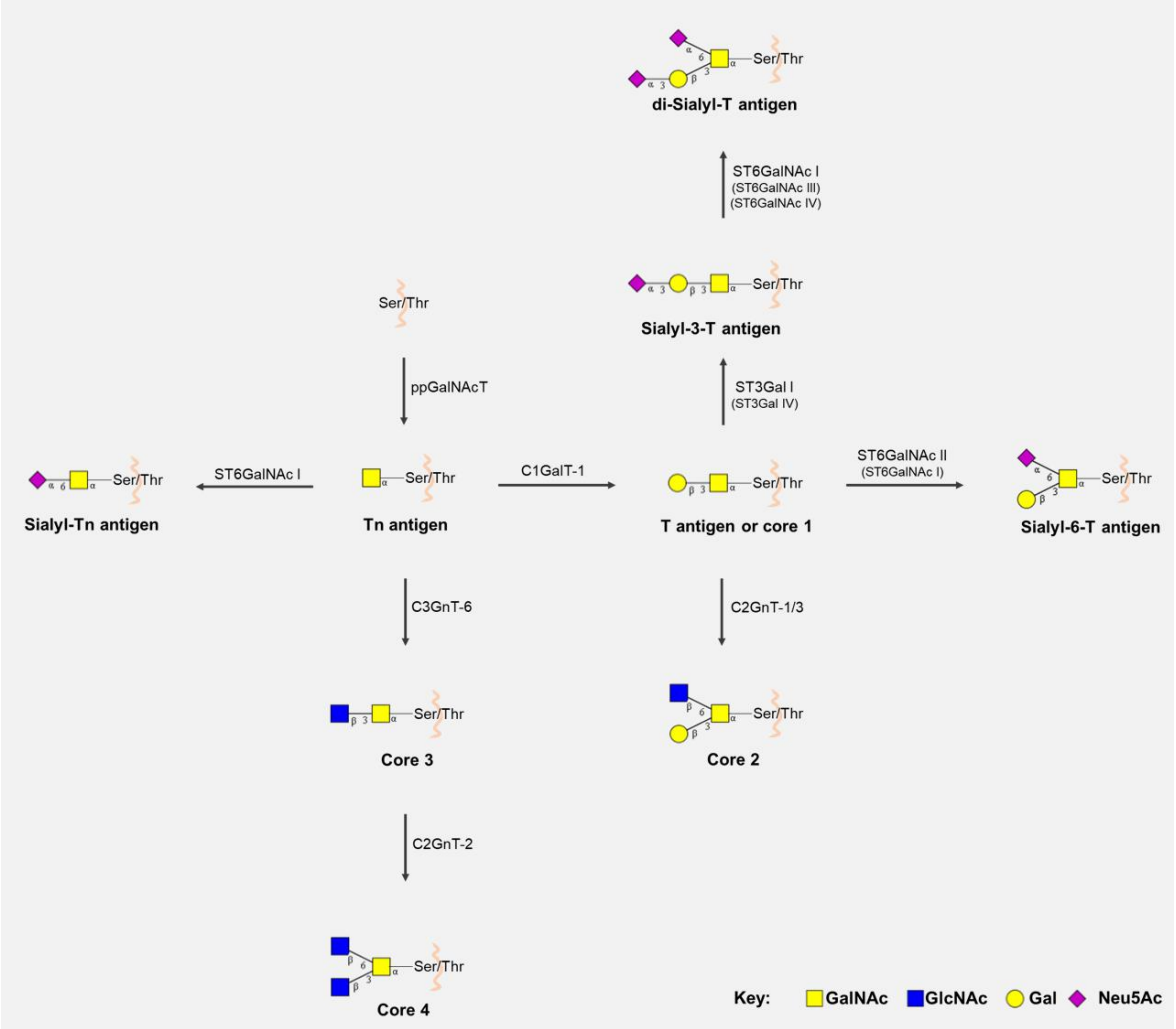

Figure 1. **Biosynthesis of core 1 to 4 and sialylated short-chain *O*-GalNAc glycans**.

Of note, glycans display essential functional roles in several development and physiological processes, including normal embryonic development, cellular differentiation,

growth, adhesion, signalling and endocytosis, protein folding, molecular trafficking and clearance, receptor activation and host-pathogen interaction[13,23-26]. Accordingly, changes in glycosylation patterns may be found in several disease settings as congenital disorders of glycosylation (CDGs)[27], immunodeficiencies[28] and cancer[24]. It has been long known that advanced tumours present severe dysregulations in glycosylation pathways, with tumour-associated carbohydrates arising from incomplete or neo-synthesis processes[29]. Of note, incomplete synthesis originating truncated structures is more common in early carcinogenesis[11], while the *de novo* synthesis of neoantigens is more frequent in advanced stages of several cancers[30]. The most reported alterations associated to cancer include the over- and/or *de novo* expression of short-chain *O*-GalNAc glycans (Tn, T, Sialyl-T, and Sialyl-Tn), Lewis blood group related antigens and their sialylated counterparts [sialyl-Lewis A (SLe^a) and X (SLe^x)], as well as complex branched *N*-glycans[31,32]. Many of these structural features are common to most advanced solid tumors and often associate with poor prognosis, suggesting common molecular mechanisms, which is yet to be proven. Nevertheless, distinct proteome signatures, glycosylation density, and glycosite distribution may ultimately dictate organ, cell-type and cancer-specific molecular signatures and clinically relevant glycoforms. The subsequent sections will specially focus on the premature stop of *O*-glycosylation extension, giving rise to the overexpression of Tn, T, ST, and STn short-chain mucin-type *O*-GalNAc glycans.

1.1.1 Expression of short-chain *O*-glycans in cancer

The most widely occurring glycosylation modifications in cancer stems from alterations in glycan length, often toward shorter *O*-glycans. The structural nature of *O*-GalNAc glycan alterations in cancer and underlying biosynthesis mechanisms have been comprehensively reviewed in recent years[12,20,33] . Briefly, these events are associated to an underlying disorganisation of secretory pathway organelles, mutations on *Cosmc*, a gene encoding the molecular chaperone of T-synthase [34], and absence or altered expression and/or activity of glycosyltransferases [35]. Altogether, these alterations functionally impact tumour cell fate. Namely, core 1 β1,3-galactosyltransferase (C1GALT1, responsible for Tn antigen biosynthesis) overexpression in hepatocellular carcinoma activates hepatocyte growth factor (HGF) signalling via modulation of MET kinase *O*-glycosylation and dimerization, thereby enhancing cell proliferation *in vivo* and *in vitro*[36]. In ovarian cancer cells, the knockout of

core 1 synthase chaperone *Cosmc*, resulting in Tn and STn *O*-glycans expression, leads to a reduction in cellular proliferation compared to the parental cell lines[37]. Notwithstanding, little is known on the functional impact of the simplest form of *O*-glycosylation in cancer.

In turn, STn is expressed by more than 80% of human carcinomas and, in all cases, it associated with adverse outcomes and decreased overall survival of patients [38], making it a potentially low risk biomarker for targeted therapeutics. Notably, most studies relayed on glycoengineered cell lines to demonstrate STn functional impact in cancer, since the antigen is rarely expressed at high levels in cell culture settings [39-41]. Such observations emphasize the intricate relationship between STn expression and the tumor microenvironment [11], which remains to be fully disclosed. In fact, in bladder cancer, it has been suggested that decreased oxygen levels may promote STn biosynthesis by suppressing the expression of glycosyltransferases involved in *O*-glycans elongation [11]; however, the microenvironmental factors driving STn expression should be further addressed in future studies. Nevertheless, gastric cancer (GC) cells glycoengineered to overexpress *ST6GALNAC1* and, consequently the STn antigen, displayed enhanced invasion capacity *in vitro* and increased metastatic ability in nude mice than the corresponding negative controls [41,42]. Moreover, MUC1 and CD44 were found to be major STn carriers [41,43], suggesting that STn might negatively impact on GC cell adhesion towards more metastatic phenotypes [42]. Furthermore, GC cells induced to overexpress *ST6GALNAC1* and *ST6GALNAC2* displayed lower proliferation rates than control cells, mostly due to an increase in the percentage of apoptotic cells and not to a G1 cell cycle delay [41]. STn expressing cells also showed markedly reduced homotypic cell–cell aggregation but increased adhesion to ECM components as collagen and fibronectin [41]. Other studies have disclosed a novel STn-dependent mechanism for chemotherapeutic resistance in GC cells [44]. Namely, STn increased galectin-3 intracellular accumulation by decreasing its interaction with cell surface glycan receptors. In this process, STn decreased chemotherapy sensitivity of cancer cells, highlighting the importance of developing novel strategies targeting galectin-3 and/or ST6GalNAc-I in GC [44]. In addition, studies involving glycoengineered *COSMC* knock-outs demonstrated that *O*-glycan shortening was accompanied by the acquisition of mesenchymal-like traits, while promoting transcriptomic remodelling towards overexpression of *SRPX2* and *RUNX1* genes (both commonly upregulated in GC tissues) [39]. STn overexpression also lead to the activation of ErbB tyrosine kinase receptors ErbB2 and EGFR in these models, implicating STn in the constitutive

activation of oncogenic signalling in GC [39]. *COSMC* knock-out mouse xenografts demonstrated decreased survival compared to wild type xenografts, vowing for the more aggressive nature of short-chain *O*-glycan overexpressing GC cells [39]. These findings highlight the role of STn in the acquisition of malignant features related to increased migration, invasion and chemoresistance in GC. In addition, overexpression of *ST6GALNAC1* enhanced STn expression in colorectal (CRC) stem cells (CSC) [45]. Particularly, STn was carried by the CSC marker CD44, and increased the sphere-forming ability and resistance to chemotherapeutic agents of CRC-CSC [45]. Furthermore, *ST6GANAC1*-overexpressing cells constitutively activated the Akt pathway, which was blocked by *LGALS3* (Galectin-3) gene knockdown. These findings suggest that *ST6GALNAC1* has a role in the maintenance of CRC-CSCs by activating the Akt pathway in cooperation with galectin-3 and that *ST6GalNAC1* or STn antigen might be reasonable molecular targets for CSC-targeted therapy [45]. Similarly, other studies reported CD44 as a major STn carrier in colorectal cancer [46], suggesting that CD44 glycosylation may be implicated in cellular adhesion alterations. The observations made for GC and CRC agree with previous reports from different types of tumours (breast, ovarian, prostate, bladder) where STn was also implicated in key oncogenic features favouring invasion and metastasis development, supporting the pancarcinoma and aggressive nature of this PTM [38,47,48]. Moreover, STn antigen is mainly observed in non-proliferative tumour areas of highly proliferative bladder tumours[49], while being overexpressed in less proliferative hypoxic bladder cancer models[11], suggesting a yet unknown indirect regulation of proliferation by *O*-glycosylation in bladder cancer. Moreover, STn reduces cell adhesion in prostate cancer[50], while increasing migration and invasion in bladder[11] and breast[41,42,51] carcinomas in a *ST6GalNAc.I*-dependent manner. Also, the increased and *de novo* expression of the STn antigen in bladder cancer cells is part of an array of molecular events underlying the establishment of mesenchymal traits[11]. Moreover, STn was mainly found in densely *O*-glycosylated adhesion proteins such as integrins and cadherins[11,30]. It is likely that the transition from extended to shorter and heavily sialylated structures may impair these proteins normal function and induce molecular and spatial reorganization at the cell-cell and cell-matrix interfaces. In agreement with these observations, STn expressing cells are frequently simultaneously observed in invasion fronts, near blood vessels and corresponding lymph nodes, as well as in distant metastasis[49,52]. Moreover, it has been recently reported

that most circulating tumor cells (CTC) in the blood of metastatic bladder cancer patients present a highly undifferentiated and more aggressive basal phenotype, while overexpressing the STn antigen[52]. As such, STn expression seems to confer a competitive advantage to neoplastic bladder cells by enabling not only invasion but also the necessary mechanisms for successful cancer dissemination. Similarly, ST6Gal.I-mediated α2,6-sialylation of breast cancer cells mediates reduced cell-cell adhesion and enhanced invasion capacity[53]. Overall, immature truncated *O*-glycophenotype of cancer cells directly induces oncogenic features, including enhanced migration and invasive capacity[54]. Both Tn and STn antigens have been classically associated to mucins due to their high glycosite density and are frequently termed simple-mucin type *O*-GalNAc glycans[55]. Nevertheless, virtually all glycoproteins presenting extracellular motifs prone to be *O*-glycosylated may express these glycoepitopes [56].

Recently, the nature of T antigen sialylation, namely the sialyl-3-T(S3T) and sialyl-6-T(S6T) sialoforms was explored in a series of bladder tumours with differing clinicopathology for short-chain *O*-glycans[30]. A predominance of sialoglycans over neutral glycoforms (Tn and T antigens) in bladder tumours was observed. In particular, the STn antigen was associated with high-grade disease and muscle invasion, in accordance with our previous observations. The S3T and S6T antigens were detected for the first time in bladder tumours, but not in healthy urothelia, highlighting their cancer-specific nature. These glycans were also overexpressed in advanced lesions, especially in cases showing muscle invasion. Glycoproteomic analyses of advanced bladder tumours resulted in the identification of several key cancer-associated glycoproteins (MUC16, CD44, integrins) carrying altered glycosylation. Of particular interest were MUC16 STn+-glycoforms, characteristic of ovarian cancers, which were found in a subset of advanced-stage bladder tumours facing the worst prognosis. In summary, significant alterations in the *O*-glycome and O-glycoproteome of bladder tumours seem to hold promise for the development of novel non-invasive diagnostic tools and targeted therapeutics. Furthermore, abnormal MUC16 glycoforms hold potential as surrogate biomarkers of poor prognosis and unique molecular signatures for designing highly specific targeted therapeutics.

1.1.2 Short-chain *O*-glycan immune response modulation

As described in previous sections, advanced stage tumours are frequently characterized by profound deregulations in glycosylation pathways, resulting in the presentation of aberrant structures at the cell surface. Importantly, these structures only render cancer cells mildly antigenic and rarely immunogenic[57]. This may occur because most cancer-associated structures have an embryonic origin or are mildly expressed in healthy tissues, allowing them to be perceived as "self" by immune system effector cells[58]. Furthermore, specialized B lymphocytes producing high-affinity antibodies against these structures might even be eliminated during development. However, glycans play a key role in the regulation of various aspects of immune response, ultimately enabling immune suppression by interacting with lectin receptors in immune cells. For instance, enhanced tumour sialylation often culminates in immune suppression and anti-inflammatory microenvironments. Accordingly, the presence of sialylated structures on melanoma cells impedes T cell mediated anti-tumour responses while promoting tumour-associated Treg cells and decreased NK cell activity[59]. Moreover, sialoglycans interact with sialic acid-binding immunoglobulin-like lectins (SIGLECs) to induce an antigen-specific tolerogenic programming, enhancing Treg cells and reducing the generation and propagation of inflammatory T cells[59]. For instance, macrophage associated Siglec-15 preferentially binds the STn antigen in myeloid tumour cells, resulting in increased TGF-β secretion into the tumour microenvironment and tumour progression[60]. Moreover, in bladder cancer, STn expression has led to impaired DC maturation while significantly reducing the production of Th1-inducing cytokines IL-12 and TNF-α[61]. Consistent with this tolerogenic profile, T cells primed by DCs pulsed with STn-expressing glycoproteins displayed a FoxP3(high) IFN-γ(low) phenotype and little capacity to trigger protective anti-tumour T cell responses[61]. More importantly, blocking STn-MUC1 and CD44 glycoforms partially reverted DC maturation, suggesting that targeting STn-expressing glycoproteins may allow circumventing tumour-induced tolerogenic mechanisms. Similarly, sialylation of the T antigen in MUC1 on breast cancer cells creates the MUC1–ST antigen which engages Siglec-9 on tumour-associated macrophages to initiate inhibitory immune signalling through the activation of the MAPK/ERK pathway[62]. In line with this, sialylated ligands of singlec-7 and−9 are expressed on cancer cells of different histological types and interactions between these lectin receptors and its ligands influence NK cell-dependent tumour immunosurveillance[63]. Moreover, hypersialylation of

tumour ligands for NKG2D receptors, expressed by NK cells, NK1.1+ T cells, γδ T cells, activated $CD8^{+}$αβ T cells and macrophages, is thought to repulse their interaction via highly negative charge repulsions, hampering immune response[64,65]. Tumour-derived sialoglycans also inhibit CD8+ T cell cytotoxicity by interfering with lytic granule trafficking and exocytosis in response to TCR engagement[66]. Thus, hypersialylation often observed on tumour cells may ultimately be amongst the mechanisms by which tumours evade immune system recognition[30,49,67,68]. Also, C2GnT-expressing bladder tumour cells express heavily core 2 *O*-glycosylated MUC1 which interacts with Gal-3 to attenuate the interaction of tumour cells with NK cells, allowing tumour cells to survive longer in host blood circulation and potentially metastasize[69]. Given these insights, sialylated antigens provided by short-chain *O*-glycans contribute to create an immunosuppressive microenvironment toward tumour cell immune escape.

1.1.3. Glycan-based clinical approaches

As previously described, short-chain *O*-glycans (Tn, T, STn, ST, dST) are the result of a premature stop in *O*-glycosylation of plasma-membrane and secreted proteins, making them accessible for serological detection. Accordingly, the CA72-4 (for the STn antigen) serological test has been long introduced in clinical practice and frequently support the assessment of gastroesophageal and colorectal cancer patients' status[70]. However, the CA72-4 antigen has been found elevated in the serum of healthy individuals as well as patients with benign conditions as gastric ulcer, polyps, atrophic gastritis and *Helicobacter pylori* infection [71]. These results indicate that routine screening of CA72-4 levels in asymptomatic patients may be ineffective due to low sensitivity and low positive predictive value [71]. Nevertheless, there is still little information on the nature and origin of the proteins in circulation carrying this PTM, which will be critical to fully disclose and potentiate its clinical meaning. Notwithstanding, the fact that these simple glycans are absent, significantly under-expressed or restricted to some cell types in healthy tissues, makes them ideal diagnostic and prognostic tools [49]. In line with this, there has been a growing interest in exploiting circulating tumour cells (CTC) for prognostication, detection of micrometastasis and as a mean to obtain more accurate insights on the molecular nature of the metastasis, as emphasized by several recent reviews[72]. Moreover, these cells have been observed in the blood of cancer patients with no evident radiological signs of metastasis [73],

reinforcing their importance for early and potentially life-saving interventions. Recently, we have demonstrated that the majority of CTC of different origins express the STn antigen at the cell-surface and that targeting this glycan could greatly expand the number of isolated CTC, thus increasing the sensitivity of current CTC detection methods[74]. Moreover, STn-CTC were identified in non-metastatic patients that subsequently experienced disease progression, further reinforcing the sensitivity of the methodology [74]. The presence of STn in CTC also provided the missing link between STn promotion of motility, invasion and immune escape and its presence in distant metastasis of advanced tumours [74]. These observations are crucial to further improve liquid biopsies and should now be extended to larger well characterized patient cohorts. It also provides the rationale for selectively targeting CTC in clinical settings and developing novel glycan-based therapeutics capable of controlling disseminated disease.

The cell-surface nature of glycans and glycoconjugates (glycoproteins and glycolipids) holds great potential for developing targeted therapeutics, including selective drug delivery, precise inhibition of key oncogenic pathways and immunotherapy[75-77]. Several monoclonal antibodies exist to target STn[78], which may be used to induce antibody-dependent cellular cytotoxicity (ADCC)[79,80], a mechanism by which many clinically available therapeutic antibodies promote anti-tumour effects[81], or block relevant oncogenic receptors [82]. These antibodies have been key tools for biomedical research but have shown limitations for theragnostic (cancer detection and therapy), including guiding drugs, CAR-Ts and immunotherapeutic agents. Again, the refinement of the glycoimmunogens poses as a critical milestone towards this end. In addition, the identification of glycoepitopes involved in interactions with the immune system may lead to the development of novel antibodies for immune check-point inhibition; however, this remains a rather unexplored field of research. As such, antibody-targeted therapies for glycoconjugates remains intimately dependent on the development of bispecific antibodies targeting glycodomains in functionally relevant proteins.

Another emerging approach relates with exploiting chimeric antigen receptor (CAR) T cells engineered to target glycosylated moieties in cancer cells, promoting selective cell death [83]. Despite boosted by advances in cell engineering, this is an old concept explored for therapeutic proposes in oncoglycobiology. In fact, the first-generation of CAR-T retrovirally transduced to efficiently target the TAG-72 glycoprotein (a well-known STn carrier) in

gastrointestinal tumour cell lines dates back to the nineties [84]. Nevertheless, the concept has only been recently translated into a clinical trial for metastatic CRC [85]. However, CAR-T cells were not able to elicit clinical response, potentially due to CAR antigenicity related to the murine origin of the scFv [86], lack of T cell co-stimulatory signalling, vowing for the inclusion of co-stimulatory molecules in CAR design, or the modest affinity of the CC49 anti-STn monoclonal antibody explored by this study [87]. In addition, Loureiro et al. has recently reported that CAR-T cells can be efficiently and safely targeted to STn-expressing cells exploiting the recently developed L2A5 monoclonal antibody [88]. These have been effective against breast- and bladder-associated tumour cells both *in vitro* and *in vivo*, but were not yet tested in digestive tract tumors[89]. Loureiro et al. also reports some degree of cross-reactivity between the most explored anti-STn antibodies and immune cells. According to this study, L2A5, B72.3 and 3F1 (also referred to as HB-STn-1) showed no affinity for NK cells; however, B72.3 and 3F1 reacted with CD4+ and CD8+ T cells but not B cells. The L2A5 antibody recognized B cells and showed weak binding to a subpopulation of CD4low T cells [89]. These critical observations demonstrated that CAR-T cells based on these antibodies carry the potential risk of fratricidal activities against T- and/or B lymphocytes. There are also concerns that STn-targeted CAR-T may significantly react against inflamed tissues, known to upregulate this glycan [90]. Collectively, these observations suggest that, even though vaccination and consequent induction of circulating STn antibodies have been proven safe [91], more potent CAR-T therapy might encompass significant and potentially limiting off-target effects. Consequently, the future of glyco-targeted CAR-T remains dependent on the identification of targetable glyconeoantigens.

Immunotherapy based on vaccination with short-chain cancer associated glycans is an appealing concept already explored in clinical trials, even though not for gastroesophageal and colorectal cancers. A pentavalent carbohydrate-based vaccine bearing several carbohydrate antigens, including STn, on a single polypeptide backbone, conjugated to keyhole limpet hemocyanin (KLH) and mixed with the QS-21 immunological adjuvant has entered in phase 1 clinical trials for patients with ovarian, fallopian tube and peritoneal cancers [92]. However, the most promising approach continues to be Theratope, an STn-KLH vaccine that reached phase 3 clinical trials for metastatic breast cancer. Despite well tolerated by the patients, vaccination did not translate into an overall benefit in terms of time to progression and overall survival [93,94]. However, it has been suggested that a prior knowledge

of the STn status of the tumours could have been crucial for patient selection and study outcome [95]. The efficacy of these approaches could also be compromised by immunological barriers raised by the STn antigen. In fact, cancer-associated glycans as STn present variable immunogenicity depending on the distribution and nature of the glycopeptide chain [96]. Moreover, STn may directly induce immune tolerance, including limited dendritic cell differentiation and induction of T-cell-mediated immunity, which are crucial for efficient cancer therapy [61,97]. As an example, densely glycosylated MUC1 sialoglycopeptides, frequently explored in the context of vaccine development, cannot be processed by antigen-presenting cells [98], impairing antigen presentation and consequent T cell activation. Nevertheless, these studies provide important lessons for choosing more adequate glycoepitopes, setting again the emphasis on glycoproteomics. There have also been attempts to overcome glycan-induced immune tolerance by coupling multiple carbohydrate antigens to specific carriers to form either clustered and/or multi-epitope conjugated vaccines [99]. Glycans have also been combined with T-cell derived peptides or immunoadjuvant epitopes to produce glycoconjugate vaccines of multicomponent nature [100]. Another strategy involves chemical modifications of glycans to improve immunogenicity. As an example, Song *et al.* recently investigated the antitumor ability of KLH-conjugated fluorinated STn analogues against a murine model of colon cancer [101]. According to the authors, vaccine constructs with substitution of two *N*-acetyl by *N*-fluoroacetyl groups in STn significantly prolonged mice survival and reduced tumour burden in the lungs compared with Theratope (STn-KLH). The fluorinated vaccine elicited stronger cytotoxic T cell and Th1 immune responses and tumour-specific anti-STn antibodies capable of inducing complement and antibody-dependent cell-mediated cytotoxicity against human tumor cells, even in the absence of an immune adjuvant [101]. Collectively, these findings suggest that strategic hapten fluorination may significantly improve the efficacy of glycan-based vaccines, even though the exact mechanism governing this immune response remains unknown. In addition, MUC1-derived glycopeptides associated with cancer are amongst the array of glycoepitopes used in vaccines explored in clinical trials [102]; however, with yet limited success. It was proposed that after first vaccination both tumour MUC1 and MHC molecules were reduced, suggesting an upfront response against these cells that was followed by therapy scape [103]. These findings highlight the need to include a diversified array of glycopeptides that mirror tumour diversity. However, surrogate T-cell pre-activation

outside the tumour bed, either in culture or by repetitive vaccination, could overcome tumour escape in MUC1 transgenic mice, offering an alternative approach to improve therapeutic schemes. Furthermore, the effective development of MUC1-based vaccines would be of great interest for patients with gastroesophageal and colorectal tumours, among others, that significantly overexpress abnormal glycoforms of this protein [104,105]. Collectively these studies demonstrate the feasibility of glycan-based anti-cancer vaccines but also highlight the importance of more accurate epitope choice and improved vehicle design, which requires a more profound knowledge of glycan-immune system interactions. The introduction of distinct T helper cell epitopes, Toll-like receptor agonists and other relevant immunogens in vaccine constructs together with the use of liposomes and nanoparticles as delivery systems may also help paving the way for improved vaccine designs [106,107].

1.2. Nanocarriers for cancer nanovaccines

Anti-tumour vaccines for cancer prevention and treatment, either alone or in combination with other immunotherapies such as adoptive cell therapy or immune checkpoint blockade, have become an attractive class of cancer immunotherapeutics in recent years. However, cancer vaccines have thus far shown suboptimal efficacy in clinical settings. In this context, nanomedicines provide key opportunities to improve the efficacy of these vaccines. A variety of nanoplatforms have been investigated for antigen encapsulation and presentation, including lipid based particulate carriers (liposomes), metallic and inorganic nanoparticles (NPs), virus like particles, biodegradable NPs, gelatine-based NPs and nanoemulsions[108-110]. Among the emerging subunit vaccines are recombinant protein- and synthetic peptide-based vaccine formulations[111,112]. However, protein, peptides and glycopeptides have a low intrinsic immunogenicity, which can be overcome through co-encapsulation of antigens with immune modulators using particulate delivery systems as poly(lactic-co-glycolic acid) (PLGA) particles. PLGA is a biocompatible and biodegradable polymer approved by U.S. Food and Drug Administration (FDA) for human use, whose particulate formulations offer many advantages for antigen delivery. Namely, PLGA nanoformulations: i) shield antigens from degradation and clearance[113]; ii) provide sustained release of encapsulated molecules (proteins, DNA, mRNA, among others)[114]; iii) allow co-encapsulation of antigens and immune modulators[114,115]; iv) can be targeted to antigen presenting cells[116]; v) increase uptake and cross-presentation by antigen presenting cells

through mimicking the size and shape of an invading pathogen[117]. Moreover, PLGA nanoparticles provide a versatile platform to encapsulate or adsorb vaccine immunogens, mostly according to its physicochemical properties [118]. Immunogen encapsulation is highly affected by frequently modest encapsulation efficiencies and incomplete release, which can lead to a weak immune response[118,119]. In turn, adsorption of immunogens can often lead to burst release or premature antigen release, which can compromise APC uptake and culminate in hampered immune responses [119]. Furthermore, PLGA nanoformulations negative charge can compromise nanoparticle uptake by APC to some extent and particle aggregation as well as particle size may limit crossing of biological barriers[119]. Notwithstanding, the multifaceted nature of nanoplatforms poses a major advantage in circumventing mythology pitfalls.

As previously mentioned, anticancer vaccines aim to induce tumour-specific CTL responses, which require activation of APCs such as dendritic cells DCs and macrophages (**Figure 2**). Therefore, a potent immunostimulatory adjuvant capable of activating APCs is an essential component of anticancer vaccines, as depicted in several recent reports[120,121]. Despite the vast panoply of immunostimulatory molecules, as saponins, cytokines and bacterial toxins, the most widespread ligands are Toll-like receptors (TLRs) agonists, which interact with DCs, macrophages and lymphocytes to incite pro-inflammatory responses[122,123]. In preclinical settings, particulate PLGA formulations have provided effective anticancer vaccination. For instance, PLGA NPs loaded with toll-like receptor 7 agonist, imiquimod (R837) and coated with cancer cell membranes with mannose modification moieties have shown enhanced uptake by DC. Moreover, in combination with checkpoint-blockade therapy, these NPs further demonstrated therapeutic efficacy against established tumours[124]. An erythrocyte membrane-enveloped PLGA nanoplatform for antigenic peptide hgp10025-33 and toll-like receptor 4 agonist monophosphoryl lipid (MPLA) also demonstrated enhanced DC uptake *in vitro*[125]. Moreover, the nanovaccine prolonged tumour-occurring time and inhibited tumour growth and metastasis in prophylactic, therapeutic, and metastatic melanoma models, respectively, while effectively enhancing IFN-γ secretion and CD8(+) T cell response[125]. Taken together, these findings demonstrate the great potential of nanoplatforms as antigen delivery systems for cancer immunotherapy. Another study introduced novel TLR 7/8 bi-specific agonists which significantly enhanced cytokine secretion compared to TLR7 mono-selective compounds[126].

Encapsulation of these TLR 7/8 agonists in PLGA NPs increased co-stimulatory molecule expression and antigen presentation via MHC I by DCs compared to the soluble agonist. When administered subcutaneously, these NPs migrated to draining lymph nodes and triggered DC activation and expansion, leading to expansion of antigen specific CD8 T cells and enhanced CTL response. This resulted in significant prophylactic and therapeutic efficacy in melanoma, bladder and renal cell carcinoma tumour models, while significantly reducing systemic metastasis[126].

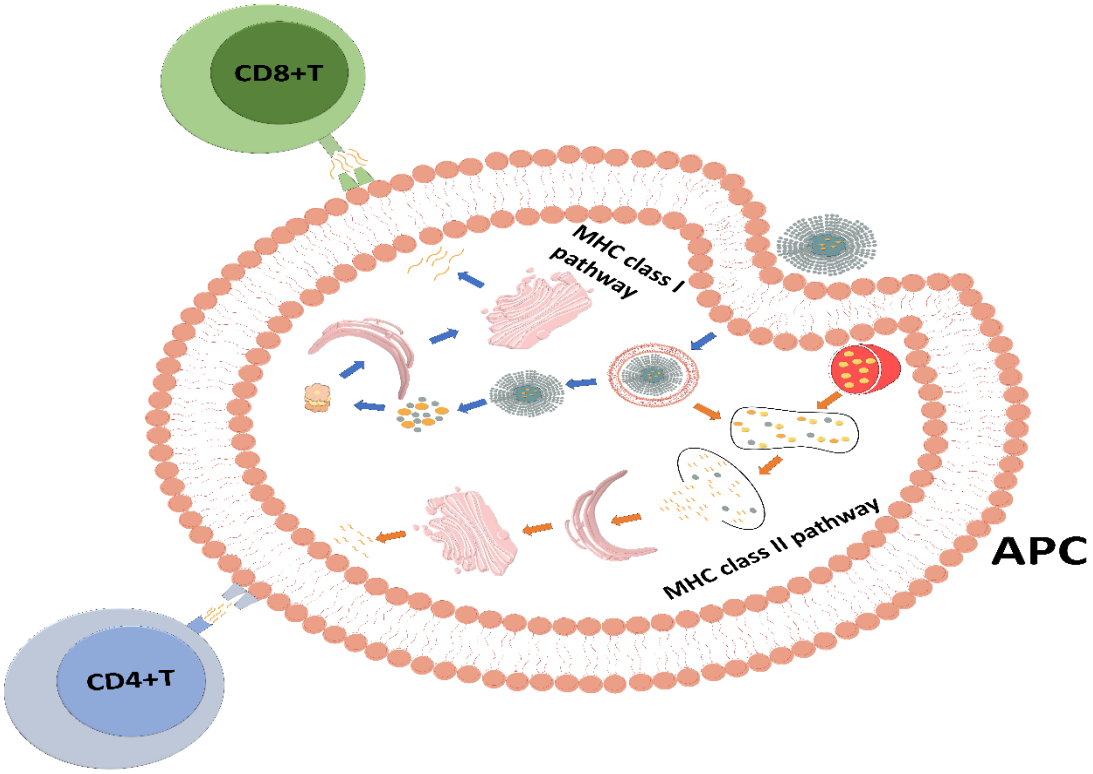

Figure 2. Immune system activation by antigens present in nanoparticles. In MHC class II pathway nanoparticles containing antigens are phagocyted with a formation of a compartment. This compartment fuses with an endosome and then antigens are transported to cell surface to be presented to CD4+T cells. In MHC class I, nanoparticles in the compartment escape from endosome and are degraded in cytosol by proteasome. Then, antigens are associated with MHC class I molecules and are presented to CD8+T cells.

Particulate PLGA nanoformulations have also been used to incite macrophage inflammatory responses. Namely, PLGA NP with or without any encapsulated bioactive compounds are avidly phagocyted by J774[127] and RAW 264.7[128] murine macrophage cells, however, the extent of inflammatory response in terms of secretion of inflammatory

cytokines seems to be dependent on the coupling of endotoxins or immunomodulators. Notwithstanding, the functional repolarization of macrophages to enhance their beneficial function and limit their detrimental properties is currently the most attractive strategy for disease treatment[129]. In this context, tremendous work is being done using polymeric nanoparticles, with most results indicating that increasing the surface ionization or adding inert polymers to the surface of nanoparticles reduces their opsonization and prevents specific nanoparticle-macrophage interactions, ultimately reducing macrophage polarization capabilities. Lessons learned from other polymeric systems could easily bring light into novel PLGA nanoformulations. Overall, nanoparticles are a promising treatment approach to modulate macrophage polarization in the tumour microenvironment, and researchers developing nanoparticle-based cancer treatments should consider the macrophage-polarizing potential of nanoparticles to maximize therapeutic efficacy.

1.3 References

1 Stratton, M. R., Campbell, P. J. & Futreal, P. A. The cancer genome. *Nature* **458**, 719-724, (2009).

2 Lee, E. Y. H. P., Muller, W. J., Sloane, B. F., Rosen, J. M. & Piwnica-worms, D. Oncogenes and Tumor Suppressor Genes. *Cold Spring Harb Perspectives in Biology* **2**, 1-18, (2014).

3 Vogelstein, B. & Kinzler, K. W. Cancer genes and the pathways they control. *Nature Medicine* **10**, 789-799, (2004).

4 Katzke, V. A., Kaaks, R. & Kuhn, T. Lifestyle and cancer risk. *The cancer journal* **21**, 104-110, (2015).

5 Wodarz, D. & Zauber, A. Risk factors and random chances. *Nature* **517**, 563-564, (2015).

6 Coulson, A., Levy, A. & Gossell-Williams, M. Monoclonal antibodies in cancer therapy: Mechanisms, successes and limitations. *West Indian Medical Journal* **63**, 650-654, (2014).

7 Qu, Z., Griffiths, G. L., Wegener, W. A., Chang, C. H., Govindan, S. V., Horak, I. D., Hansen, H. J. & Goldenberg, D. M. Development of humanized antibodies as cancer therapeutics. *Methods* **36**, 84-95, (2005).

8 Pardoll, D. M. The blockade of immune checkpoints in cancer immunotherapy. *Nature Reviews Cancer* **12**, 252-264, (2012).

9 Hu, Z., Ott, P. A. & Wu, C. J. Towards personalized, tumour-specific, therapeutic vaccines for cancer. *Nature Reviews Immunology* **18**, 168-182, (2018).

10 Desrichard, A., Snyder, A. & Chan, T. A. Cancer neoantigens and applications for immunotherapy. *Clinical Cancer Research* **22**, 807-812, (2016).

11 Peixoto, A., Fernandes, E., Gaiteiro, C., Lima, L., Azevedo, R., Soares, J., Cotton, S., Parreira, B., Neves, M., Amaro, T., Tavares, A., Teixeira, F., Palmeira, C.,

Rangel, M., Silva, A. M., Reis, C. A., Santos, L. L., Oliveira, M. J. & Ferreira, J. A. Hypoxia enhances the malignant nature of bladder cancer cells and concomitantly antagonizes protein O-glycosylation extension. *Oncotarget* **7**, 63138-63157, (2016).

12 Pinho, S. S. & Reis, C. A. Glycosylation in cancer : mechanisms and clinical implications. *Nature Publishing Group* **16**, 540-550, (2015).

13 Rodrigues, J. G., Balmaña, M., Macedo, J. A., Poças, J., Fernandes, Â., De-Freitas-Junior, J. C. M., Pinho, S. S., Gomes, J., Magalhães, A., Gomes, C., Mereiter, S. & Reis, C. A. Glycosylation in cancer: Selected roles in tumour progression, immune modulation and metastasis. *Cellular Immunology* **8749**, 30121-30127, (2018).

14 Christiansen, M. N., Chik, J., Lee, L., Anugraham, M., Abrahams, J. L. & Packer, N. H. Cell surface protein glycosylation in cancer. *Proteomics* **14**, 525-546, (2014).

15 Hakomori, S. Glycosylation defining cancer malignancy: new wine in an old bottle. *Pnas* **99**, 10231-10233, (2002).

16 Tan, H. T., Low, J., Lim, S. G. & Chung, M. C. M. Serum autoantibodies as biomarkers for early cancer detection. *FEBS Journal* **276**, 6880-6904, (2009).

17 Li, M., Song, L. & Qin, X. Glycan changes: Cancer metastasis and anti-cancer vaccines. *Journal of Biosciences* **35**, 665-673, (2010).

18 Holmberg, L. A. & Sandmaier, B. M. Theratope ® vaccine (STn-KLH). *Expert Opinion on Biological Therapy* **1**, 881-891, (2001).

19 An, H. J., Kronewitter, S. R., Leoz, M. L. A. D. & Lebrilla, C. B. Glycomics and disease markers. *Current Opinion in Chemical Biology* **13**, 601-607, (2009).

20 Azevedo, R., Peixoto, A., Gaiteiro, C., Fernandes, E., Neves, M., Lima, L., Santos, L. L. & Ferreira, J. A. *Over forty years of bladder cancer glycobiology: Where do glycans stand facing precision oncology?* , Vol. 8 (2017).

21 Shrimal, S., Cherepanova, N. A. & Gilmore, R. Cotranslational and posttranslocational N-glycosylation of proteins in the endoplasmic reticulum. *Semin Cell Dev Biol* **41**, 71-78, (2015).

22 Ju, T., Aryal, R. P., Kudelka, M. R., Wang, Y. & Cummings, R. D. The Cosmc connection to the Tn antigen in cancer. *Cancer Biomark* **14**, 63-81, (2014).

23 Ghazarian, H., Idoni, B. & Oppenheimer, S. B. A glycobiology review : Carbohydrates , lectins and implications in cancer therapeutics. *Acta histochemica* **113**, 236-247, (2011).

24 Ohtsubo, K. & Marth, J. D. Glycosylation in Cellular Mechanisms of Health and Disease. *Cell* **126**, 855-867, (2006).

25 Helenius, A. & Aebi, M. Intracellular functions of N-linked glycans. *Science* **291**, 2364-2369, (2001).

26 Kannagi, R., Izawa, M., Koike, T., Miyazaki, K. & Kimura, N. Carbohydrate-mediated cell adhesion in cancer metastasis and angiogenesis. *Cancer Sci* **95**, 377-384, (2004).

27 Aebi, M. & Hennet, T. Congenital disorders of glycosylation: genetic model systems lead the way. *Trends Cell Biol* **11**, 136-141, (2001).

28 Lyons, J. J., Milner, J. D. & Rosenzweig, S. D. Glycans Instructing Immunity: The Emerging Role of Altered Glycosylation in Clinical Immunology. *Front Pediatr* **3**, 54, (2015).

29 Hakomori, S. & Kannagi, R. Glycosphingolipids as tumor-associated and differentiation markers. *J Natl Cancer Inst* **71**, 231-251, (1983).

30 Cotton, S., Azevedo, R., Gaiteiro, C., Ferreira, D., Lima, L., Peixoto, A., Fernandes, E., Neves, M., Neves, D., Amaro, T., Cruz, R., Tavares, A., Rangel, M., Silva, A. M.

N., Santos, L. L. & Ferreira, J. A. Targeted O-glycoproteomics explored increased sialylation and identified MUC16 as a poor prognosis biomarker in advanced-stage bladder tumours. *Mol Oncol* **11**, 895-912, (2017).

31 Orntoft, T. F., Wolf, H., Clausen, H., Hakomori, S. & Dabelsteen, E. Blood group ABO and Lewis antigens in fetal and normal adult bladder urothelium: immunohistochemical study of type 1 chain structures. *J Urol* **138**, 171-176, (1987).

32 Nakamori, S., Kameyama, M., Imaoka, S., Furukawa, H., Ishikawa, O., Sasaki, Y., Izumi, Y. & Irimura, T. Involvement of carbohydrate antigen sialyl Lewis(x) in colorectal cancer metastasis. *Dis Colon Rectum* **40**, 420-431, (1997).

33 Ferreira, J. A., Magalhães, A., Gomes, J., Peixoto, A., Gaiteiro, C., Fernandes, E., Santos, L. L. & Reis, C. A. Protein glycosylation in gastric and colorectal cancers: Toward cancer detection and targeted therapeutics. *Cancer Letters* **387**, 32-45, (2017).

34 Ju, T., Lanneau, G. S., Gautam, T., Wang, Y., Xia, B., Stowell, S. R., Willard, M. T., Wang, W., Xia, J. Y., Zuna, R. E., Laszik, Z., Benbrook, D. M., Hanigan, M. H. & Cummings, R. D. Human tumor antigens Tn and sialyl Tn arise from mutations in Cosmc. *Cancer Res* **68**, 1636-1646, (2008).

35 Reis, C. A., Osorio, H., Silva, L., Gomes, C. & David, L. Alterations in glycosylation as biomarkers for cancer detection. *J Clin Pathol* **63**, 322-329, (2010).

36 Wu, Y. M., Liu, C. H., Huang, M. J., Lai, H. S., Lee, P. H., Hu, R. H. & Huang, M. C. C1GALT1 enhances proliferation of hepatocellular carcinoma cells via modulating MET glycosylation and dimerization. *Cancer Res* **73**, 5580-5590, (2013).

37 Coelho, R., Marcos-Silva, L., Mendes, N., Pereira, D., Brito, C., Jacob, F., Steentoft, C., Mandel, U., Clausen, H., David, L. & Ricardo, S. Mucins and Truncated O-Glycans Unveil Phenotypic Discrepancies between Serous Ovarian Cancer Cell Lines and Primary Tumours. *Int J Mol Sci* **19**, (2018).

38 Julien, S., Videira, P. A. & Delannoy, P. Sialyl-tn in cancer: (how) did we miss the target? *Biomolecules* **2**, 435-466, (2012).

39 Freitas, D., Campos, D., Gomes, J., Pinto, F., Macedo, J. A., Matos, R., Mereiter, S., Pinto, M. T., Polonia, A., Gartner, F., Magalhaes, A. & Reis, C. A. O-glycans truncation modulates gastric cancer cell signaling and transcription leading to a more aggressive phenotype. *EBioMedicine* **40**, 349-362, (2019).

40 Marcos, N. T., Pinho, S., Grandela, C., Cruz, A., Samyn-Petit, B., Harduin-Lepers, A., Almeida, R., Silva, F., Morais, V., Costa, J., Kihlberg, J., Clausen, H. & Reis, C. A. Role of the human ST6GalNAc-I and ST6GalNAc-II in the synthesis of the cancer-associated sialyl-Tn antigen. *Cancer Res* **64**, 7050-7057, (2004).

41 Pinho, S., Marcos, N. T., Ferreira, B., Carvalho, A. S., Oliveira, M. J., Santos-Silva, F., Harduin-Lepers, A. & Reis, C. A. Biological significance of cancer-associated sialyl-Tn antigen: modulation of malignant phenotype in gastric carcinoma cells. *Cancer Lett* **249**, 157-170, (2007).

42 Ozaki, H., Matsuzaki, H., Ando, H., Kaji, H., Nakanishi, H., Ikehara, Y. & Narimatsu, H. Enhancement of metastatic ability by ectopic expression of ST6GalNAcI on a gastric cancer cell line in a mouse model. *Clin Exp Metastasis* **29**, 229-238, (2012).

43 Mereiter, S., Martins, A. M., Gomes, C., Balmana, M., Macedo, J. A., Polom, K., Roviello, F., Magalhaes, A. & Reis, C. A. O-glycan truncation enhances cancer-related functions of CD44 in gastric cancer. *FEBS Lett* **593**, 1675-1689, (2019).

44 Santos, S. N., Junqueira, M. S., Francisco, G., Vilanova, M., Magalhaes, A., Dias Baruffi, M., Chammas, R., Harris, A. L., Reis, C. A. & Bernardes, E. S. O-glycan sialylation alters galectin-3 subcellular localization and decreases chemotherapy sensitivity in gastric cancer. *Oncotarget* **7**, 83570-83587, (2016).

45 Ogawa, T., Hirohashi, Y., Murai, A., Nishidate, T., Okita, K., Wang, L., Ikehara, Y., Satoyoshi, T., Usui, A., Kubo, T., Nakastugawa, M., Kanaseki, T., Tsukahara, T., Kutomi, G., Furuhata, T., Hirata, K., Sato, N., Mizuguchi, T., Takemasa, I. & Torigoe, T. ST6GALNAC1 plays important roles in enhancing cancer stem phenotypes of colorectal cancer via the Akt pathway. *Oncotarget* **8**, 112550-112564, (2017).

46 Singh, R., Campbell, B. J., Yu, L. G., Fernig, D. G., Milton, J. D., Goodlad, R. A., FitzGerald, A. J. & Rhodes, J. M. Cell surface-expressed Thomsen-Friedenreich antigen in colon cancer is predominantly carried on high molecular weight splice variants of CD44. *Glycobiology* **11**, 587-592, (2001).

47 Munkley, J. The Role of Sialyl-Tn in Cancer. *Int J Mol Sci* **17**, 275, (2016).

48 Azevedo, R., Peixoto, A., Gaiteiro, C., Fernandes, E., Neves, M., Lima, L., Santos, L. L. & Ferreira, J. A. Over forty years of bladder cancer glycobiology: Where do glycans stand facing precision oncology? *Oncotarget* **8**, 91734-91764, (2017).

49 Ferreira, J. A., Videira, P. A., Lima, L., Pereira, S., Silva, M., Carrascal, M., Severino, P. F., Fernandes, E., Almeida, A., Costa, C., Vitorino, R., Amaro, T., Oliveira, M. J., Reis, C. A., Dall'Olio, F., Amado, F. & Santos, L. L. Overexpression of tumour-associated carbohydrate antigen sialyl-Tn in advanced bladder tumours. *Mol Oncol* **7**, 719-731, (2013).

50 Munkley, J., Oltean, S., Vodak, D., Wilson, B. T., Livermore, K. E., Zhou, Y., Star, E., Floros, V. I., Johannessen, B., Knight, B., McCullagh, P., McGrath, J., Crundwell, M., Skotheim, R. I., Robson, C. N., Leung, H. Y., Harries, L. W., Rajan, P., Mills, I. G. & Elliott, D. J. The androgen receptor controls expression of the cancer-associated sTn antigen and cell adhesion through induction of ST6GalNAc1 in prostate cancer. *Oncotarget* **6**, 34358-34374, (2015).

51 Julien, S., Adriaenssens, E., Ottenberg, K., Furlan, A., Courtand, G., Vercoutter-Edouart, A. S., Hanisch, F. G., Delannoy, P. & Le Bourhis, X. ST6GalNAc I expression in MDA-MB-231 breast cancer cells greatly modifies their O-glycosylation pattern and enhances their tumourigenicity. *Glycobiology* **16**, 54-64, (2006).

52 Lima, L., Neves, M., Oliveira, M. I., Dieguez, L., Freitas, R., Azevedo, R., Gaiteiro, C., Soares, J., Ferreira, D., Peixoto, A., Fernandes, E., Montezuma, D., Tavares, A., Ribeiro, R., Castro, A., Oliveira, M., Fraga, A., Reis, C. A., Santos, L. L. & Ferreira, J. A. Sialyl-Tn identifies muscle-invasive bladder cancer basal and luminal subtypes facing decreased survival, being expressed by circulating tumor cells and metastases. *Urol Oncol* **35**, 675 e671-675 e678, (2017).

53 Lin, S., Kemmner, W., Grigull, S. & Schlag, P. M. Cell surface alpha 2,6 sialylation affects adhesion of breast carcinoma cells. *Exp Cell Res* **276**, 101-110, (2002).

54 Radhakrishnan, P., Dabelsteen, S., Madsen, F. B., Francavilla, C., Kopp, K. L., Steentoft, C., Vakhrushev, S. Y., Olsen, J. V., Hansen, L., Bennett, E. P., Woetmann, A., Yin, G., Chen, L., Song, H., Bak, M., Hlady, R. A., Peters, S. L., Opavsky, R., Thode, C., Qvortrup, K., Schjoldager, K. T., Clausen, H., Hollingsworth, M. A. & Wandall, H. H. Immature truncated O-glycophenotype of cancer directly induces oncogenic features. *Proc Natl Acad Sci U S A* **111**, E4066-4075, (2014).

55 Kudelka, M. R., Ju, T., Heimburg-Molinaro, J. & Cummings, R. D. Simple sugars to complex disease--mucin-type O-glycans in cancer. *Adv Cancer Res* **126**, 53-135, (2015).
56 Steentoft, C., Vakhrushev, S. Y., Joshi, H. J., Kong, Y., Vester-Christensen, M. B., Schjoldager, K. T., Lavrsen, K., Dabelsteen, S., Pedersen, N. B., Marcos-Silva, L., Gupta, R., Bennett, E. P., Mandel, U., Brunak, S., Wandall, H. H., Levery, S. B. & Clausen, H. Precision mapping of the human O-GalNAc glycoproteome through SimpleCell technology. *EMBO J* **32**, 1478-1488, (2013).
57 Fukuda, M. Possible roles of tumor-associated carbohydrate antigens. *Cancer Res* **56**, 2237-2244, (1996).
58 Speiser, D. E., Miranda, R., Zakarian, A., Bachmann, M. F., McKall-Faienza, K., Odermatt, B., Hanahan, D., Zinkernagel, R. M. & Ohashi, P. S. Self antigens expressed by solid tumors Do not efficiently stimulate naive or activated T cells: implications for immunotherapy. *J Exp Med* **186**, 645-653, (1997).
59 Perdicchio, M., Cornelissen, L. A., Streng-Ouwehand, I., Engels, S., Verstege, M. I., Boon, L., Geerts, D., van Kooyk, Y. & Unger, W. W. Tumor sialylation impedes T cell mediated anti-tumor responses while promoting tumor associated-regulatory T cells. *Oncotarget* **7**, 8771-8782, (2016).
60 Takamiya, R., Ohtsubo, K., Takamatsu, S., Taniguchi, N. & Angata, T. The interaction between Siglec-15 and tumor-associated sialyl-Tn antigen enhances TGF-beta secretion from monocytes/macrophages through the DAP12-Syk pathway. *Glycobiology* **23**, 178-187, (2013).
61 Carrascal, M. A., Severino, P. F., Guadalupe Cabral, M., Silva, M., Ferreira, J. A., Calais, F., Quinto, H., Pen, C., Ligeiro, D., Santos, L. L., Dall'Olio, F. & Videira, P. A. Sialyl Tn-expressing bladder cancer cells induce a tolerogenic phenotype in innate and adaptive immune cells. *Mol Oncol* **8**, 753-765, (2014).
62 Beatson, R., Tajadura-Ortega, V., Achkova, D., Picco, G., Tsourouktsoglou, T. D., Klausing, S., Hillier, M., Maher, J., Noll, T., Crocker, P. R., Taylor-Papadimitriou, J. & Burchell, J. M. The mucin MUC1 modulates the tumor immunological microenvironment through engagement of the lectin Siglec-9. *Nat Immunol* **17**, 1273-1281, (2016).
63 Jandus, C., Boligan, K. F., Chijioke, O., Liu, H., Dahlhaus, M., Demoulins, T., Schneider, C., Wehrli, M., Hunger, R. E., Baerlocher, G. M., Simon, H. U., Romero, P., Munz, C. & von Gunten, S. Interactions between Siglec-7/9 receptors and ligands influence NK cell-dependent tumor immunosurveillance. *J Clin Invest* **124**, 1810-1820, (2014).
64 Cohen, M., Elkabets, M., Perlmutter, M., Porgador, A., Voronov, E., Apte, R. N. & Lichtenstein, R. G. Sialylation of 3-methylcholanthrene-induced fibrosarcoma determines antitumor immune responses during immunoediting. *J Immunol* **185**, 5869-5878, (2010).
65 Lanier, L. L. NKG2D Receptor and Its Ligands in Host Defense. *Cancer Immunol Res* **3**, 575-582, (2015).
66 Lee, H. C., Wondimu, A., Liu, Y., Ma, J. S., Radoja, S. & Ladisch, S. Ganglioside inhibition of CD8+ T cell cytotoxicity: interference with lytic granule trafficking and exocytosis. *J Immunol* **189**, 3521-3527, (2012).
67 Schultz, M. J., Swindall, A. F. & Bellis, S. L. Regulation of the metastatic cell phenotype by sialylated glycans. *Cancer metastasis reviews* **31**, 501-518, (2012).

68 Costa, C., Pereira, S., Lima, L., Peixoto, A., Fernandes, E., Neves, D., Neves, M., Gaiteiro, C., Tavares, A., Gil da Costa, R. M., Cruz, R., Amaro, T., Oliveira, P. A., Ferreira, J. A. & Santos, L. L. Abnormal Protein Glycosylation and Activated PI3K/Akt/mTOR Pathway: Role in Bladder Cancer Prognosis and Targeted Therapeutics. *PLoS One* **10**, e0141253, (2015).

69 Suzuki, Y., Sutoh, M., Hatakeyama, S., Mori, K., Yamamoto, H., Koie, T., Saitoh, H., Yamaya, K., Funyu, T., Habuchi, T., Arai, Y., Fukuda, M., Ohyama, C. & Tsuboi, S. MUC1 carrying core 2 O-glycans functions as a molecular shield against NK cell attack, promoting bladder tumor metastasis. *Int J Oncol* **40**, 1831-1838, (2012).

70 Piantino, P., Taccone, W., Fusaro, A., Daziano, E., Polloni, R. & Mosso, R. Significance of CA 72.4 serum levels in gastrointestinal diseases. *Int J Biol Markers* **5**, 77-80, (1990).

71 Hu, P. J., Chen, M. Y., Wu, M. S., Lin, Y. C., Shih, P. H., Lai, C. H. & Lin, H. J. Clinical Evaluation of CA72-4 for Screening Gastric Cancer in A Healthy Population: A Multicenter Retrospective Study. *Cancers (Basel)* **11**, (2019).

72 Paterlini-Brechot, P. & Benali, N. L. Circulating tumor cells (CTC) detection: clinical impact and future directions. *Cancer Lett* **253**, 180-204, (2007).

73 Alunni-Fabbroni, M., Muller, V., Fehm, T., Janni, W. & Rack, B. Monitoring in metastatic breast cancer: is imaging outdated in the era of circulating tumor cells? *Breast Care (Basel)* **9**, 16-21, (2014).

74 Neves, M., Azevedo, R., Lima, L., Oliveira, M. I., Peixoto, A., Ferreira, D., Soares, J., Fernandes, E., Gaiteiro, C., Palmeira, C., Cotton, S., Mereiter, S., Campos, D., Afonso, L. P., Ribeiro, R., Fraga, A., Tavares, A., Mansinho, H., Monteiro, E., Videira, P. A., Freitas, P. P., Reis, C. A., Santos, L. L., Dieguez, L. & Ferreira, J. A. Exploring sialyl-Tn expression in microfluidic-isolated circulating tumour cells: A novel biomarker and an analytical tool for precision oncology applications. *N Biotechnol* **49**, 77-87, (2019).

75 Ferreira, J. A., Magalhaes, A., Gomes, J., Peixoto, A., Gaiteiro, C., Fernandes, E., Santos, L. L. & Reis, C. A. Protein glycosylation in gastric and colorectal cancers: Toward cancer detection and targeted therapeutics. *Cancer Lett* **387**, 32-45, (2017).

76 Pinho, S. S. & Reis, C. A. Glycosylation in cancer: mechanisms and clinical implications. *Nat Rev Cancer* **15**, 540-555, (2015).

77 Mereiter, S., Balmana, M., Campos, D., Gomes, J. & Reis, C. A. Glycosylation in the Era of Cancer-Targeted Therapy: Where Are We Heading? *Cancer Cell* **36**, 6-16, (2019).

78 Prendergast, J. M., Galvao da Silva, A. P., Eavarone, D. A., Ghaderi, D., Zhang, M., Brady, D., Wicks, J., DeSander, J., Behrens, J. & Rueda, B. R. Novel anti-Sialyl-Tn monoclonal antibodies and antibody-drug conjugates demonstrate tumor specificity and anti-tumor activity. *MAbs* **9**, 615-627, (2017).

79 Liu, S. D., Chalouni, C., Young, J. C., Junttila, T. T., Sliwkowski, M. X. & Lowe, J. B. Afucosylated antibodies increase activation of FcgammaRIIIa-dependent signaling components to intensify processes promoting ADCC. *Cancer Immunol Res* **3**, 173-183, (2015).

80 Loureiro, L. R., Carrascal, M. A., Barbas, A., Ramalho, J. S., Novo, C., Delannoy, P. & Videira, P. A. Challenges in Antibody Development against Tn and Sialyl-Tn Antigens. *Biomolecules* **5**, 1783-1809, (2015).

81 Seo, Y., Ishii, Y., Ochiai, H., Fukuda, K., Akimoto, S., Hayashida, T., Okabayashi, K., Tsuruta, M., Hasegawa, H. & Kitagawa, Y. Cetuximab-mediated ADCC activity

is correlated with the cell surface expression level of EGFR but not with the KRAS/BRAF mutational status in colorectal cancer. *Oncol Rep* **31**, 2115-2122, (2014).

82 Duarte, H. O., Balmana, M., Mereiter, S., Osorio, H., Gomes, J. & Reis, C. A. Gastric Cancer Cell Glycosylation as a Modulator of the ErbB2 Oncogenic Receptor. *Int J Mol Sci* **18**, (2017).

83 Benmebarek, M. R., Karches, C. H., Cadilha, B. L., Lesch, S., Endres, S. & Kobold, S. Killing Mechanisms of Chimeric Antigen Receptor (CAR) T Cells. *Int J Mol Sci* **20**, (2019).

84 Hombach, A., Heuser, C., Sircar, R., Tillmann, T., Diehl, V., Kruis, W., Pohl, C. & Abken, H. T cell targeting of TAG72+ tumor cells by a chimeric receptor with antibody-like specificity for a carbohydrate epitope. *Gastroenterology* **113**, 1163-1170, (1997).

85 Hege, K. M., Bergsland, E. K., Fisher, G. A., Nemunaitis, J. J., Warren, R. S., McArthur, J. G., Lin, A. A., Schlom, J., June, C. H. & Sherwin, S. A. Safety, tumor trafficking and immunogenicity of chimeric antigen receptor (CAR)-T cells specific for TAG-72 in colorectal cancer. *J Immunother Cancer* **5**, 22, (2017).

86 Kim, S. J. & Hong, H. J. Guided selection of human antibody light chains against TAG-72 using a phage display chain shuffling approach. *J Microbiol* **45**, 572-577, (2007).

87 Muraro, R., Kuroki, M., Wunderlich, D., Poole, D. J., Colcher, D., Thor, A., Greiner, J. W., Simpson, J. F., Molinolo, A., Noguchi, P. & et al. Generation and characterization of B72.3 second generation monoclonal antibodies reactive with the tumor-associated glycoprotein 72 antigen. *Cancer Res* **48**, 4588-4596, (1988).

88 Loureiro, L. R., Sousa, D. P., Ferreira, D., Chai, W., Lima, L., Pereira, C., Lopes, C. B., Correia, V. G., Silva, L. M., Li, C., Santos, L. L., Ferreira, J. A., Barbas, A., Palma, A. S., Novo, C. & Videira, P. A. Novel monoclonal antibody L2A5 specifically targeting sialyl-Tn and short glycans terminated by alpha-2-6 sialic acids. *Sci Rep* **8**, 12196, (2018).

89 Loureiro, L. R., Feldmann, A., Bergmann, R., Koristka, S., Berndt, N., Arndt, C., Pietzsch, J., Novo, C., Videira, P. & Bachmann, M. Development of a novel target module redirecting UniCAR T cells to Sialyl Tn-expressing tumor cells. *Blood Cancer J* **8**, 81, (2018).

90 Itzkowitz, S. H., Young, E., Dubois, D., Harpaz, N., Bodian, C., Chen, A. & Sachar, D. B. Sialosyl-Tn antigen is prevalent and precedes dysplasia in ulcerative colitis: a retrospective case-control study. *Gastroenterology* **110**, 694-704, (1996).

91 O'Boyle, K. P., Zamore, R., Adluri, S., Cohen, A., Kemeny, N., Welt, S., Lloyd, K. O., Oettgen, H. F., Old, L. J. & Livingston, P. O. Immunization of colorectal cancer patients with modified ovine submaxillary gland mucin and adjuvants induces IgM and IgG antibodies to sialylated Tn. *Cancer Res* **52**, 5663-5667, (1992).

92 O'Cearbhaill, R. E., Ragupathi, G., Zhu, J., Wan, Q., Mironov, S., Yang, G., Spassova, M. K., Iasonos, A., Kravetz, S., Ouerfelli, O., Spriggs, D. R., Danishefsky, S. J. & Sabbatini, P. J. A Phase I Study of Unimolecular Pentavalent (Globo-H-GM2-sTn-TF-Tn) Immunization of Patients with Epithelial Ovarian, Fallopian Tube, or Peritoneal Cancer in First Remission. *Cancers (Basel)* **8**, (2016).

93 Miles, D., Roche, H., Martin, M., Perren, T. J., Cameron, D. A., Glaspy, J., Dodwell, D., Parker, J., Mayordomo, J., Tres, A., Murray, J. L., Ibrahim, N. K. & Theratope Study, G. Phase III multicenter clinical trial of the sialyl-TN (STn)-keyhole limpet

hemocyanin (KLH) vaccine for metastatic breast cancer. *Oncologist* **16**, 1092-1100, (2011).

94 Ibrahim, N. K., Murray, J. L., Zhou, D., Mittendorf, E. A., Sample, D., Tautchin, M. & Miles, D. Survival Advantage in Patients with Metastatic Breast Cancer Receiving Endocrine Therapy plus Sialyl Tn-KLH Vaccine: Post Hoc Analysis of a Large Randomized Trial. *J Cancer* **4**, 577-584, (2013).

95 Zeichner, S. B. The Failed Theratope Vaccine: 10 Years Later. *The Journal of the American Osteopathic Association* **112**, 482-483, (2012).

96 Pedersen, J. W., Blixt, O., Bennett, E. P., Tarp, M. A., Dar, I., Mandel, U., Poulsen, S. S., Pedersen, A. E., Rasmussen, S., Jess, P., Clausen, H. & Wandall, H. H. Seromic profiling of colorectal cancer patients with novel glycopeptide microarray. *Int J Cancer* **128**, 1860-1871, (2011).

97 Rughetti, A., Pellicciotta, I., Biffoni, M., Backstrom, M., Link, T., Bennet, E. P., Clausen, H., Noll, T., Hansson, G. C., Burchell, J. M., Frati, L., Taylor-Papadimitriou, J. & Nuti, M. Recombinant tumor-associated MUC1 glycoprotein impairs the differentiation and function of dendritic cells. *J Immunol* **174**, 7764-7772, (2005).

98 Ninkovic, T. & Hanisch, F. G. O-glycosylated human MUC1 repeats are processed in vitro by immunoproteasomes. *J Immunol* **179**, 2380-2388, (2007).

99 Gaidzik, N., Westerlind, U. & Kunz, H. The development of synthetic antitumour vaccines from mucin glycopeptide antigens. *Chem Soc Rev* **42**, 4421-4442, (2013).

100 Abdel-Aal, A. B., Lakshminarayanan, V., Thompson, P., Supekar, N., Bradley, J. M., Wolfert, M. A., Cohen, P. A., Gendler, S. J. & Boons, G. J. Immune and anticancer responses elicited by fully synthetic aberrantly glycosylated MUC1 tripartite vaccines modified by a TLR2 or TLR9 agonist. *Chembiochem* **15**, 1508-1513, (2014).

101 Song, C., Zheng, X. J., Liu, C. C., Zhou, Y. & Ye, X. S. A cancer vaccine based on fluorine-modified sialyl-Tn induces robust immune responses in a murine model. *Oncotarget* **8**, 47330-47343, (2017).

102 Taylor-Papadimitriou, J., Burchell, J. M., Graham, R. & Beatson, R. Latest developments in MUC1 immunotherapy. *Biochem Soc Trans* **46**, 659-668, (2018).

103 Lakshminarayanan, V., Supekar, N. T., Wei, J., McCurry, D. B., Dueck, A. C., Kosiorek, H. E., Trivedi, P. P., Bradley, J. M., Madsen, C. S., Pathangey, L. B., Hoelzinger, D. B., Wolfert, M. A., Boons, G. J., Cohen, P. A. & Gendler, S. J. MUC1 Vaccines, Comprised of Glycosylated or Non-Glycosylated Peptides or Tumor-Derived MUC1, Can Circumvent Immunoediting to Control Tumor Growth in MUC1 Transgenic Mice. *PLoS One* **11**, e0145920, (2016).

104 Reis, C. A., David, L., Seixas, M., Burchell, J. & Sobrinho-Simoes, M. Expression of fully and under-glycosylated forms of MUC1 mucin in gastric carcinoma. *Int J Cancer* **79**, 402-410, (1998).

105 Wang, Y., Liao, X., Ye, Q. & Huang, L. Clinic implication of MUC1 O-glycosylation and C1GALT1 in esophagus squamous cell carcinoma. *Sci China Life Sci* **61**, 1389-1395, (2018).

106 Stergiou, N., Gaidzik, N., Heimes, A. S., Dietzen, S., Besenius, P., Jakel, J., Brenner, W., Schmidt, M., Kunz, H. & Schmitt, E. Reduced Breast Tumor Growth after Immunization with a Tumor-Restricted MUC1 Glycopeptide Conjugated to Tetanus Toxoid. *Cancer Immunol Res* **7**, 113-122, (2019).

107 Hossain, M. K. & Wall, K. A. Immunological Evaluation of Recent MUC1 Glycopeptide Cancer Vaccines. *Vaccines (Basel)* **4**, (2016).
108 Fontana, F., Liu, D., Hirvonen, J. & Santos, H. A. Delivery of therapeutics with nanoparticles: what's new in cancer immunotherapy? *Wiley Interdisciplinary Reviews: Nanomedicine and Nanobiotechnology* **9**, 1-26, (2017).
109 Joshi, M. D., Unger, W. J., Storm, G., Van Kooyk, Y. & Mastrobattista, E. Targeting tumor antigens to dendritic cells using particulate carriers. *Journal of Controlled Release* **161**, 25-37, (2012).
110 Krishnamachari, Y., Geary, S. M., Lemke, C. D. & Salem, A. K. Nanoparticle delivery systems in cancer vaccines. *Pharmaceutical Research* **28**, 215-236, (2011).
111 Buskas, T., Ingale, S. & Boons, G. J. Towards a fully synthetic carbohydrate-based anticancer vaccine: synthesis and immunological evaluation of a lipidated glycopeptide containing the tumor-associated tn antigen. *Angew Chem Int Ed Engl* **44**, 5985-5988, (2005).
112 Skwarczynski, M. & Toth, I. Peptide-based synthetic vaccines. *Chem Sci* **7**, 842-854, (2016).
113 Leleux, J. & Roy, K. Micro and nanoparticle-based delivery systems for vaccine immunotherapy: an immunological and materials perspective. *Adv Healthc Mater* **2**, 72-94, (2013).
114 Demento, S. L., Cui, W., Criscione, J. M., Stern, E., Tulipan, J., Kaech, S. M. & Fahmy, T. M. Role of sustained antigen release from nanoparticle vaccines in shaping the T cell memory phenotype. *Biomaterials* **33**, 4957-4964, (2012).
115 Elamanchili, P., Lutsiak, C. M. E., Hamdy, S., Diwan, M. & Samuel, J. "Pathogen-mimicking" nanoparticles for vaccine delivery to dendritic cells. *Journal of Immunotherapy* **30**, 378-395, (2007).
116 Cruz, L. J., Rosalia, R. A., Kleinovink, J. W., Rueda, F., Lowik, C. W. & Ossendorp, F. Targeting nanoparticles to CD40, DEC-205 or CD11c molecules on dendritic cells for efficient CD8(+) T cell response: a comparative study. *J Control Release* **192**, 209-218, (2014).
117 Zwaveling, S., Ferreira Mota, S. C., Nouta, J., Johnson, M., Lipford, G. B., Offringa, R., van der Burg, S. H. & Melief, C. J. Established human papillomavirus type 16-expressing tumors are effectively eradicated following vaccination with long peptides. *J Immunol* **169**, 350-358, (2002).
118 Pavot, V., Berthet, M., Rességuier, J., Legaz, S., Gilbert, S. C., Paul, S. & Verrier, B. Poly (lactic acid) and poly (lactic- co -glycolic acid) particles as versatile carrier platforms for vaccine delivery. *Nanomedicine* **9**, 2703-2718, (2014).
119 Silva, A. L., Soema, P. C., Slütter, B., Ossendorp, F. & Jiskoot, W. PLGA particulate delivery systems for subunit vaccines: Linking particle properties to immunogenicity. *Human Vaccines and Immunotherapeutics* **12**, 1056-1069, (2016).
120 Marciani, D. J. Vaccine adjuvants: Role and mechanisms of action in vaccine immunogenicity. *Drug Discovery Today* **8**, 934-943, (2003).
121 Petrovsky, N. & Aguilar, J. C. Vaccine adjuvants: Current state and future trends. *Immunology and Cell Biology* **82**, 488-496, (2004).
122 Dubensky, T. W. & Reed, S. G. Adjuvants for cancer vaccines. *Seminars in Immunology* **22**, 155-161, (2010).
123 Saxena, M. & Bhardwaj, N. Turbocharging vaccines: emerging adjuvants for dendritic cell based therapeutic cancer vaccines. *Current Opinion in Immunology* **47**, 35-43, (2017).

124 Yang, R., Xu, J., Xu, L., Sun, X., Chen, Q., Zhao, Y., Peng, R. & Liu, Z. Cancer Cell Membrane-Coated Adjuvant Nanoparticles with Mannose Modification for Effective Anticancer Vaccination. *ACS Nano* **12**, 5121-5129, (2018).
125 Guo, Y., Wang, D., Song, Q., Wu, T., Zhuang, X., Bao, Y., Kong, M., Qi, Y., Tan, S. & Zhang, Z. Erythrocyte Membrane-Enveloped Polymeric Nanoparticles as Nanovaccine for Induction of Antitumor Immunity against Melanoma. *ACS Nano* **9**, 6918-6933, (2015).
126 Kim, H., Niu, L., Larson, P., Kucaba, T. A., Murphy, K. A., James, B. R., Ferguson, D. M., Griffith, T. S. & Panyam, J. Polymeric nanoparticles encapsulating novel TLR7/8 agonists as immunostimulatory adjuvants for enhanced cancer immunotherapy. *Biomaterials* **164**, 38-53, (2018).
127 Nicolete, R., dos Santos, D. F. & Faccioli, L. H. The uptake of PLGA micro or nanoparticles by macrophages provokes distinct in vitro inflammatory response. *Int Immunopharmacol* **11**, 1557-1563, (2011).
128 Lee, S. Y. & Cho, H. J. Dopamine-conjugated poly(lactic-co-glycolic acid) nanoparticles for protein delivery to macrophages. *J Colloid Interface Sci* **490**, 391-400, (2017).
129 Hu, G., Guo, M., Xu, J., Wu, F., Fan, J., Huang, Q., Yang, G., Lv, Z., Wang, X. & Jin, Y. Nanoparticles Targeting Macrophages as Potential Clinical Therapeutic Agents Against Cancer and Inflammation. *Frontiers in Immunology* **10**, (2019).

CHAPTER II

Aims and Scopes

2. Aims and Scopes

Cancer management has experienced significant advances in recent years with the introduction of targeted therapies and immune check point inhibitors immunotherapy. Moreover, cancer vaccines based on peptide neoantigens, resulting from genetic and epigenetic alterations, have been gaining momentum. So far, several preclinical studies and clinical trials have demonstrated its capacity to elicit effective immune responses against cancer cells with limited off-target effects. Cancer vaccines also have the capability to elicit protective immunological memory against recurrences, which remain a critical aspect in cancer management. More recently, cancer vaccines are being tested in combination with immune checkpoint inhibitors, with encouraging results. However, the low mutational burden of many primary lesions and metastasis has constituted a major challenge for vaccine generalization to different tumours, reinforcing the need to explore alternative antigens.

In this context, it is well known that cancer cells experience significant glycoproteome remodelling, often driven by the overexpression of short-chain *O*-glycans. This may result in unique molecular fingerprints at the cell-surface, which are not reflected by healthy tissues, holding tremendous potential for precise cancer targeting. Moreover, short-chain *O*-glycans are ubiquitous drivers of important oncogenic features such as sustained proliferation, migration and invasion. Not surprisingly, short-chain *O*-glycans and cancer-associated glycoproteins carrying abnormal glycosylation patterns are frequently associated with unfavourable outcomes in most solid tumours. The downside to the tremendous potential of cancer glycoepitopes resides in their immunosuppressive or poorly immunogenic nature. In fact, short-chain *O*-glycans such as the Tn, sialyl-Tn, T and sialylated T antigens are key regulators of immunological homeostasis. Furthermore, they are part of key mechanisms exploited by cancer cells to evade immune responses. These include the interaction with lectins at the surface of antigen presenting cells (APCs), ultimately leading to immune suppressive signals. This has frustrated the establishment of effective glycan-based vaccines exploiting conventional immunogenic vehicles. Therefore, the development of effective strategies to bypass or increase the low immunogenicity of many glycoepitopes will be critical for the establishment of more effective anti-cancer vaccines capable of addressing different types of solid tumours.

Nanotechnology appears as a promising strategy to help overtaking this limitation by offering a nanoscale particle size, which facilitates uptake by phagocytic cells, the gut-

associated lymphoid tissue and the mucosa-associated lymphoid tissue, leading to efficient antigen recognition and presentation. Namely, PLGA has emerged as an FDA-approved biopolymer of election towards this end, given its ability to shield antigens from degradation and clearance, provide sustained release of encapsulated molecules, the possibility of co-encapsulation of antigens and imunemodulators and its increased uptake and cross-presentation by APCs through mimicking of size and shape of invading pathogens. Based on these considerations, the present document aims to set the molecular bases and cell models for the future development of innovative glycan-based cancer nanovaccines. This includes the establishment of easy methods for glycoepitope synthesis, the development of immunogenic protein glycoconjugates and glyconanoconstructs for potential vaccine applications. Envisaging these goals, cancer associated MUC16 glycoforms, expressed by many solid tumours and associated with cancer malignancy, are exploited as model glycoepitopes. Lastly, a glycoengineered cell model expressing the cancer-associated Tn glycan at the cell-surface, thus mimicking more aggressive tumours, was developed. This work also devotes to exploiting the functional implications of this antigen in relevant cancer cell features (proliferation, migration, invasion) as well as immune modulation. The goal is to provide a well characterized model capable of supporting the development of innovative cancer therapies, with emphasis on cancer vaccines. Facing this objective, we have elected the T24 urothelial cell line isolated from a solid tumour typically expressing the Tn antigen at advanced stages.

As such, this work comprehends the following specific objectives:

I. Chemoenzymatic synthesis of a library of cancer-associated MUC16 glycoforms (MUC16-Tn, MUC16-STn, MUC16-S3T, MUC16-S6T) and potentially immunogenic glycopeptide-protein glycoconjugates to support vaccine development;
II. Synthesis and physicochemical characterization of MUC16-Tn PLGA vehicles for potential vaccine applications;
III. Establishment of CRISPR/Cas9 glycoengineered cancer cells displaying homogenous Tn antigen expression at the cell surface for future development of innovative targeted therapeutics and immunotherapy.

These objectives are addressed in chapters III, IV and V of this dissertation. The chapters follow a research paper format, including an abstract, introduction, materials and methods, results, discussion and conclusions. Chapter VI provides concluding remarks and future perspectives.

CHAPTER III

Single-pot enzymatic synthesis of cancer-associated MUC16 O-glycopeptides protein glycoconjugates for bioanalytical and biomedical applications

Single-pot enzymatic synthesis of cancer-associated MUC16 *O*-glycopeptides, protein glycoconjugates for bioanalytical and biomedical applications

Rui Freitas[a,b,*], Rita Azevedo[a,c,*], Elisabete Fernandes[a,c,d,*], Marta Relvas-Santos[a], Andreia Peixoto[a,c,d], Dylan Ferreira[a], Lúcio Lara Santos[a,c,e,f,g], André M. N. Silva[g,h], José Alexandre Ferreira[a,g,i]

[a]Experimental Pathology and Therapeutics Group, Portuguese Institute of Oncology, 4200-162 Porto, Portugal; [b]Department of Chemistry, QOPNA&REQIMTE-LAQV, University of Aveiro, 3810-193 Aveiro, Portugal; [c]Institute of Biomedical Sciences Abel Salazar, University of Porto, 4050-013 Porto, Portugal; [d]Instituto de Investigação e Inovação em Saúde, Universidade do Porto, 4200-135 Porto, Portugal; [e]Health School of University Fernando Pessoa, 4249-004 Porto, Portugal; [f]Department of Surgical Oncology, Portuguese Institute of Oncology, 4200-072 Porto, Portugal; [g]GlycoMatters Biotech, Portuguese Institute of Oncology of Porto, 4200-162 Porto, Portugal; [h]UCIBIO-REQUIMTE/Department of Chemistry and Biochemistry, Faculty of Sciences, 4169-007 University of Porto, Portugal; [i]Porto Comprehensive Cancer Center (P.ccc), 4200-162 Porto Porto, Portugal.

*These authors have equally contributed to the work

Corresponding author:

José Alexandre Ferreira (jose.a.ferreira@ipoporto.min-saude.pt)

Experimental Pathology and Therapeutics Group, Research Centre, Portuguese Oncology Institute of Porto, R. Dr. António Bernardino de Almeida 62, 4200-162 Porto, Portugal; Tel. +351 225084000 (ext. 5111).

Running head: Synthesis of glycopeptides and glycoconjugates

[¥] The chapter results from a collaboration between the first authors. As such, most of its content is also part of the PhD thesis by Rita Azevedo, entitled "Development of Monoclonal antibodies for bladder cancer based on glycobiomarkers: Identification of relevant glycoantigens and synthesis methodologies thereof" and defended in July 2019 at ICBAS-UP

3.1 Abstract

Cancer cells overexpress and often express *de novo* glycoproteins modified with short-chain sialylated *O*-glycans such as the sialyl-Tn (STn), sialyl-3-T (S3T) and sialyl-6-T (S6T) antigens. Such events mirror profound deregulations in protein glycosylation pathways, creating unique molecular fingerprints holding potential for antibody development and carbohydrate-based vaccines. However, the generation of glycopeptide libraries composed by pure and structurally defined standards remains a critical step for carbohydrate metrology and glycobiomarker identification. Moreover, it has hampered glycoepitope determination for therapeutic development. Those antigens can be used in immunotherapy as a promising alternative to conventional treatments. However, those antigens are uncapable of proper immune system stimulation. This work explores a simple and fast multi-enzymatic single-pot method for the generation of a wide array of STn, S3T and S6T glycopeptides. Emphasis was set on glycopeptides derived from MUC16 variable tandem repeats, given the clinical relevance of this protein in bladder, ovarian and other solid tumours. Moreover, it explores combinations of reverse phase chromatography with TiO_2 enrichment to isolate different sialoglycopeptides, setting the basis for carbohydrate metrology. Finally, it describes the conjugation of multiple glycopeptides with the immunogenic molecule Keyhole Limpet Hemocyanin (KLH) foreseeing multivalent glycoepitopes that may pave the way for immunotherapy.

3.2 Introduction

Glycan-based therapeutics face some drawbacks as lack of pure and structurally well-defined carbohydrates and glycoconjugates to develop analytical methods and therapeutics applications[1,2]. Chemical and enzymatic methods have been developed for oligosaccharide synthesis in the development of many applications such as vaccines and antibodies[3,4]. However, chemical synthesis could be hard to perform due to multiple steps of protection, deprotection and purification, being expensive and time consuming[4]. The need for more efficient approaches to oligosaccharides and glycoconjugates lead to the development of chemo-enzymatic methods in which synthetic oligosaccharides and/or peptides act as substrates for glycosyltransferases to give rise to more complex glycans and glycoconjugates, allowing the preparation of complex glycopeptides and the establishment of glycoconjugates libraries[5,6]. Some advantages of employing enzymes in biosynthetic processed include high regio or stereospecificity with no need of protection and deprotection reactions to obtain chemo selectivity. As such, enzymatic methods have been successfully applied to the biosynthesis of both *O*- and *N*-glycosides that constitute the main post-translational modification of membrane glycoproteins[7,8].

The exploitation of chemoenzymatic synthesis of immunogenic glycopeptides and glycoconjugates to develop antibodies and carbohydrate-based vaccine prototypes has significantly increased in recent years[9,10]. The possibility of acquiring highly pure synthetic peptides at accessible prices to use as scaffolds for enzymatic glycosylation contributed for this interest[11]. In addition, the increasing availability of a wide array of recombinant glycosyltransferases with distinct substrate specificities and well-defined kinetic properties enables a highly controlled glycopeptide synthesis[12,13]. However, ensuring the desired glycosylation pattern of *O*-GalNAc glycopeptides remains particularly challenging. This requires the precision setting of the initial glycosylation step, consisting in the covalent link of a GalNAc residue to serine or threonine amino acids, catalysed by polypeptide *N*-acetylgalactosamine transferases (ppGalNAcTs) in the presence of UDP-GalNAc[14,15]. Many ppGalNAcTs show both complementary and overlapping activities, acting in a coordinated manner defining the *O*-GalNAc glycosites on a given protein. Moreover, most ppGalNAcTs target multiple glycosites in a given peptide chain producing a wide array of glycopatterns, which poses a significant challenge for producing uniform products. Notably, bioinformatics tools such as ISOGlyP and NetOGlyc have been developed to assist the election of ppGalNAcTs better suited for generating glycopeptides of interest as well as predicting the diversity and abundance of potential glycosites[16,17]. After the first glycosylation step, *O*-

GalNAc glycans can be further elongated by several glycosyltransferases to produce glycans ultimately presenting sialylated terminal structures. As such, these methods have been successfully applied to the synthesis of sialyl-Tn (STn)- and sialyl-3-T (S3T)-MUC1 glycopeptides commonly overexpressed by cancer cells[18-20]. In addition, many studies explored the coupling of these glycopeptides with immunogenic proteins such as the keyhole limpet hemocyanin (KLH), foreseeing the development of targeted therapeutics and cancer vaccines[21-23]. Envisaging similar goals, this work describes the enzymatic synthesis of STn-, S3T- and S6T-MUC16 glycopeptides using synthetic MUC16 variable tandem repeat (VTR) peptides as starting point. It further exploits purification methods to tackle the wide array of glycosides synthetized. Finally, it focuses on developing multivalent MUC16-Tn glycopeptide-KLH conjugates, envisaging novel therapeutics for aggressive ovarian, bladder and other solid tumours known to overexpress abnormally glycosylated MUC16 glycoforms. It is anticipated that the synthesis and purification methods developed herein may be translatable to other targets, ultimately providing the necessary epitopes to support carbohydrate-based theragnostic applications for cancer.

3.3. Materials and Methods

3.3.1 Bioinformatics-assisted selection of MUC16-glycopeptide epitopes

The MUC16 protein sequence from NCBI database (NP_078966.2) presents 60+ tandem repeats (TR) of approximately 156 amino acids (aa) each. Accordingly, antigen synthesis was based on these highly repeated and *O*-glycosylated epitopes in MUC16. Specifically, the 156 aa repeats were analysed using the *O*-glycosylation site determination bioinformatics tool NetOGlyc, following the selection of the 20 aa sequence within the TR comprising more *O*-glycosylation sites. Subsequently, the elected sequence was run using the ISOGlyP (Isoform Specific O-Glycosylation Prediction)[16,17] bioinformatics tool to determine the fitness of human polypeptide *N*-acetylgalactosaminyltransferases (EC 2.4.1.41) to *O*-glycosylate this particular sequence of aa. Hence, GalNAc-T1 was designated as the GalNAc-transferase isoform with higher probability of successful activity.

3.3.2 Enzymatic synthesis of MUC16-glycopeptide epitopes

A MUC16 20-mer peptide (VDVGTSGTPSSSPSPTTAGP) (with a cysteine tag) from the TR region was purchased from GenScript Biotech (Netherlands). Synthesis of glycopeptides carrying the Tn-epitope (GalNAcα-O-Ser/Thr) was performed in 100 µL reaction mixtures containing glycosylation buffer (125 mM Cacodylate, 50 mM MnCl2, pH

7.4; Sigma-Aldrich, MO, USA), 0.5 mM UDP-GalNAc (Sigma-Aldrich), 50 μg of MUC16 20-mer peptide and 0.025 μg GalNAc-T1 (R&D Systems, MN, USA). Tn-epitope sialylation, rendering STn-peptides, was performed through the overnight incubation at 37ºC of the Tn-peptides in glycosylation buffer, 0.5 mM CMP-NeuAc (Sigma-Aldrich) and 0.020 μg ST6GalNAc-I (R&D Systems), a human α-*N*-acetylgalactosaminide α-2,6-sialyltransferase (EC 2.4.99.3). Synthesis of glycopeptides carrying the T epitope was performed in 100 μL reaction mixtures containing the Tn-peptides in glycosylation buffer, 0.5 mM UDP-Gal, 0.015 μg C1GalT1/C1GalT1C, a *N*-acetylgalactosaminide β-1,3-galactosyltransferase (EC 2.4.1.122) and its chaperone. T epitope sialylation, rendering S6T-peptides, was performed by overnight incubation at 37ºC of T-peptides in glycosylation buffer, 0.5 mM CMP-NeuAc (Sigma-Aldrich) and 0.024 μg ST6GalNAc-II (R&D Systems), an α-*N*-acetylgalactosaminide alpha-2,6-sialyltransferase (EC 2.4.99.3) preferentially acting upon T antigens over Tn epitopes[24,25]. S3T-peptides were synthetized following the same strategy but in the presence of 0.025 μg ST3Gal-I, a human β-galactoside α-2,3-sialyltransferase (EC 2.4.99.4). All MUC16 glycopeptides were purified using the High-Select™ TiO_2 Phosphopeptide Enrichment Kit (ThermoFisher Scientific), according to the manufacturer instructions.

3.3.3 BSA-MUC16-STn and KLH-MUC16-Tn glycoconjugates

Cysteine-tagged MUC16-STn and MUC16-Tn glycopeptides were conjugated to bovine serum albumin (BSA, Sigma-Aldrich) and keyhole limpet hemocyanin (KLH, Sigma-Aldrich)[22] respectively, to render immunogenic glycoepitopes. Briefly, 0.01mg/μL KLH or BSA in 0.01 M phosphate buffer (pH 7, Sigma-Aldrich) were incubated for 30 min at room temperature under agitation with 0.015mg/μL 3-maleimidobenzoic acid N-hydroxysuccinimide ester (MBS, Sigma-Aldrich) in dimethylformamide (DMF, Sigma-Aldrich). Posteriorly, KLH/MBS and BSA/MBS solutions were passed through a PD-10 desalting column (Sigma-Aldrich) conditioned with 0.05 M phosphate buffer (pH 6). Desalted KLH/MBS and BSA/MBS solutions were incubated with 10 μg of glycopeptides in 25 μL DMF pH 7.0 and incubated at 4°C overnight under rotation, following evaporation in a SpeedVac. The products of conjugation with BSA were characterized by SDS-PAGE on 4–20% precast polyacrylamide gels (BIORAD) and stained with Coomassie blue (Sigma-Aldrich). In parallel, the products were analysed by western blot in 0.45 μm nitrocellulose membranes (Amersham). The membranes were blotted for the Tn antigen with biotinylated *Vicia villosa* (VVA) lectin (Vector Laboratories) and vectastain RTU elite ABC reagent

(Vector Laboratories). Membranes subjected to digestion *in situ* with sialidase were analysed in parallel for Tn expression. The products of conjugation with KLH were analysed by dot blot in a 0.45 μm polyvinylidene difluoride membrane (PVDF; ThermoFisher Scientific). The membrane was subsequently blotted for the Tn antigen with biotinylated VVA lectin (Vector Laboratories) and vectastain RTU elite ABC reagent (Vector Laboratories).

3.3.4 nanoLC-LTQ-Orbitrap mass spectrometry

Synthesized glycopeptides were characterized by nanoLC-ESI-MS on a nanoLC system (Dionex, 3000 Ultimate nano-LC) coupled online to an LTQ-Orbitrap XL mass spectrometer (ThermoFisher Scientific) equipped with a nano-electrospray ion source (ThermoFisher Scientific, EASY-Spray source). Eluent A was aqueous formic acid (0.2%) and eluent B was formic acid (0.2%) in acetonitrile. Samples (20 μl) were injected directly into a trapping column (C18 PepMap 100, 5 μm particle size) and washed with an isocratic flux of 95% eluent A and 5% eluent B at a flow rate of 30 μl/min. After 3 minutes, the flux was redirected to the analytical column (EASY-Spray C18 PepMap, 100 Å, 150 mm × 75μm ID and 3 μm particle size) at a flow rate of 0.3 μl/min. Column temperature was set at 35°C. Peptide separation occurred using a linear gradient of 5–40% eluent B over 90 min., 50–90% eluent B over 5 min and 5 min with 90% eluent B. The mass spectrometer was operated in the positive ion mode, with a spray voltage of 1.9 kV and a transfer capillary temperature of 250°C. Tube lens voltage was set to 120 V. MS survey scans were acquired at an Orbitrap resolution of 60,000 for an m/z range from 300 to 2000. Data were recorded with Xcalibur software version 2.1. Analysis were conducted in triplicates. Reported ions are presented in terms of relative abundance in relation to the total glycopeptides abundance.

3.3.5 MUC16-Tn and MUC16-STn purification for yield determination

MUC16-Tn glycopeptides were purified in an agarose-bound *Vicia Villosa* (VVA; Vector Laboratories) agglutinin column. Briefly, the sample containing MUC16-Tn was loaded on a agarose-bound VVA column and washed 10 times with 200 μL of LAC A + glucose buffer (0.4M glucose in LAC A buffer: 20mM of Tris/HCl pH 7.4, 150mM of NaCl, 1M of Urea, 0.1M of $CaCl_2$, $MgCl_2$, $MnCl_2$ and $ZnCl_2$) followed by 4 times with 200 μL of 50mM NH_4HCO_3 (all reagents were purchased from Sigma-Aldrich). The glycopeptides were then eluted with 3 x 100 μL 3% ammonium bicarbonate (Sigma-Aldrich). Finally, MUC16-Tn glycopeptides were quantified with Pierce™ Quantitative Fluorometric Peptide

Assay Kit (ThermoFisher Scientific). MUC16-Tn yield of synthesis was calculated by the following equation:

Yield of synthesis (%) =

$$1 - \left(\frac{amount\ of inicial\ MUC16 - \ amount\ of\ obtained\ MUC16\ Tn}{amount\ of\ inicial\ MUC16}\right) x\ 100$$

MUC16-STn glycopeptides were purified using the High-Select™ TiO_2 Phosphopeptide Enrichment Kit (ThermoFisher Scientific), according to the manufacturer instructions. MUC16-STn yield of synthesis according to MUC16-Tn amounts was calculated by the following equation:

Yield of synthesis (%) =

$$1 - \left(\frac{amount\ of\ obtained\ MUC16\ Tn - \ amount\ of\ MUC16\ STn\ obtained}{amount\ of\ obtained\ MUC16\ Tn}\right) x\ 100$$

MUC16-STn yield of synthesis according to initial MUC16 amounts was calculated by the following equation:

Yield of synthesis (%) =

$$1 - \left(\frac{amount\ of inicial\ MUC16\ used - \ amount\ of\ obtained\ MUC16\ STn}{amount\ of\ inicial\ MUC16\ used}\right) x\ 100$$

3.4 Results and Discussion

MUC16 glycoforms yielding short-chain sialylated *O*-glycans are frequently expressed by more aggressive bladder tumours and, due to its cell-surface nature, hold potential for targeted therapeutics and immunotherapy[26,27]. These glycoforms include the STn antigen, associated with poor prognosis and chemoresistance and, possibly, different forms of sialylated T antigens, namely S3T and S6T. Therefore, this work has been devoted to the establishment of rapid and easy enzymatic synthesis and purification of STn-, S3T- and S6T-MUC16 derived glycopeptides. For proof-of-concept, we have elected a MUC16 20-mer target peptide from the variable tandem repeat region containing approximately 9 potential *O*-glycosylation sites (T5, S6, T8, S10, S11, S12, S14, T16, T17; according to NetOGlyc). ppGalNAcT1 was elected as initiation enzyme to mimic the *O*-glycosites

presented by cancer cells, given its overexpression in more aggressive bladder tumours in relation to the healthy urothelium and association with poor prognosis according to Oncomine and the Human Protein Atlas[28-30]. According to a bioinformatics prediction, ppGalNAcT1 will preferentially target the S12 residue (approximately 40% probability of *O*-glycosylation) and, to much less extent, S10, S14 and T17 (approximately 10%). The probability of obtaining glycopeptides substituted at other positions is lower than 5%. Notably, mixtures of peptides presenting distinct combinations of glycosylation patterns are likely to occur using this strategy. While this effect is desirable foreseeing multivalent vaccines mimicking the structural diversity observed in solid tumours, it raises concerns related with the purity of standards for bioanalytical applications. As such, emphasis was also set on exploring potential purification strategies.

3.4.1 MUC16-Tn and MUC16-STn purification for yield determination

With the objective of determine MUC16-Tn/STn synthesis yields, both glycopeptides species were purified by affinity chromatography. For MUC16-Tn purification agarose-bound VVA was used, while for MUC16-STn a TiO_2 Enrichment Kit was employed. Then, both species were quantified by a Fluorometric Peptide Assay Kit. Glycosylation of MUC16 with GalNAc, generating MUC16-Tn, presented a yield of 22,60%, while the sialylation step yielded 9,52% (according to the initial amount of MUC16). When compared with the amount of MUC16-Tn, MUC16-STn yielded 34,94 (***Figure 3***) .The yields presented herein are lower than others obtained for these kinds of glycosylations of other mucins[31]. These findings may be explained by the use of only one enzyme to perform the GalNac incorporation reaction instead of an enzymatic cocktail which would probably generate more Tn epitopes in potential glycosylation sites. Therefore, the second reaction step will be affected by the number of aa with Tn epitopes, since ST6GalNAc-I will add sialic acid moieties to aa carrying Tn epitopes.

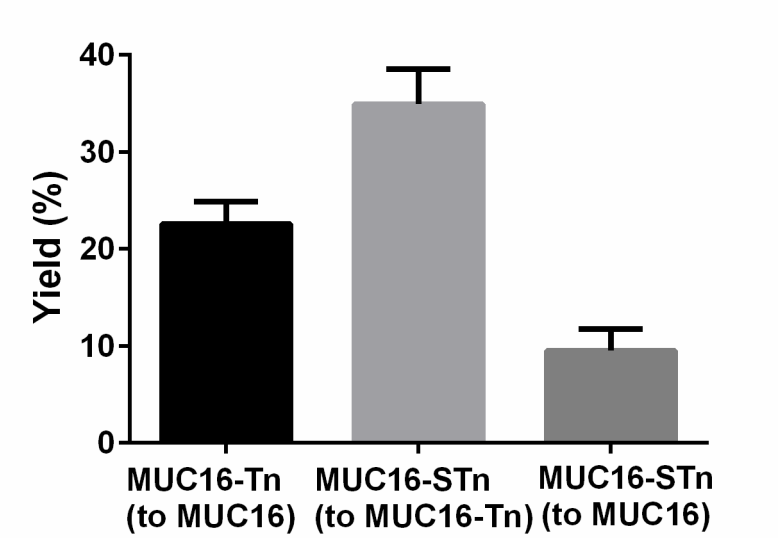

Figure 3. Synthesis yields obtained for each glycoform of MUC16 mer Cys Tag. Determination of yields for MUC16-Tn (total amount of MUC16 as reference) and MUC16-STn (both total amount of MUC16 and MUC16-Tn as reference).

3.4.2 Characterization of MUC16 glycosites density

The initial step in MUC16 *O*-glycosylation concerns the substitution of either Ser or Thr residues with GalNAc, originating the Tn antigen, which is crucial for defining glycosites before downstream *O*-glycans extension and sialylation. The reaction products were subsequently analysed by nanoLC-ESI-MS. According to **Figure 4**, di-glycosylated peptides were predominant in relation to mono-glycosylated forms (43% vs 18% of total glycosylated species), followed by the production of similar amounts of tri- and tetra-glycospecies (11-13%). Lower amounts of MUC16 with up to 8 glycosylation sites could also be detected (1-6%). NanoLC analysis further highlighted acceptable chromatographic separations for neutral species, suggesting it may be used as starting point for isolation/analysis of these molecules. In particular, the used chromatographic conditions enabled a reasonable isolation of single and double glycosylated MUC16-Tn glycopeptides (**Figure 4**). Complementary tandem mass spectrometry studies by Electron-transfer dissociation (ETD) are now required for glycosite annotation envisaging fully characterized products. Notably, only vestigial signs (<1% of total species; data not shown) of unglycosylated MUC16 glycopeptides were observed, suggesting complete glycosylation.

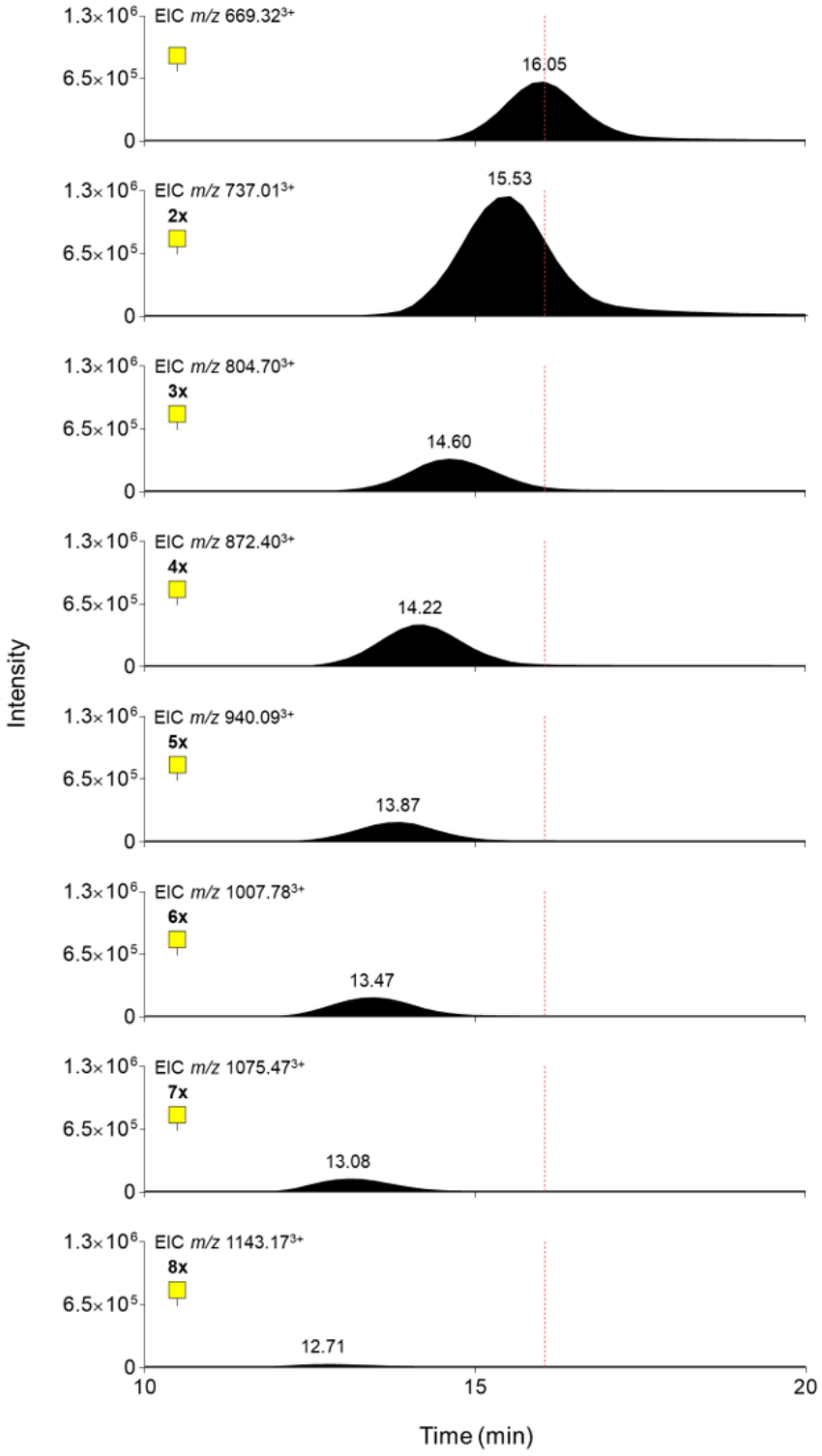

Figure 4. C18 reverse phase nanoLC-ESI-MS profiles for reaction products resulting from the glycosylation of 20 mer MUC16-VRT peptide by ppGalNAc-T1. The main products correspond to the mono- and di-glycosylated peptides, followed by tri- and tetra-glycosylated species. MUC16 glycopeptides with up to eight glycosites could also be detected, however in much lower abundance.

3.4.3 Synthesis and purification of MUC16-STn glycopeptides

Efforts were also devoted to the synthesis of MUC16 carrying the STn antigen using a combination of ppGalNAcT1 and ST6GaLNAc-I in the presence of UDP-GalNAc and CMP-Neu5Ac in a stepwise manner. This led to the formation of a wide array of glycosides presented in Table 1. Twenty-seven species were identified, which can be classified in three groups: i) neutral glycopeptides, presenting the Tn antigen; ii) hybrid glycopeptides, bearing both STn- and Tn antigens; and iii) sialylated glycopeptides, exhibiting STn as sole type of glycosylation. Notably, neutral and hybrid glycopeptides were present in similar proportions and corresponded to almost 90% of the total amount of identified species (**Table 1**). However, both groups were highly heterogeneous (8 neutral species, 16 hybrid species) in comparison to sialylated glycopeptides (3 species). Moreover, experimental conditions favoured the formation of neutral and hybrid glycopeptides with two glycosites (2 Tn, 1Tn/1STn), which correspond to approximately 40% of total glycopeptides. Contrastingly, sialylated glycopeptides mainly presented a single glycosite. The prevalence of single over multiple sialylation in both hybrid and sialo- groups suggests that multiple glycosites may reduce the efficiency of sialylation under the described experimental conditions. It should also be noticed that glycopeptides containing up to 8 glycosylation sites could be identified, close to the maximum predicted by bioinformatics. Nevertheless, approximately 70% of the identified species presented more than two glycosites and were present in very low abundance (<3%). In summary, the most abundant glycopeptides arising from this synthesis corresponded to the neutral precursor MUC16-2Tn and MUC16-Tn/STn. Therefore, TiO_2 chromatography was introduced to improve the isolation of sialylated glycopeptides[32]. TiO_2 enrichment significantly decreased the abundance of neutral glycopeptides, while enriching it for hybrid glycopeptides (now composing 90% of the sample; **Table 1** and **Figure 5**) by reducing the dynamic range of glycopeptides concentrations.

Table 1. Products from the single-pot enzymatic synthesis of MUC16-STn glycopeptides analyzed by C18 reverse phase nanoLC-ESI-MS before and after TiO2 enrichment

O-glycans	Glycopeptides Monoisotopic mass $[M+3H]^{3+}$	Apex Retention time (min)	Without enrichment Relative abundance (%)	Enrichment with TiO_2 Relative abundance (%)
Neutral glycopeptides				
1 Tn	669.32	16.18	7.66	0.00
2 Tn	737.01	15.73	18.28	2.31
3 Tn	804.70	14.83	4.68	0.59
4 Tn	872.40	14.45	5.70	0.54
5 Tn	940.09	14.07	2.48	0.42
6 Tn	1007.78	13.73	2.41	0.48
7 Tn	1075.47	13.53	1.51	0.33
8 Tn	1143.17	12.84	0.24	0.00
Hybrid glycopeptides				
1 Tn + 1 STn	834.04	16.10	20.13	7.16
1 Tn + 2 STn	998.77	15.56	1.11	4.12
1 Tn + 3 STn	1163.49	15.02	0.19	4.96
1 Tn + 5 STn	1492.94	15.21	0.00	0.14
2 Tn + 1 STn	901.73	15.21	6.35	3.31
2 Tn + 2 STn	1066.46	14.83	2.45	11.19
2 Tn + 3 STn	1231.18	14.64	0.10	3.44
2 Tn + 4 STn	1395.91	14.64	0.00	1.83
3 Tn + 1 STn	969.43	14.64	5.93	6.57
3 Tn + 2 STn	1134.15	14.45	0.89	6.30
3 Tn + 3 STn	1298.88	14.25	0.11	5.93
3 Tn + 4 STn	1463.60	14.45	0.00	0.65
4 Tn + 1 STn	1037.12	14.25	2.84	3.83
4 Tn + 2 STn	1201.85	14.07	0.97	10.82
4 Tn + 3 STn	1366.57	14.07	0.04	2.46
5 Tn + 1 STn	1104.81	13.89	2.97	7.03
5 Tn + 2 STn	1269.54	13.73	0.48	5.92
6 Tn + 1 STn	1172.51	13.73	1.45	3.62
6 Tn + 2 STn	1337.23	13.53	0.00	0.28
7 Tn + 1 STn	1240.20	13.34	0.09	0.37
Sialylated glycopeptides				
1 STn	766.35	16.67	9.45	2.11
2 STn	931.07	16.29	1.43	1.67
3 STn	1095.80	15.40	0.06	0.80
4 STn	1260.52	15.40	0.00	0.79

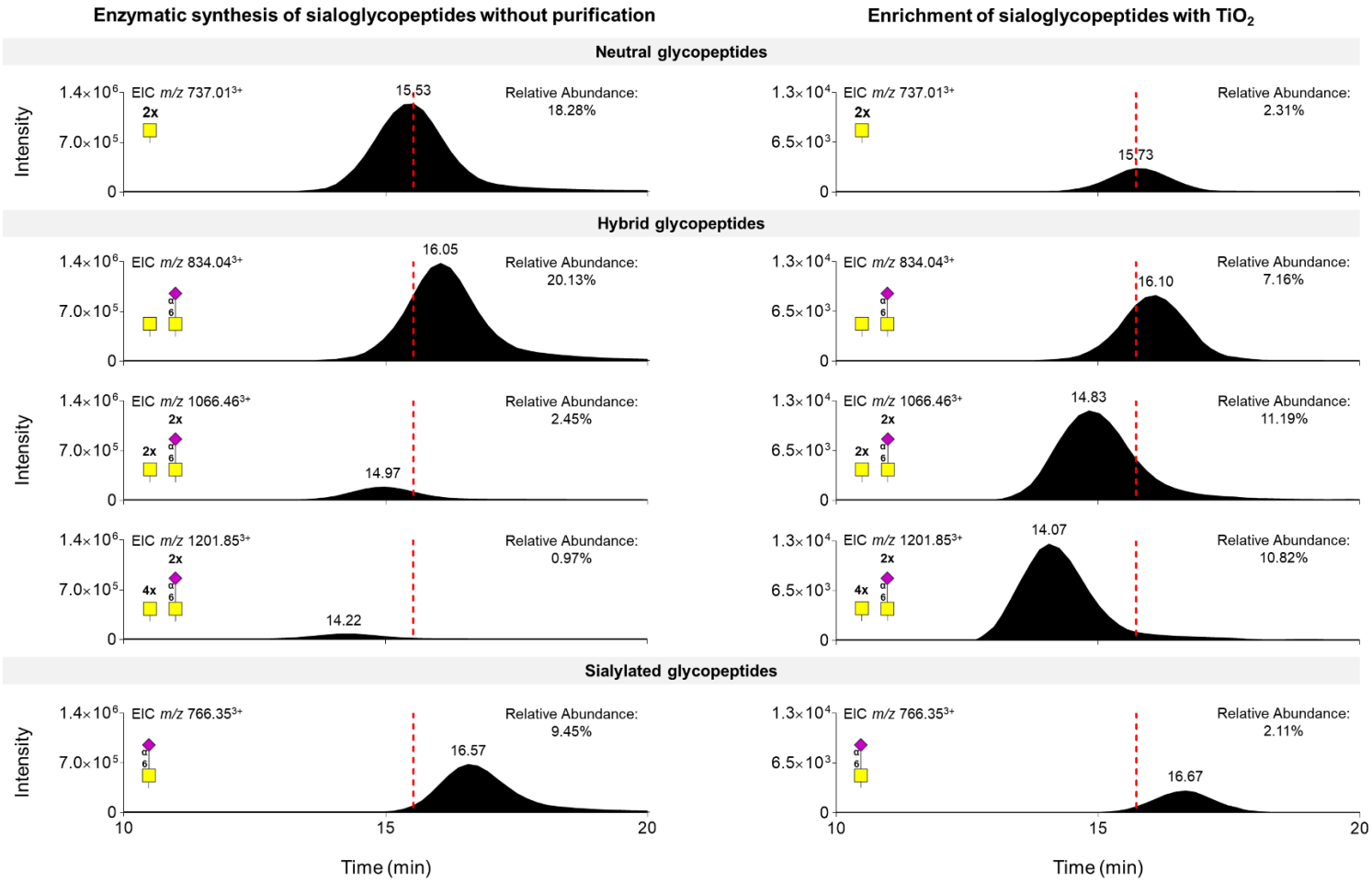

Figure 5. C18 reverse phase nanoLC-ESI-MS profiles for the main reaction products resulting from single-pot enzymatic synthesis of MUC16-STn glycopeptides before and after TiO_2 enrichment. Single-pot enzymatic synthesis of MUC16-STn led to the formation of a wide array of glycoforms, including neutral, hybrid and sialospecies. Most abundant glycopeptides correspond to the neutral precursor MUC16-2Tn and MUC16-Tn/STn. TiO_2 enrichment enabled a significant decrease in the abundance of neutral glycopeptides and increase in di-, tetra and hexa glycopeptides containing either 1 or 2 STn residues.

3.4.4 Synthesis of MUC16-S3T glycopeptides

MUC16-S3T glycopeptides were synthesized using a combination of ppGalNAcT1, C1GalT1, C1GalT1 chaperone C1GalT1C1and ST3Gal-I, in the presence of UDP-GalNAc, UDP-Gal and CMP-Neu5Ac. Table 2 shows that over 65% of the total amount of glycopeptides identified in the final reaction mixture (21 glycopeptides) were solely glycosylated with the Tn antigen, the initial synthesis intermediate. The second most abundant class corresponded to glycopeptides yielding both Tn and ST antigens, whereas a small percentage (4%) corresponded to glycopeptides presenting only the ST antigen. The di-glycosylated peptides were the most abundant, irrespectively of the type of glycosylation, followed by tri and tetra-glycosylated species, in agreement with observations for STn synthesis. Notably, no intermediates carrying the T antigen were observed, strongly suggesting that the rate limiting step of reaction was core 1 synthesis. The elevated number of Tn precursors emphasizes the low reaction efficiency, requiring further optimization in future studies. It is possible that C1GalT1C1 could be inhibited by either products and/or high substrate concentrations, which should be subjected to comprehensive evaluation to improve reaction yields[33]. Nevertheless, C18 reverse phase chromatography enabled the resolution of MUC16-S3T glycopeptides in comparison to other neutral and hybrid species present in the mixture, suggesting it may be a useful purification tool in this context. Finally, we explored the possibility of TiO_2 enrichment to improve purification. This significantly enriched the samples for sialylated glycopeptides, while removing neutral species (**Figure 6**), as previously observed for MUC16-STn synthesis. Namely, it enriched the sample for a wider array of hybrid glycopeptides, with emphasis on glycospecies containing 2 S3T and a Tn glycosite.

Table 2. Products from the single-pot enzymatic synthesis of MUC16-S3T glycopeptides analysed by C18 reverse phase nanoLC-ESI-MS before and after TiO2 enrichment

O-glycans	Glycopeptides Monoisotopic mass $[M+3H]^{3+}$	Apex Retention time (min)	Without Enrichment	Enrichment with TiO_2
			Relative abundance (%)	Relative abundance (%)
Neutral glycopeptides				
1 Tn	669.32	15.95	2.91	0.00
2 Tn	737.01	15.43	20.21	0.00
3 Tn	804.70	14.72	17.63	0.00
4 Tn	872.40	14.19	17.43	0.00
5 Tn	940.09	13.85	5.63	0.00
6 Tn	1007.78	13.46	2.11	0.00
7 Tn	1075.47	13.08	0.45	0.00
1 Tn + 1 T	791.03	15.08	0.07	0.00
2 Tn + 1 T	858.72	14.37	0.03	0.00
3 Tn + 1 T	926.41	14.72	0.03	0.00
4 Tn + 1 T	994.11	13.46	0.01	0.00
Hybrid glycopeptides				
1 Tn + 1 ST	888.06	16.12	14.62	1.55
1 Tn + 2 ST	1106.80	16.12	0.00	20.02
1 Tn + 3 ST	1325.54	16.30	0.00	10.22
1 Tn + 4 ST	1544.29	16.30	0.00	0.36
2 Tn + 1 ST	955.75	15.60	5.01	0.54
2 Tn + 2 ST	1174.49	15.60	0.40	6.29
2 Tn + 3 ST	1393.24	15.41	0.00	1.56
3 Tn + 1 ST	1023.44	14.84	6.60	0.07
3 Tn + 2 ST	1242.19	14.84	0.14	0.48
4 Tn + 1 ST	1091.14	14.37	1.95	0.00
5 Tn + 1 ST	1158.83	13.85	0.51	0.00
6 Tn + 1 ST	1226.52	13.66	0.08	0.00
1 T + 1 ST	942.08	15.60	0.00	1.34
1 T + 2 ST	1160.82	15.76	0.00	3.60
1 T + 3 ST	1379.56	15.76	0.00	0.64
2 T + 1 ST	1063.79	14.84	0.00	0.07
2 T + 2 ST	1282.53	15.04	0.00	0.06
1 Tn + 1 T + 1 ST	1009.77	15.23	0.00	1.97
1 Tn + 1 T + 2 ST	1228.51	15.23	0.00	1.31
1 Tn + 1 T + 3 ST	1447.25	15.04	0.00	0.16
2 Tn + 1 T + 1 ST	1077.46	14.65	0.00	0.19
2 Tn + 1 T + 2 ST	1296.21	14.47	0.00	0.20
Sialylated Glycopeptides				
1 ST	820.37	16.66	0.88	1.30
2 ST	1039.11	16.66	3.32	19.77
3 ST	1257.85	16.83	0.00	26.13
4 ST	1476.59	17.19	0.00	2.13
5 ST	1695.34	17.35	0.00	0.04

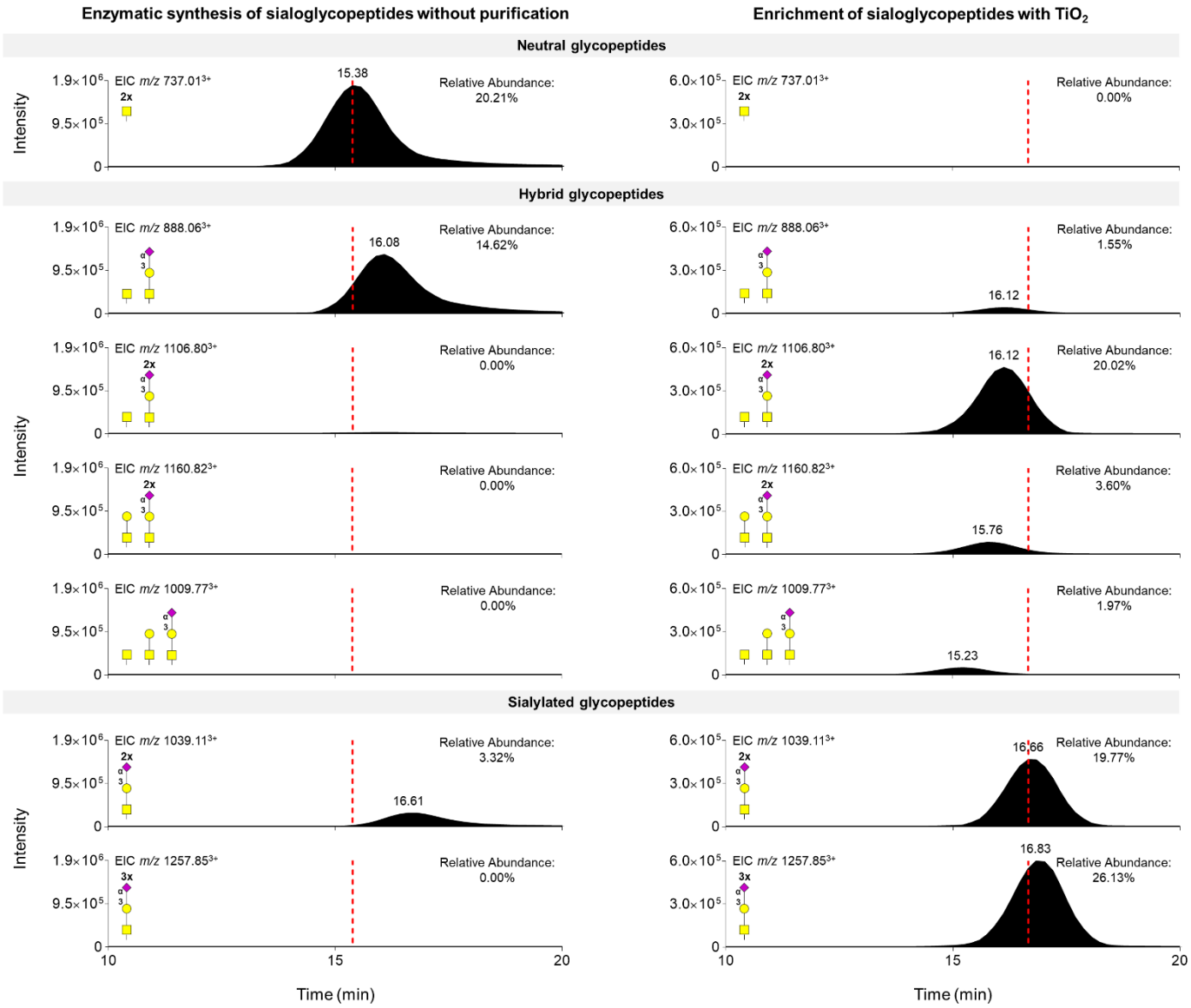

Figure 6. C18 reverse phase nanoLC-ESI-MS profiles for the main reaction products resulting from single-pot enzymatic synthesis of MUC16-S3T glycopeptides before and after TiO_2 enrichment. According to the presented profiles, enzymatic synthesis produces mostly di-glycosylated neutral peptides and mono-sialylated sialoglycopeptides. TiO_2 enrichment enables a significant enrichment for sialylated glycopeptides, while successfully removing neutral species. Moreover, it enriches the sample for a wider array of hybrid glycopeptides, with emphasis for glycospecies containing 2 S3T and a Tn glycosite. Overall, TiO_2 enrichment was significantly effective in the removal of neutral species.

3.4.5 Synthesis and purification of MUC16-S6T glycopeptides

MUC16-S6T glycopeptides were synthesized using a combination of ppGalNAcT1, C1GalT1 and its chaperone C1GalT1C1 as well as ST6GalNAc-II, in the presence of UDP-GalNAc, UDP-Gal and CMP-Neu5Ac. ST6GalNAC-II was elected ever ST6GalNA-I used for STn synthesis based on previous reports supporting its higher affinity for the T antigen. Overall 27 species were identified, 7 of them corresponding to Tn precursors that together comprehended approximately 80% of the total amount of glycopeptides in the sample, as previously observed for S3T. The remaining 20 glycopeptide species derived from different combinations of MUC16 with all other types of glycans (T, STn, S6T) in low or vestigial amounts (≤5%) (Table 3). Such observations suggest the low efficiency of *O*-6 sialylation under the described experimental conditions. Nevertheless, the introduction of TiO_2 purification steps tremendously enriched the sample for hybrid glycopeptides containing the S6T antigen (MUC16-1T/ST, MUC16-1T/2ST, MUC16-2T/ST and MUC16-Tn/T/ST), mostly at the expenses of MUC16-Tn glycopeptides (**Figure 7**, **Table 3**). Future studies should devote to improving the efficacy of T antigen *O*-6 sialylation and the isolation of pure glycospecies.

Table 3. Products from the single-pot enzymatic synthesis of MUC16-S6T glycopeptides analysed by C18 reverse phase nanoLC-ESI-MS before and after TiO_2 enrichment

O-glycans	Glycopeptides Monoisotopic mass $[M+3H]^{3+}$	Apex Retention time (min)	Without enrichment	Enrichment with TiO_2
			Relative abundance (%)	Relative abundance (%)
Neutral glycopeptides				
1 Tn	669.32	16.15	12.46	0.00
2 Tn	737.01	15.40	40.21	0.06
3 Tn	804.70	14.73	11.94	0.00
4 Tn	872.40	14.37	11.40	0.00
5 Tn	940.09	13.81	3.74	0.00
6 Tn	1007.78	13.61	1.70	0.00
7 Tn	1075.47	13.23	0.24	0.00
1 T	723.33	15.40	0.45	0.36
2 T	845.04	14.66	0.04	2.65
3 T	966.76	13.91	0.00	1.55
4 T	1088.47	12.81	0.00	0.18
1 Tn + 1 T	791.03	15.02	4.89	1.00
1 Tn + 2 T	912.74	14.30	0.00	5.23
1 Tn + 3 T	1034.45	13.17	0.00	0.79
1 Tn + 4 T	1156.16	12.64	0.00	0.13
2 Tn + 1 T	858.72	14.30	0.67	0.46
2 Tn + 2 T	980.43	13.72	0.00	0.73
2 Tn + 3 T	1102.14	12.81	0.00	0.16
3 Tn + 1 T	926.41	13.81	1.10	0.00
3 Tn + 2 T	1048.12	13.17	0.00	0.12
4 Tn + 1 T	994.11	13.61	0.19	0.00
5 Tn + 1 T	1061.80	13.23	0.04	0.00
Hybrid glycopeptides				
1 Tn + 1 STn	834.04	16.33	0.71	0.00
3 Tn + 1 STn	969.43	14.73	0.48	0.00
4 Tn + 1 STn	1037.12	14.55	0.04	0.00
1 Tn + 1 ST	888.06	15.40	5.32	1.10
1 Tn + 2 ST	1106.80	15.21	0.00	7.83
1 Tn + 3 ST	1325.54	15.21	0.00	0.37
2 Tn + 1 ST	955.75	15.02	0.93	0.32
2 Tn + 2 ST	1174.49	14.83	0.00	0.99
3 Tn + 1 ST	1023.44	14.55	0.99	0.00
3 Tn + 2 ST	1242.19	14.30	0.00	0.07
4 Tn + 1 ST	1091.14	14.20	0.16	0.00
1 T + 1 ST	942.08	15.21	0.37	12.95
1 T + 2 ST	1160.82	15.02	0.00	8.14
1 T + 3 ST	1379.56	14.66	0.00	0.18
2 T + 1 ST	1063.79	14.47	0.00	10.73
2 T + 2 ST	1282.53	14.11	0.00	0.79
3 T + 1 ST	1185.50	13.53	0.00	1.30
3 T + 2 ST	1404.24	13.17	0.00	0.08
1 Tn + 1 T + 1 ST	1009.77	14.83	0.04	20.64
1 Tn + 2 T + 1 ST	1131.48	13.91	0.00	5.63
1 Tn + 3 T + 1 ST	1253.19	12.98	0.00	0.78
1 Tn + 1 T + 2 ST	1228.51	14.66	0.00	3.45
1 Tn + 2 T + 2 ST	1350.22	13.53	0.00	0.35
2 Tn + 1 T + 1 ST	1077.46	14.30	0.04	2.91
2 Tn + 2 T + 1 ST	1199.17	13.35	0.00	1.48
2 Tn + 1 T + 2 ST	1296.21	13.91	0.00	0.37
3 Tn + 1 T + 1 ST	1145.16	13.72	0.00	0.54
Sialylated glycopeptides				
1 STn	766.35	16.69	0.08	0.00
1 ST	820.37	15.97	1.68	0.50
2 ST	1039.11	15.78	0.11	3.93
3 ST	1257.85	15.58	0.00	1.19

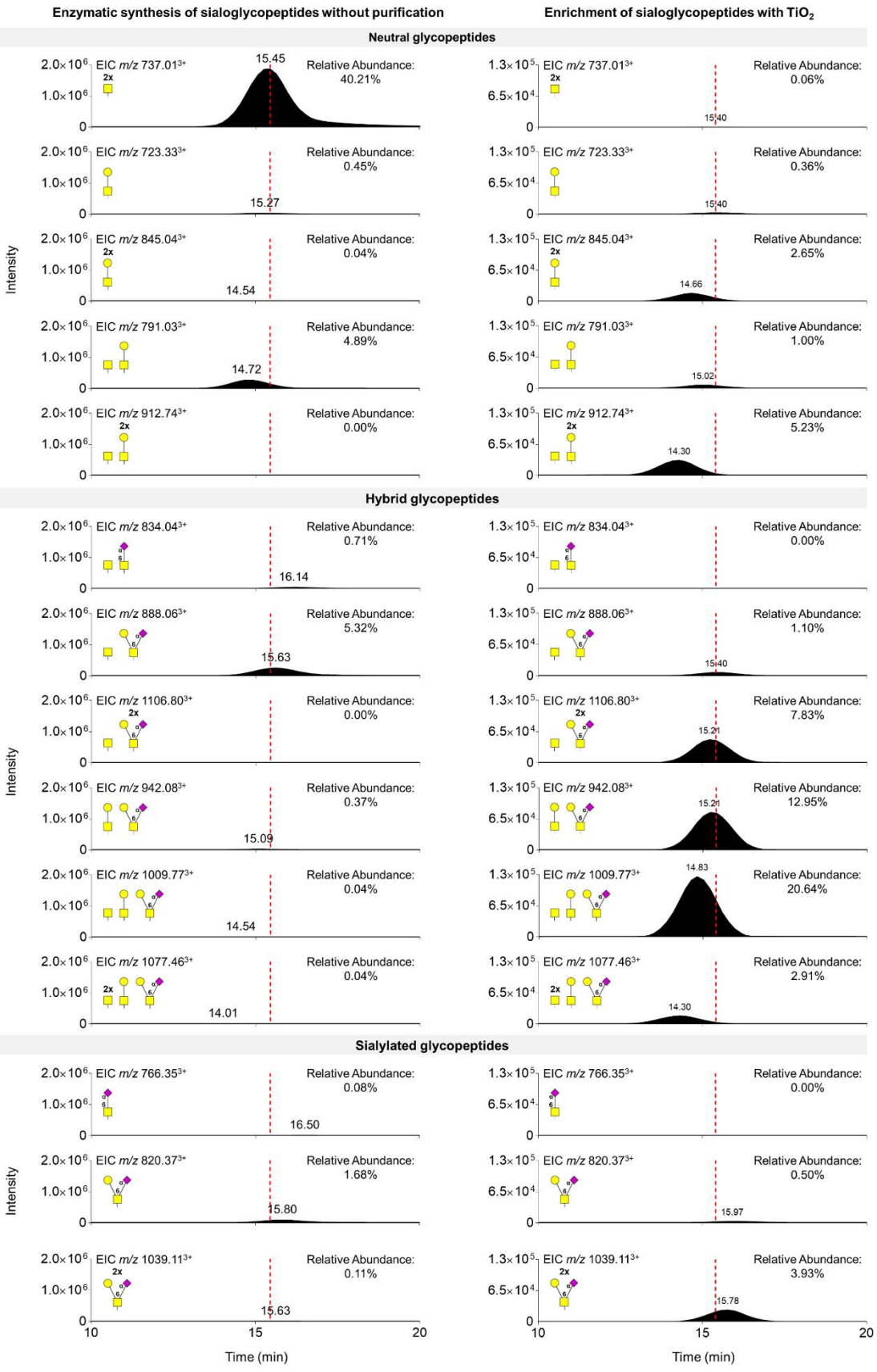
Enzymatic synthesis of sialoglycopeptides without purification
Enrichment of sialoglycopeptides with TiO2
Neutral glycopeptides
Hybrid glycopeptides
Sialylated glycopeptides
Intensity
Time (min)
EIC m/z 737.01 3+
Relative Abundance: 40.21%
Relative Abundance: 0.06%
EIC m/z 723.33 3+
Relative Abundance: 0.45%
Relative Abundance: 0.36%
EIC m/z 845.04 3+
Relative Abundance: 0.04%
Relative Abundance: 2.65%
EIC m/z 791.03 3+
Relative Abundance: 4.89%
Relative Abundance: 1.00%
EIC m/z 912.74 3+
Relative Abundance: 0.00%
Relative Abundance: 5.23%
EIC m/z 834.04 3+
Relative Abundance: 0.71%
Relative Abundance: 0.00%
EIC m/z 888.06 3+
Relative Abundance: 5.32%
Relative Abundance: 1.10%
EIC m/z 1106.80 3+
Relative Abundance: 0.00%
Relative Abundance: 7.83%
EIC m/z 942.08 3+
Relative Abundance: 0.37%
Relative Abundance: 12.95%
EIC m/z 1009.77 3+
Relative Abundance: 0.04%
Relative Abundance: 20.64%
EIC m/z 1077.46 3+
Relative Abundance: 0.04%
Relative Abundance: 2.91%
EIC m/z 766.35 3+
Relative Abundance: 0.08%
Relative Abundance: 0.00%
EIC m/z 820.37 3+
Relative Abundance: 1.68%
Relative Abundance: 0.50%
EIC m/z 1039.11 3+
Relative Abundance: 0.11%
Relative Abundance: 3.93%

Figure 7. C18 reverse phase nanoLC-ESI-MS profiles for the main reaction products resulting from single-pot enzymatic synthesis of MUC16-S6T glycopeptides before and after TiO_2 enrichment. The enzymatic synthesis of MUC16 glycopeptides with S6T modifications presented very low yields, as translated by the high amount of neutral species in relation to hybrid and sialoglycans mostly presenting one S6T glycosite. TiO_2 enabled the enrichment for a wider number of hybrid glycopeptides.

3.4.6 Synthesis of BSA-MUC16-STn and KLH-MUC16-Tn glycoconjugates

MUC16-Tn glycoforms have been associated with worst cancer prognosis and recently with decreased bladder cancer response to cisplatin[26]. As such, we have devoted to the production of glycoepitopes aiming towards the development of novel MUC16-STn/MUC16-Tn targeting antibodies and cancer vaccines. To overcome their poor immunogenicity, MUC16-STn glycopeptides were covalently linked to BSA, a strategy that has been proven capable of inducing antibody production against relevant glycopeptides in animal models[31]. As such, BSA was incubated with MBS (m-maleimidobenzoyl-N-hydroxysuccinamide ester), an amino-to-sulfhydryl crosslinker containing NHS-ester and a maleimide reactive groups at opposite ends of a short aromatic spacer arm. The maleimide linker was subsequently used to link MUC16-STn cysteine-tagged glycopeptides. Efforts were set on the development of protein-glycopeptide conjugates presenting a diversified array of hybrid and sialylated glycoepitopes, in an attempt to translate the structural diversity of glycoepitopes presented by cancer cells[26,30,34]. The efficacy of the conjugation reaction was later confirmed by observing the migration of BSA's major band in SDS-PAGE gels above 55 kDa to near 70 kDa upon introduction of the MBS linker. MALDI-TOF analysis latter confirmed the presence of a major signal at approximately 66 kDa corresponding to BSA that shifted to 70 kDa, suggesting the incorporation of approximately 21 MBS linker residues (70613 kDa). The addition of the glycopeptides to the reaction media promoted a shift in the BSA-MBS band to approximately 150 kDa, strongly suggesting glycopeptide conjugation, which was latter validated by western blot. In fact, as shown in (**Figure 8A**) BSA and BSA-MBS conjugates showed no reactivity to the VVA lectin, which has affinity for the Tn antigen. On the other hand, two major bands above 150 and 200 kDa were observed in the lanes corresponding to BSA-MUC16-STn/Tn hybrid glycoconjugates. These signals were further enhanced after sialidase digestion that exposes cryptic Tn epitopes by sialylation. Taken together, these observations support the successful conjugation of both

hybrid and sialoglycoepitopes to BSA. Notably, bands at molecular weights above 150 kDa could also be observed for BSA, which may relate with protein DTT-irreversible multimerization, as previously reported[35]. SDS-PAGE and western blot analysis suggests that these bands may also be experiencing linker functionalization and glycoconjugation, which warrants future validation.

After performing a conjugation of MUC16-STn with BSA as a proof of concept, we conjugated MUC16-Tn with a classical immunogenic carrier, namely KLH, using the same methodology[36]. KLH is a high-molecular-weight glycoprotein that is known by inducing both cell-mediated and humoral responses in animals and humans. Because of its high immunogenicity, low toxicity associated and its availability as a clinical grade product, this carrier is used extensively as a natural immunostimulant for basic research and clinical applications[37]. The efficacy of the conjugation reaction was later confirmed by Dot Blot. In fact, as shown in (**Figure 8B**), KLH and KLH-MBS conjugates showed no reactivity to the VVA lectin, which has affinity for the Tn antigen. On the other hand, one major dot was observed in the area corresponding to KLH-MUC16-Tn glycoconjugates. These observations support the successful conjugation of both hybrid and sialoglycoepitopes to KLH. In summary, this sets the bases for producing different protein-glycopeptide conjugates for biomedical applications, with emphasis on antibody production.

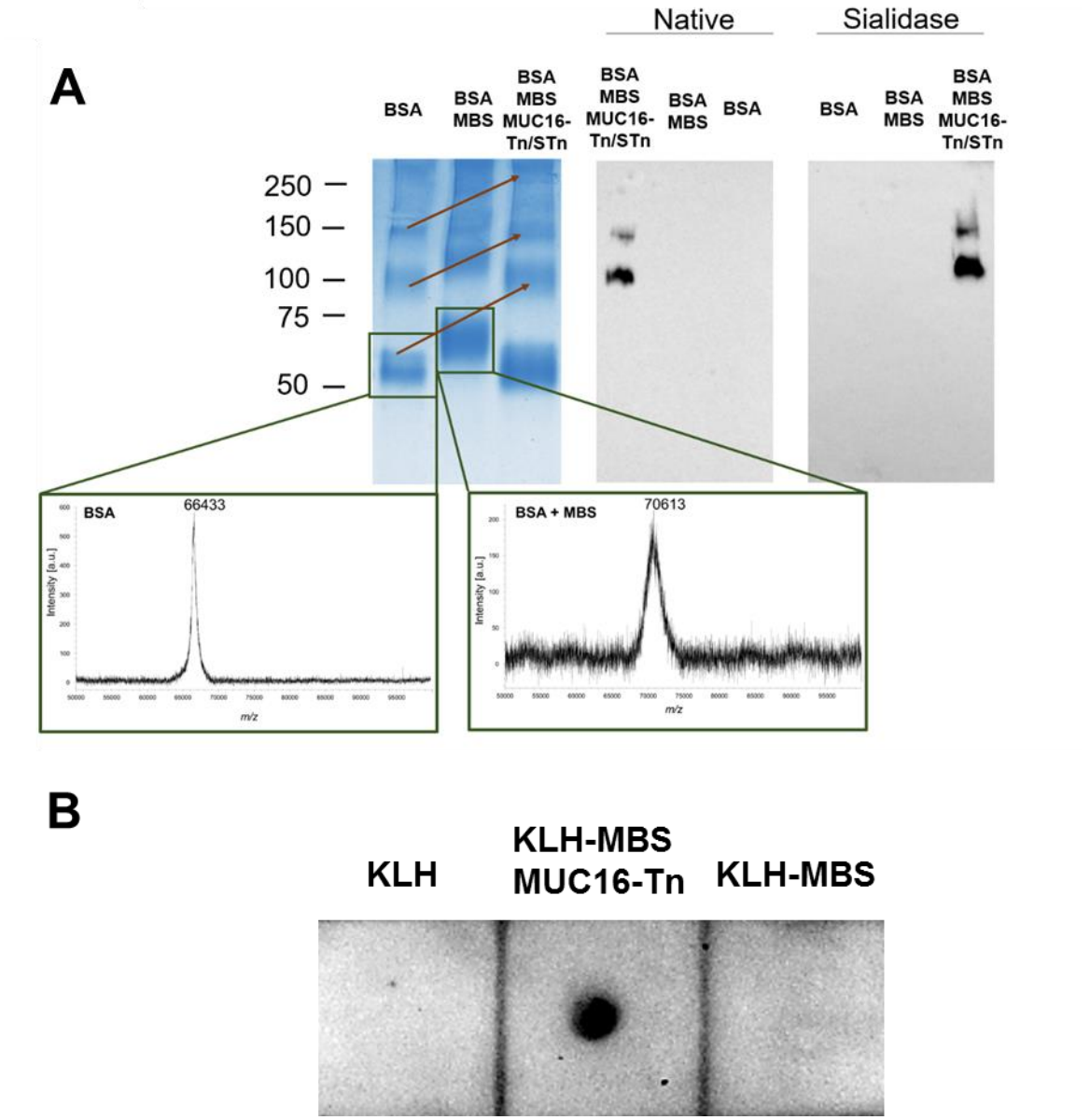

Figure 8. A) Monitoring reaction products of MUC16-Tn/STn biosynthesis by SDS-PAGE, Western blot and MALDI-TOF-MS; SDS-PAGE shows a main band above 55 kDa, which was later confirmed to be BSA by MALDI-TOF-MS (band at m/z 66433 in the left panel MS spectrum). Higher molecular weight bands of lower intensity could also be observed above 100 kDa most likely resulting from BSA multidimers. However, these were not observed by MALDI-TOF-MS probably due to difficulties in the ionization of higher molecular weight species. The addition of MBS to the reaction pot drifted this band to approximately 70 kDa, as highlighted by SDS-PAGE and later confirmed by MALDI-TOF-MS (right panel MS spectrum). Notably, a mass increase could also be observed for the molecular bands above 100 kDa, also suggesting substitutions with MBS. The addition of

hybrid MUC16-Tn/STn glycopeptides increased the molecular weight to above 100 kDa. In this case, a higher amount of BSA was used for conjugation in relation to MBS, explaining the presence of unconjugated BSA in the SDS-PAGE gel. Successful conjugation was then confirmed by western blot using the VVA lectin targeting the Tn antigen. Briefly, the left side western blot supports the presence of Tn expressing proteins above 100 and 150 kDa. Membrane incubation with sialidase increased the affinity for VVA for these proteins, also supporting the presence of STn antigen. Notably, bands corresponding to BSA and BSA-MBS were not recognized by the lectin, confirming signal specificity. The arrows in SDS-PAGE gels attempt to highlight the increase in molecular weight during the different conjugation steps leading to BSA-MBS-MUC16-Tn/STn conjugates**. B) Monitoring of reaction products of MUC16-Tn biosynthesis by DotBlot.** KLH, KLH-MBS conjugates showed no reactivity to the VVA lectin. On the other hand, one major dot was observed in the area corresponding to KLH-MUC16-Tn glycoconjugates.

3.5 Concluding Remarks

The synthesis of *O*-glycopeptides for bioanalytical and medical applications has been a challenging research topic. Exploiting human recombinant glycosyltransferases for glycosites definition and glycan chains extension offers significant advantages over organic synthesis, enabling an easy, rapid, less expensive and sustainable production of glycan chains with desired conformations. Nevertheless, it requires a fine tuning of the myriad of initial ppGalNATs to ensure the correct definition of glycosites. In particular, the enzymatic synthesis of short-chain sialylated peptides mimicking cancer-associated epitopes may be achievable by one-pot combination of glycosyltranferases, chaperones and cofactors. Accordingly, these methodologies have been used to generate MUC1-Tn, STn, T and S3T antigens with relative success[18,31]. However, even though tremendously straightforward, these procedures generate complex glycopeptide mixtures with distinct glycosite patterns and different combinations of glycan chains, often presenting all synthesis intermediates. Mixtures of different epitopes may likely translate the *in vivo* context and therefore be desirable envisaging multivalent carbohydrate-based vaccines. However, the lack of pure products still poses difficulties for bioanalytical applications and the design of highly specific targeted therapeutics. As such, this work was devoted to setting the synthesis and analytical bases for future enzymatic production of glycopeptides of medical interest

presenting sialylated short-chain *O*-glycans and their conjugation with PLGA based nanoparticles. It successfully explored one-pot enzymatic synthesis to produce a wide array of MUC16-Tn, STn, S3T and, for the first time, S6T glycopeptides. These glycopeptides are expressed in bladder cancer and may also be present in other solid tumours overexpressing MUC16 as ovarian[27], breast[38], and pancreatic cancer[39]. A combination of reverse phase chromatography with and without TiO_2 enrichment has also been tested to establish purification protocols. Reverse phase chromatography allowed a reasonable separation between neutral and fully sialylated glycopeptides, irrespectively of their nature. Moreover, it enabled a good separation of glycopeptides with different Tn-glycosites which may be introduced at initial stages as precursors for downstream glycosylation. Nevertheless, future studies should explore combinations of different ppGalNAcTs to diversify the array of products. Moreover, the characterization of isolated glycopeptides by ETD-fragmentation should be envisaged to support glycosites annotation. Finally, while there is still room to improve chromatographic settings, reverse phase chromatography has demonstrated limited capacity to fully resolve hybrid glycopeptides presenting both neutral and sialoglycans. This limitation may be significantly improved in the future with the introduction of HILIC chromatography, which enables good separation between neutral and sialoglycopeptides[32]. A possible combination with reverse phase chromatography in 2D settings may significantly increase the quality of these procedures. In addition, TiO_2 enrichment may be used to improve the isolation of hybrid MUC16-STn glycopeptides as well as sialylated MUC16-S3T and S6T. These observations suggest that combinations of different enrichment/purification strategies may be used according to the outlined objectives. Moreover, testing these different settings will significantly improve purification and provide an important setup for future glycoproteomics studies supporting glycobiomarkers discovery.

The second part of this work relates with setting up a protocol for construction of immunogenic MUC16-STn/Tn glycopeptides-protein glycoconjugates for future work, including the generation of antibodies in relevant animal models and carbohydrate-based vaccines. MUC16-STn and MUC16-Tn were elected for proof-of-concept studies, given its clinical relevance for targeting chemoresistant bladder tumours[26]. No particular purification steps were introduced at this stage in an attempt to provide a multivalent construct presenting a wide myriad of glycoepitopes. The future construction of glycoconjugates with distinct

glycoepitopes and immunogenic proteins with tailored properties to improve immunogenicity, half-life in circulation, amongst other critical aspects may be now envisaged. This will pave the way for formulations capable of eliciting antibody production in different animal models that may be ultimately tested as carbohydrate-based vaccines.

In summary, this work sets important foundations for translating *O*-glycobiomarker research into glycan libraries aiding biomedical research and the development of glycan-inspired targeted therapeutics, namely immunotherapy. Moreover, important observations have been made for more in-depth studies towards carbohydrate metrology, a crucial milestone for fostering carbohydrate-based biotechnological applications.

3.6 References

1 Hudak, J. E. & Bertozzi, C. R. Glycotherapy: new advances inspire a reemergence of glycans in medicine. *Chem Biol* **21**, 16-37, (2014).

2 Zhang, P., Woen, S., Wang, T., Liau, B., Zhao, S., Chen, C., Yang, Y., Song, Z., Wormald, M. R., Yu, C. & Rudd, P. M. Challenges of glycosylation analysis and control: an integrated approach to producing optimal and consistent therapeutic drugs. *Drug Discov Today* **21**, 740-765, (2016).

3 Lepenies, B., Yin, J. & Seeberger, P. H. Applications of synthetic carbohydrates to chemical biology. *Curr Opin Chem Biol* **14**, 404-411, (2010).

4 Palcic, M. M. Glycosyltransferases as biocatalysts. *Curr Opin Chem Biol* **15**, 226-233, (2011).

5 Boltje, T. J., Buskas, T. & Boons, G. J. Opportunities and challenges in synthetic oligosaccharide and glycoconjugate research. *Nat Chem* **1**, 611-622, (2009).

6 Schmaltz, R. M., Hanson, S. R. & Wong, C. H. Enzymes in the synthesis of glycoconjugates. *Chem Rev* **111**, 4259-4307, (2011).

7 Ati, J., Lafite, P. & Daniellou, R. Enzymatic synthesis of glycosides: from natural O- and N-glycosides to rare C- and S-glycosides. *Beilstein J Org Chem* **13**, 1857-1865, (2017).

8 Murata, T. & Usui, T. Enzymatic synthesis of oligosaccharides and neoglycoconjugates. *Biosci Biotechnol Biochem* **70**, 1049-1059, (2006).

9 Brocke, C. & Kunz, H. Synthesis of tumor-associated glycopeptide antigens. *Bioorg Med Chem* **10**, 3085-3112, (2002).

10 Rao, T. D., Fernandez-Tejada, A., Axelrod, A., Rosales, N., Yan, X., Thapi, S., Wang, A., Park, K. J., Nemieboka, B., Xiang, J., Lewis, J. S., Olvera, N., Levine, D. A., Danishefsky, S. J. & Spriggs, D. R. Antibodies Against Specific MUC16 Glycosylation Sites Inhibit Ovarian Cancer Growth. *ACS Chem Biol* **12**, 2085-2096, (2017).

11 Geyer, H. & Geyer, R. Strategies for analysis of glycoprotein glycosylation. *Biochim Biophys Acta* **1764**, 1853-1869, (2006).

12 Bennett, E. P., Hassan, H., Mandel, U., Mirgorodskaya, E., Roepstorff, P., Burchell, J., Taylor-Papadimitriou, J., Hollingsworth, M. A., Merkx, G., van Kessel, A. G., Eiberg, H., Steffensen, R. & Clausen, H. Cloning of a human UDP-N-acetyl-alpha-D-Galactosamine:polypeptide N-acetylgalactosaminyltransferase that complements

other GalNAc-transferases in complete O-glycosylation of the MUC1 tandem repeat. *J Biol Chem* **273**, 30472-30481, (1998).

13 Wandall, H. H., Hassan, H., Mirgorodskaya, E., Kristensen, A. K., Roepstorff, P., Bennett, E. P., Nielsen, P. A., Hollingsworth, M. A., Burchell, J., Taylor-Papadimitriou, J. & Clausen, H. Substrate specificities of three members of the human UDP-N-acetyl-alpha-D-galactosamine:Polypeptide N-acetylgalactosaminyltransferase family, GalNAc-T1, -T2, and -T3. *J Biol Chem* **272**, 23503-23514, (1997).

14 Pohl, N. Cellular addresses; step one in creating a glycocode. *Chem Biol* **11**, 891-892, (2004).

15 Pratt, M. R., Hang, H. C., Ten Hagen, K. G., Rarick, J., Gerken, T. A., Tabak, L. A. & Bertozzi, C. R. Deconvoluting the functions of polypeptide N-alpha-acetylgalactosaminyltransferase family members by glycopeptide substrate profiling. *Chem Biol* **11**, 1009-1016, (2004).

16 Gerken, T. A., Jamison, O., Perrine, C. L., Collette, J. C., Moinova, H., Ravi, L., Markowitz, S. D., Shen, W., Patel, H. & Tabak, L. A. Emerging paradigms for the initiation of mucin-type protein O-glycosylation by the polypeptide GalNAc transferase family of glycosyltransferases. *J Biol Chem* **286**, 14493-14507, (2011).

17 Hansen, J. E., Lund, O., Tolstrup, N., Gooley, A. A., Williams, K. L. & Brunak, S. NetOglyc: prediction of mucin type O-glycosylation sites based on sequence context and surface accessibility. *Glycoconj J* **15**, 115-130, (1998).

18 Beatson, R., Maurstad, G., Picco, G., Arulappu, A., Coleman, J., Wandell, H. H., Clausen, H., Mandel, U., Taylor-Papadimitriou, J., Sletmoen, M. & Burchell, J. M. The Breast Cancer-Associated Glycoforms of MUC1, MUC1-Tn and sialyl-Tn, Are Expressed in COSMC Wild-Type Cells and Bind the C-Type Lectin MGL. *PLoS One* **10**, e0125994, (2015).

19 Beatson, R., Tajadura-Ortega, V., Achkova, D., Picco, G., Tsourouktsoglou, T. D., Klausing, S., Hillier, M., Maher, J., Noll, T., Crocker, P. R., Taylor-Papadimitriou, J. & Burchell, J. M. The mucin MUC1 modulates the tumor immunological microenvironment through engagement of the lectin Siglec-9. *Nat Immunol* **17**, 1273-1281, (2016).

20 Taylor-Papadimitriou, J., Burchell, J. M., Graham, R. & Beatson, R. Latest developments in MUC1 immunotherapy. *Biochem Soc Trans* **46**, 659-668, (2018).

21 Cai, H., Huang, Z. H., Shi, L., Sun, Z. Y., Zhao, Y. F., Kunz, H. & Li, Y. M. Variation of the glycosylation pattern in MUC1 glycopeptide BSA vaccines and its influence on the immune response. *Angew Chem Int Ed Engl* **51**, 1719-1723, (2012).

22 Lateef, S. S., Gupta, S., Jayathilaka, L. P., Krishnanchettiar, S., Huang, J. S. & Lee, B. S. An improved protocol for coupling synthetic peptides to carrier proteins for antibody production using DMF to solubilize peptides. *J Biomol Tech* **18**, 173-176, (2007).

23 Naito, S., Takahashi, T., Onoda, J., Uemura, S., Ohyabu, N., Takemoto, H., Yamane, S., Fujii, I., Nishimura, S. I. & Numata, Y. Generation of Novel Anti-MUC1 Monoclonal Antibodies with Designed Carbohydrate Specificities Using MUC1 Glycopeptide Library. *ACS Omega* **2**, 7493-7505, (2017).

24 Kurosawa, N., Kojima, N., Inoue, M., Hamamoto, T. & Tsuji, S. Cloning and expression of Gal beta 1,3GalNAc-specific GalNAc alpha 2,6-sialyltransferase. *J Biol Chem* **269**, 19048-19053, (1994).

25 Marcos, N. T., Pinho, S., Grandela, C., Cruz, A., Samyn-Petit, B., Harduin-Lepers, A., Almeida, R., Silva, F., Morais, V., Costa, J., Kihlberg, J., Clausen, H. & Reis, C. A. Role of the human ST6GalNAc-I and ST6GalNAc-II in the synthesis of the cancer-associated sialyl-Tn antigen. *Cancer Res* **64**, 7050-7057, (2004).

26 Cotton, S., Azevedo, R., Gaiteiro, C., Ferreira, D., Lima, L., Peixoto, A., Fernandes, E., Neves, M., Neves, D., Amaro, T., Cruz, R., Tavares, A., Rangel, M., Silva, A. M. N., Santos, L. L. & Ferreira, J. A. Targeted O-glycoproteomics explored increased sialylation and identified MUC16 as a poor prognosis biomarker in advanced-stage bladder tumours. *Mol Oncol* **11**, 895-912, (2017).

27 Felder, M., Kapur, A., Gonzalez-Bosquet, J., Horibata, S., Heintz, J., Albrecht, R., Fass, L., Kaur, J., Hu, K., Shojaei, H., Whelan, R. J. & Patankar, M. S. MUC16 (CA125): tumor biomarker to cancer therapy, a work in progress. *Mol Cancer* **13**, 129, (2014).

28 Azevedo, R., Silva, A. M. N., Reis, C. A., Santos, L. L. & Ferreira, J. A. In silico approaches for unveiling novel glycobiomarkers in cancer. *J Proteomics* **171**, 95-106, (2018).

29 Gomes, J., Mereiter, S., Magalhaes, A. & Reis, C. A. Early GalNAc O-Glycosylation: Pushing the Tumor Boundaries. *Cancer Cell* **32**, 544-545, (2017).

30 Steentoft, C., Vakhrushev, S. Y., Joshi, H. J., Kong, Y., Vester-Christensen, M. B., Schjoldager, K. T., Lavrsen, K., Dabelsteen, S., Pedersen, N. B., Marcos-Silva, L., Gupta, R., Bennett, E. P., Mandel, U., Brunak, S., Wandall, H. H., Levery, S. B. & Clausen, H. Precision mapping of the human O-GalNAc glycoproteome through SimpleCell technology. *EMBO J* **32**, 1478-1488, (2013).

31 Sorensen, A. L., Reis, C. A., Tarp, M. A., Mandel, U., Ramachandran, K., Sankaranarayanan, V., Schwientek, T., Graham, R., Taylor-Papadimitriou, J., Hollingsworth, M. A., Burchell, J. & Clausen, H. Chemoenzymatically synthesized multimeric Tn/STn MUC1 glycopeptides elicit cancer-specific anti-MUC1 antibody responses and override tolerance. *Glycobiology* **16**, 96-107, (2006).

32 Palmisano, G., Lendal, S. E., Engholm-Keller, K., Leth-Larsen, R., Parker, B. L. & Larsen, M. R. Selective enrichment of sialic acid-containing glycopeptides using titanium dioxide chromatography with analysis by HILIC and mass spectrometry. *Nat Protoc* **5**, 1974-1982, (2010).

33 Yoshino, M. & Murakami, K. Analysis of the substrate inhibition of complete and partial types. *Springerplus* **4**, 292, (2015).

34 Campos, D., Freitas, D., Gomes, J., Magalhães, A., Steentoft, C., Gomes, C., Vester-Christensen, M., Ferreira, J. A., Afonso, L., L. Santos, L., Pinto de Sousa, J., Mandel, U., Clausen, H., Vakhrushev, S. & Reis, C. A. Probing the O-glycoproteome of gastric cancer cell lines for biomarker discovery. *Molecular & cellular proteomics : MCP* **14**, 1616-1629, (2015).

35 Borzova, V. A., Markossian, K. A., Kara, D. A., Chebotareva, N. A., Makeeva, V. F., Poliansky, N. B., Muranov, K. O. & Kurganov, B. I. Quantification of anti-aggregation activity of chaperones: a test-system based on dithiothreitol-induced aggregation of bovine serum albumin. *PLoS One* **8**, e74367, (2013).

36 Swaminathan, A., Lucas, R. M., Dear, K. & McMichael, A. J. Keyhole limpet haemocyanin - a model antigen for human immunotoxicological studies. *Br J Clin Pharmacol* **78**, 1135-1142, (2014).

37 Wimmers, F., de Haas, N., Scholzen, A., Schreibelt, G., Simonetti, E., Eleveld, M. J., Brouwers, H. M., Beldhuis-Valkis, M., Joosten, I., de Jonge, M. I., Gerritsen, W.

R., de Vries, I. J., Diavatopoulos, D. A. & Jacobs, J. F. Monitoring of dynamic changes in Keyhole Limpet Hemocyanin (KLH)-specific B cells in KLH-vaccinated cancer patients. *Sci Rep* **7**, 43486, (2017).

38 Lakshmanan, I., Ponnusamy, M. P., Das, S., Chakraborty, S., Haridas, D., Mukhopadhyay, P., Lele, S. M. & Batra, S. K. MUC16 induced rapid G2/M transition via interactions with JAK2 for increased proliferation and anti-apoptosis in breast cancer cells. *Oncogene* **31**, 805-817, (2012).

39 Haridas, D., Chakraborty, S., Ponnusamy, M. P., Lakshmanan, I., Rachagani, S., Cruz, E., Kumar, S., Das, S., Lele, S. M., Anderson, J. M., Wittel, U. A., Hollingsworth, M. A. & Batra, S. K. Pathobiological implications of MUC16 expression in pancreatic cancer. *PLoS One* **6**, e26839, (2011).

CHAPTER IV

PLGA Nano-vehicles for Selective Delivery of MUC16-Tn Glycopeptides to Immune Cells

PLGA Nano-vehicles for Selective Delivery of MUC16-Tn Glycopeptides to Immune Cells

Rui Freitas[a,b], Elisabete Fernandes[a,c,d,] , Dylan Ferreira[a,c,d], Andreia Peixoto[a,c,d,e], Marta Relvas-Santos[a,c,d,e,f], Carlos Palmeira[a,g,h], Andre M. N.Silva[f], Lúcio Lara Santos[a ,e,h,i,j], Bruno Sarmento[c,d], José Alexandre Ferreira[a,e,j]

[a]Experimental Pathology and Therapeutics Group, Portuguese Institute of Oncology, 4200-162 Porto, Portugal; [b]QOPNA & LAQV-REQUIMTE, Department of Chemistry, University of Aveiro, Aveiro, Portugal; [c]Institute for Research and Innovation in Health (i3s), University of Porto, 4200-135 Porto, Portugal; [d]Institute for Biomedical Engineering (INEB), Porto, Portugal, 4200-135 Porto, Portugal; [e]Institute of Biomedical Sciences Abel Salazar (ICBAS), University of Porto, 4050-013 Porto, Portugal; [f]REQUIMTE-LAQV, Department of Chemistry and Biochemistry, Faculty of Sciences of the University of Porto, 4069-007 Porto, Portugal; [g]Immunology Department, Portuguese Institute of Oncology of Porto, 4200-162 Porto, Portugal; [h]Health Science Faculty, University of Fernando Pessoa, 4249-004 Porto, Portugal; [i]Department of Surgical Oncology, Portuguese Institute of Oncology of Porto, 4200-162 Porto, Portugal; [j]Porto Comprehensive Cancer Centre (P.ccc), 4200-162 Porto, Portugal;

Corresponding author:

José Alexandre Ferreira (jose.a.ferreira@ipoporto.min-saude.pt)
Experimental Pathology and Therapeutics Group, Research Centre, Portuguese Oncology Institute of Porto, R. Dr. António Bernardino de Almeida 62, 4200-162 Porto, Portugal; Tel. +351 225084000 (ext. 5111).

Keywords: Cancer Vaccines, Glycoepitopes, immunotherapy, cancer glycosylation, nanovaccines.

4.1 Abstract

Alterations in the glycosyation of proteins at the cell-surface of cancer cells are often responsible for creating unique molecular signatures that are not reflected by healthy tissues. Amongst the most common alterations in cancer is the overexpression of the Tn antigen, a short-chain *O*-glycan resulting from a premature stop in glycans elongation. Its cancer specific nature holds tremendous potential for immunotherapy by vaccination once their immunosuppressive nature is overcome. Based on previous reports, we anticipate that glycopeptides presentation to the immune system using nanoconstructs may constitute a key strategy to surpass Tn immunosuppressive features. Envisaging the molecular rationale towards this end, we have synthesized several MUC16-Tn glycopeptides that were covalently immobilized at the surface of PLGA nanoparticles. In parallel, we have also adsorbed the glypeptide at the surface of PLGA nanoparticles. These nanoconstructs presented a spherical nature and dimensions lower than 200nm, a low polydispersion index and high stability at physiological pH, suggesting potential for delivery of glycoepitopes to antigen presenting cells. The successful immobilization/adsorption of the glycopeptide to nanoparticles was confirmed by proton Nuclear Magnetic Resonance (^{1}H NMR). We also observed that the nanoconstructs could be internalized by immature macrophages at non-toxic concentrations. This has created the rational for pursuing the development of innovative glycan-based nanovaccines.

4.2 Introduction

Cancer cells frequently overexpress at the cell surface short-chain *O*-glycans such as Tn and sialyl-Tn antigens, which result from a premature stop in protein *O*-glycosylation due to profound deregulations in secretory pathways[1,2]. The substitution of more elongated glycoforms by shorter species is known to induce the activation of relevant oncogenic pathways such as PI3K/AKT[3] and hyperactivation of the mitogenic ErbB2 tyrosine kinase receptor (RTK)[4], ultimately favouring cancer cell migration[5], invasion[6] and metastasis development[7]. Consequently, increased levels of these glycans are frequently associated with worst prognosis in most human solid tumours[8-10], supporting their pancarcinomic nature. These events are frequently associated to mucins (MUC) overexpression that, due to their elevated molecular weight and dense number of *O*-glycosites, tremendously amplify

abnormal glycosylation at the cell surface[11-13]. Nevertheless, virtually any protein at the cell-surface presenting serine and/or threonine residues and undergoing transport across the secretory pathways may exhibit these common post-translational modifications[14]. Short-chain *O*-glycans are generally not expressed by non-malignant cells or exhibit a sparse expression restricted to cells specialized in secretion and facing the lumen of the gastrointestinal and respiratory tracts[15]. In addition, they have not yet been observed in the bloodstream or lymph, suggesting potential for cancer targeted therapeutics and immunotherapy.

Cancer vaccines, alone or in combination with other immunotherapies such as adoptive cell therapy or immune checkpoint inhibitors, are considered a promising alternative to conventional cancer therapy[16]. These may stimulate specific and deleterious immune responses against tumours with minimal impact on healthy cells[17-19]. The capacity to elicit immune memory and long-term protection against recurrences is also a key advantage compared to existing therapeutics[20,21]. Several vaccine constructs have been developed exploiting either synthetic short-chain *O*-glycans[22,23] or abnormally glycosylated MUC- glycopeptides[24] coupled to different types of immunogens. However, the success of such approaches has been challenged by these glycans immunosuppressive nature[25]. In fact, Tn and STn antigens are endogenous ligands of different lectins at the surface of antigen presenting cells (APCs) and glycan-lectin recognition has been found responsible by preventing APCs maturation and damping effective anti-tumour immune responses[26,27]. Namely, both Tn and STn antigens are targeted by macrophage galactose type C-type lectin (MGL) exclusively expressed by dendritic cells (DCs) and activated macrophages[27,28], driving the activation of immune-inhibitory programmes characterized by increased IL-10 production and the induction of effector T cell apoptosis[27]. Moreover, STn-positive mucins secreted by cancer cells impair DCs maturation and lead to DC-mediated induction of high levels of the Treg cell-associated transcription factor forkhead box protein P3 (FOXP3) and low IFNγ[29] in T cells. Recognition by sialic acid-binding immunoglobulin-like lectins (Siglecs) expressed at the surface of APCs are regarded to play a key role in these events[25,26,30]. Therefore, more effective vaccine formulations are required to tackle the current limitation of conventional vaccination on APCs. Nanomedicine offers unique opportunities to improve the suboptimal efficacy of cancer vaccines and may constitute a key opportunity to foster the exploitation of glycans in this context[31-33]. A plethora of

nanoplatforms have been proposed to deliver molecular, cellular or subcellular vaccines to target cells and lymphoid tissues, while promoting the potency and durability of anti-tumor immunity and reducing adverse side effects[34-36]. Namely, poly(lactic-co-glycolic acid) (PLGA)-based nanovaccines have been exploited to improve the delivery of neoantigens to APCs[37-39]. PLGA-formulations have been used to encapsulate different types of immunogens (proteins, peptides, nucleic acids, immunostimulatory molecules) preventing premature degradation and enhancing their stability[38,40,41]. Moreover, PLGA nanoparticles may be easily grafted by simple click-chemistry reactions with different epitopes and/or immunostimulatory molecules such as Toll-Like Receptors (TLR), enabling a more effective targeting of relevant APCs subpopulations[42,43]. Many of these strategies have been elegantly used to induce the efficient uptake and presentation of cancer antigens by APCs, promoting their activation and capacity to elicit effector T cell responses[44,45].

As such, the present chapter devotes to designing innovative PLGA nano-vehicles for selective delivery of Tn-glycoepitopes to immune cells. We hypothesize that PLGA nanoparticles may be used to boost more effective immune responses and/or hinder the glycopeptides from recognition by APC cell surface receptors, bypassing the downstream activation of immunosuppressive signals. The variable tandem repeat of MUC16 containing several potential *O*-glycosylation sites was used as model glycopeptide. We anticipate that this may constitute the molecular basis for the development of a multivalent glycan-based vaccine for a wide number of solid tumours overexpressing abnormally glycosylated MUC16 (bladder[46], ovarian[47], cervical[48], lung[49]) and where this glycoprotein plays a key role in cancer development towards poor prognosis[50-52].

4.3 Material and Methods

4.3.1 Nanoparticles production for MUC16-Tn encapsulation

PLGA-PEG-MAL NPs for MUC16-Tn encapsulation were generated by a modified water-in-oil-in-water (w/o/w) double emulsion-solvent evaporation technique[53,54,55]. Briefly, 19 mg of PLGA (Corbion-Purac Biomaterials) and 1mg of PLGA-PEG-MAL (for PLGA-PEG-MAL NPs) were dissolved in 4 mL ethyl acetate (Sigma-Aldrich), following the addition of 20, 30 or 40 µg/mL MUC16-Tn and emulsification at 70% amplitude for 30 s using a Vibra-Cell™ ultrasonic processor in an ice bath. The second emulsion was achieved by adding 2% Pluronic F-127 (6 mL) (Sigma-Aldrich) to the first emulsion, following Vibra-Cell™ ultrasonic homogenization for 60 s and addition of the resulting mixture to 12 mL of

the same surfactant. Ethyl acetate evaporation from the final solution occurred for 5 h under magnetic stirring at 250 rpm. Nanoparticles were isolated by ultracentrifugation at 120 000g for 40 min.

4.3.2 Nanoparticles production for MUC16-Tn adsorption or functionalization

Briefly, 19 mg of PLGA (Corbion-Purac Biomaterials) and 1 mg PLGA-PEG-MAL were dissolved in 1 mL ethyl acetate, following the addition of 100 µL Mili-Q water to form the primary (w/o) emulsion and homogenization in a Vibra-Cell™ ultrasonic processor for 30 seconds. The second (w/o/w) emulsion was achieved by adding 2% Pluronic F-127 (4 mL) and homogenization for 1minute. The final mixture was finally added to another solution of pluronic 2% (15 mL) and left under magnetic stirring at 300 rpm for 3h envisaging ethyl acetate evaporation. This resulted in the synthesis of both PLGA and PLGA-PEG-MAL (95:5 % w/w) NPs. Formulations were washed three times with ultrapure water using Amicon centrifuge filters (100kDa MWCO) at 1,500g for 10 minutes at 4ºC, followed by resuspension in 5,4 mL of ultrapure water.

MUC16-Tn glycopeptides were conjugated to the surface of NPs by maleimide chemistry[56,57]. To allowmild reduction of C-terminal cysteines in the glycopeptide, tris(2-carboxyethyl) phosphine hydrochloride (TCEP) was added to MUC16-Tn 20 mer CysTag at a final proportion of 1:1 and incubated for 1 hour at room temperature under 70 rpm agitation in the presence of 0,1% of TWEEN-20. To this mixture, 2mg of NPs were added and incubated overnight at 4ºC under 250 rpm agitation. NPs with adsorbed peptide were produces similarly but in the absence of TCEP. After overnight incubation, formulations were washed three times with phosphate buffer pH 7 using Amicon centrifuge filters (3kDa) at 1,500 g for 5 minutes at 4ºC and finally resuspended in the same buffer. Functionalization with 10, 20, 30 and 40 µg of MUC16-Tn were attempted for PLGA-PEG-MAL NPs. The supernatants were stored for further peptide quantification using the Pierce™ Quantitative Colorimetric Peptide Assay Kit (Thermo Fisher Scientific). The conjugation efficiency was determined according to the following equation:

$$Conjugation\ efficiency\ (\%) = \frac{amount\ of glycopeptide - \ amount\ of\ glycopeptide\ in\ supernatant}{amount\ of\ glycopeptide}\ x\ 100$$

Fluorescent PLGA-PEG-MAL NPs were produced through a modified nanoprecipitation method[58]. Accordingly, 20 mg PLGA-PEG-MAL was dissolved in acetone (Sigma-Aldrich) and added to 0.8 mg of coumarin (C6; Sigma-Aldrich) dissolved in acetone. This organic solution was transferred through a 25 G needle to an aqueous solution of 1% Pluronic F-127 (15 mL) and solvent evaporation occurred under magnetic stirring at 250 rpm for 3 h. Fluorescent NPs were washed three times with ultrapure water using Amicon centrifuge filters (100kDa MWCO) at 1,500g for 10 minutes at 4ºC, followed by resuspension in 5,4 mL of ultrapure water. Functionalization of 15 μg of MUC16-Tn were attempted for fluorescent NPs.

4.3.3 Characterization of nanoparticles

4.3.3.1 Nanoparticles physicochemical and morphological characterization

The size and polydispersity index (PdI) of formulations were determined by Dynamic Light Scattering (DLS), while surface charge of NPs was determined by laser Doppler anemometry (LDA). After dispersion, NPs were diluted in 10mM sodium chloride solution (pH 7.0) (Sigma-Aldrich) and DLS and LDA were performed with a Nano ZS Zetasizer (Malvern, Worcestershire, UK) at 25 °C using the Smoluchowski model. Data is presented as the average of the triplicate NP formulations. Surface morphology and NPs size confirmation were performed by transmission electron microscopy (TEM) using a JEM-1400 microscope (JEOL, Tokyo, Japan) at an acceleration voltage of 80 kV.

4.3.3.2 Nuclear magnetic resonance analysis

PLGA nanoparticles were washed with ultrapure water and poured into semi-stoppered glass vials with slotted rubber closures at a maximal formulation volume of 2 mL The samples were frozen by ramped cooling at −40ºC for 4 h followed by lyophilization using a VirTis Advantage Plus Benchtop lyophilizer from SP Scientific (Warminster, PA, USA). The condenser surface temperature was maintained at -60 ± 5ºC. The primary drying occurred at -32ºC and 150 mtorr during 24 h, while secondary drying occurred at 20 ºC and 50 mtorr during 6 h.

^{1}H NMR spectra of PLGA NPs, PLGA-PEG-MAL NPs, and MUC16-Tn adsorbed or covalently linked to PLGA-PEG-MAL NPs were acquired, at room temperature, on a Brüker AMX 300 spectrometer operating at 400.13 MHz. The samples were analysed at the final concentration of 2 mg/mL in 1:3 H_2O-d_6:DMSO-d_6. The chemical shifts are expressed

in δ (ppm) values relative to tetramethylsilane (TMS) as internal reference and coupling constants (J) are given in Hz.

4.3.4 Functionalized nanoparticles evaluation in human macrophages

4.3.4.1 Cell culture maintenance conditions

The human THP-1 cell line was acquired from ATCC (Manassas, USA) and cultured in RPMI 1640 + GlutaMAX™ medium (GibcoTM, Thermo Fisher Sientific) supplemented with 10% heat-inactivated FBS (GibcoTM, Thermo Fisher Sientific) and 1% penicillin-streptomycin (10,000 Units/mL penicillin; 10,000 µg/mL streptomycin; Gibco™, Thermo Fisher Sientific) at 37°C in a 5% CO2 humidified atmosphere.

4.3.4.2 *In vitro* uptake studies on dTHP-1

THP-1 cells were differentiated into macrophage-like cells (dTHP) with 100 ng/mL phorbol 12-myristate 13-acetate (PMA; Sigma-Aldrich) for 48 h, following a 24h incubation with fresh medium to achieve the M0 phenotype. For NP uptake evaluation, cells were incubated with 20, 2, 0.2 or 0.01 ng/µL of functionalized or adsorbed MUC16-Tn-PLGA-NPs loaded with fluorescent coumarin 6 (C6) as well as with the same amounts of MUC16-Tn free peptide in OptiMEM. Medium (Gibco) for 4 h at 37 °C. Cells were then fixed with 4% PFA and stained with CellMask™ Orange 0.5x (Invitrogen) for 10 min at room temperature in obscurity. The uptake of fluorescent NPs was evaluated under inverted fluorescence microscopy (Leica DMI 6000 from Leica), detecting NPs through the GFP channel and CellMask™ stained cells through the TXR channel. Tilescans were captured using the LAS X software.

4.3.4.3 Nanoparticles cytotoxicity profiles

The cytotoxicity of free MUC16-Tn and both MUC16-Tn functionalized and adsorbed NPs were determined by MTT assay. Accordingly, dTHP-1were seeded into 96 well plates at a cell density of 10 000 cells/well, and exposed to increasing doses of free glycopeptides and NPs formulations. After 24 h exposure, conditioned media was replaced by 100 µL fresh culture medium and 10 µL of a 12mM 3-(4,5-dimethylthiazol-2-yl)-2,5-diphenyltetrazolium bromide (MTT, ThermoFisher Scientific) stock solution was added to each well, following a 4 h incubation at 37 °C in a humidified chamber. 75 µL of conditioned medium was

removed from the wells and 50 µL of DMSO (Sigma-Aldrich) was added to solubilize formazan crystals. Plates were incubated at 37 °C for 10 min and absorbances were read at 540 nm in a microplate spectrophotometer. Positive controls (untreated cells; empty NPs exposed cells) and a negative control (cells treated with 1% triton-X 100) were included. Thus, the metabolic activity (%) of living cells was calculated through the following the equation:

$$Metabolic\ activity\ (\%) = \frac{absorvance\ of\ treated\ cells}{absorbance\ of\ positive\ control}\ x\ 100$$

4.3.5 Statistical analysis

Statistical analysis and data mining Statistical analysis was performed using the Student's T-test for unpaired samples. Differences were considered to be significant when $p < 0.05$.

4.4 Results and Discussion

The main goal of this work was to establish nanovaccine constructs for cancer immunotherapy. As proof of concept, we have produced nanovehicles to deliver MUC16-Tn glycoepitopes to antigen presenting cells (APCs). We anticipate that this may constitute an important milestone for developing affective anti-cancer vaccines against this antigen, which is widely expressed in many aggressive solid tumours, including bladder[46], ovarian[47], cervical[48], and lung[49] tumours. Moreover, it may help creating a rationale for exploiting other relevant glycoepitopes for cancer immunotherapy.

4.4.1 Synthesis and Physicochemical characterization

We started by producing MUC16-Tn glycopeptides with the same sequence and glycosylation patterns described in Chapter III and using the single pot chemoenzymatic synthesis method. This strategy allowed to produce multiple glycopeptides carrying different levels of glycosylation, which better reflects the heterogeneous nature at the surface of cancer cells.

In parallel, we have produced PLGA-PEG-MAL nanoparticles by the double emulsion-solvent evaporation technique[55]. Nanoparticles surfaces were subsequentially functionalized with MUC16-Tn glycopeptides, originating PLGA-PEG-MAL-MUC16-Tn

molecular constructs. The cysteine TAG at the reducing end of the glycopeptide was explored towards this end after reduction with TCEP, enabling to control the reaction stoichiometry while allowing a more homogeneous orientation of the glycopeptide upon functionalization. Alternatively, we have also promoted the adsorption of the glycopeptides at the nanoparticles surface, originating PLGA-PEG-MAL/MUC16-Tn molecular assemblies. According to **Figure 9**, using different amounts of glycopeptide (10-40 μg), we obtained similar adsorption and functionalization yields (80-90%) and immobilized a maximum of 36 μg in the nanoparticles for downstream physicochemical evaluation of toxicity and APCs uptake. We have also attempted to encapsulate the glycopeptide in PLGA using the double emulsion method[53,54]; however, with no success (**Figure 9**) reflecting the difficulty to encapsulate highly hydrophilic molecules such as MUC16-Tn in PLGA[55,59]. These observations support the need to adopt alternative scaffolds of more hydrophilic natures such as chitosan[60,61] or liposomes[62-64] for efficient MUC16-Tn encapsulation. Finally, we performed controlled release experiments at physiological pH to estimate the stability of the adsorbed and covalently linked MUC-16-Tn PLGA vehicles. No glycopeptide was release from both constructs over a 72 hours period, suggesting efficient covalent immobilization and high affinity of the glycopeptide to the nanoparticles.

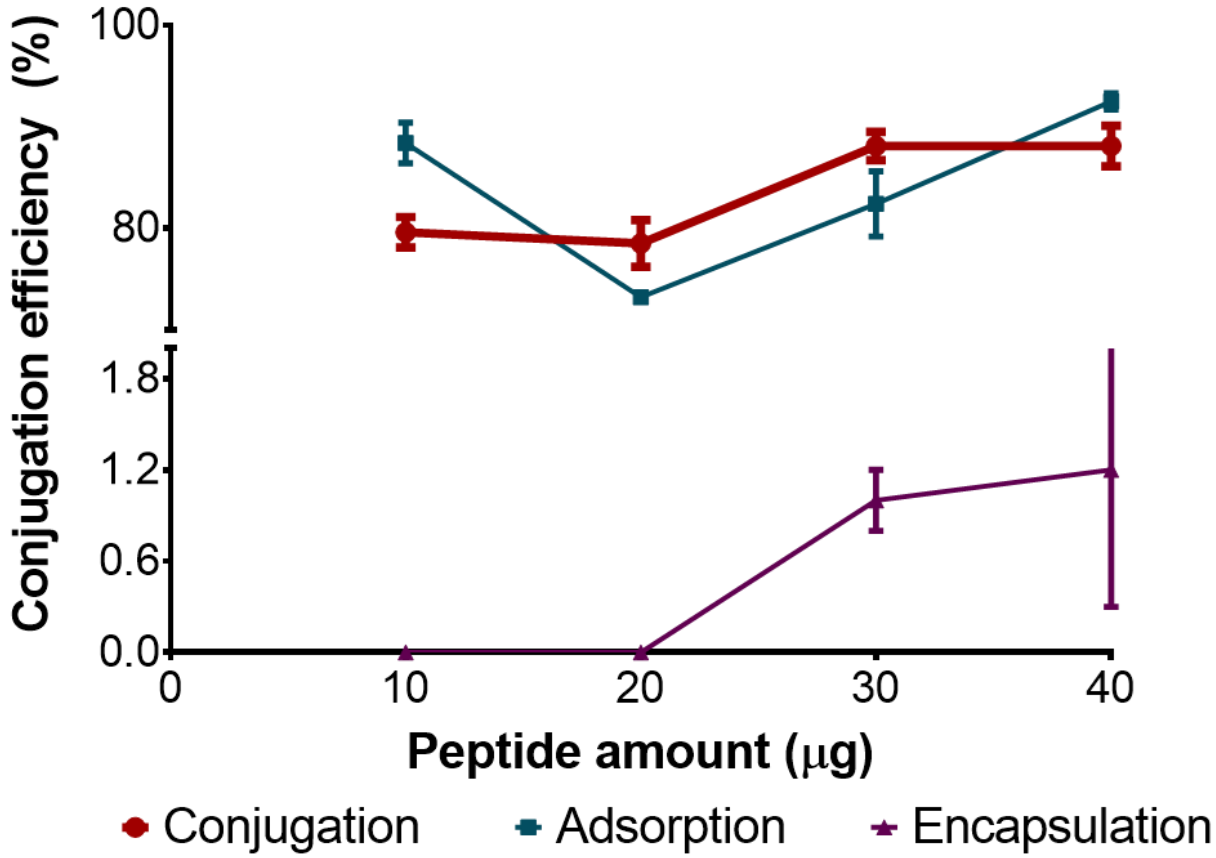

Figure 9. Percentage of MUC16-Tn conjugation (covalent link of MUC16-Tn to the surface of PLGA-PEG-MAL-NPs), adsorption and encapsulation. The amount of MUC16-Tn in the nanoparticles increased with the amount of available MUC16-Tn for conjugated and adsorbed molecular constructs. Contrastingly, PLGA-PEG-MAL did not encapsulate the glycopeptides even in the presence of higher amounts of MUC16-Tn.

Nanoparticles size, as determined by dynamic light scattering (DLS), ranged between 156-199 nm. The polydispersion index (PdI) of NPs suspensions ranged between 0.2 and 0.5, demonstrating little polydispersion in all cases (**Table *4***). Notably, slightly higher dimensions and polydispersion were observed for functionalized nanoparticles (199 nm; 0.5 PdI), supporting the notion that functionalization may contribute to increase the nanoparticles size and originate some degree of heterogeneity (**Table *4***), as highlighted by previous studies[55,65].

Table 4. Properties of PLGA-PEG-MAL, MUC16-Tn functionalized (PLGA-PEG-MAL-MUC16-Tn) and MUC16-Tn adsorbed (PLGA-PEG-MAL/MUC16-Tn) nanoparticles. The values are represented as mean values ± SD (n = 3).

	Size (nm)	PDI	Potential (mV)
PLGA-PEG-MAL	156,1±3,580	0,225±0,007	-0,3777±0,055
PLGA-PEG-MAL-MUC16-Tn	199,3±8,3338	0,503±0,035	-1,264±0,1036
PLGA-PEG-MAL/MUC16-Tn	150,6±4,574	0,294±0,020	-0,6746

Nevertheless, all formulations presented negative zeta potentials, demonstrating stability and low aggregation probability as well as low potential to undergo repulsion by negatively charged cell surfaces[66]. Notably, the presence of MUC16-Tn glycopeptides at the nanoparticles surface significantly contributed towards their stabilization, being more accentuated upon covalent glycopeptide linkage. Furthermore, transmission electron microscopy (TEM) demonstrated similar nanoparticle spherical shape, size range and polydispersion to DLS analysis (**Figure 10A**). Notably, MUC16-Tn containing PLGA nanoparticles also changed their colour from bright white to dark under TEM analysis, supporting the presence of the glycopeptide. Moreover, elementary analysis confirmed an increase in the relative amount of carbon in the nanoparticles carrying MUC16-Tn in comparison to controls (**Figure 10B**), reinforcing the presence of the glycopeptide. In addition, MUC16 functionalized nanoparticles also presented an increased sulfur content consistent with the presence of the cysteine tag at the reducing end. However, sulfur could not be detected in adsorbed MUC16-Tn nanoconstructs, suggesting that adsorption to the nanoparticles may interfere with TEM analysis due to sufur groups sublimation[67].

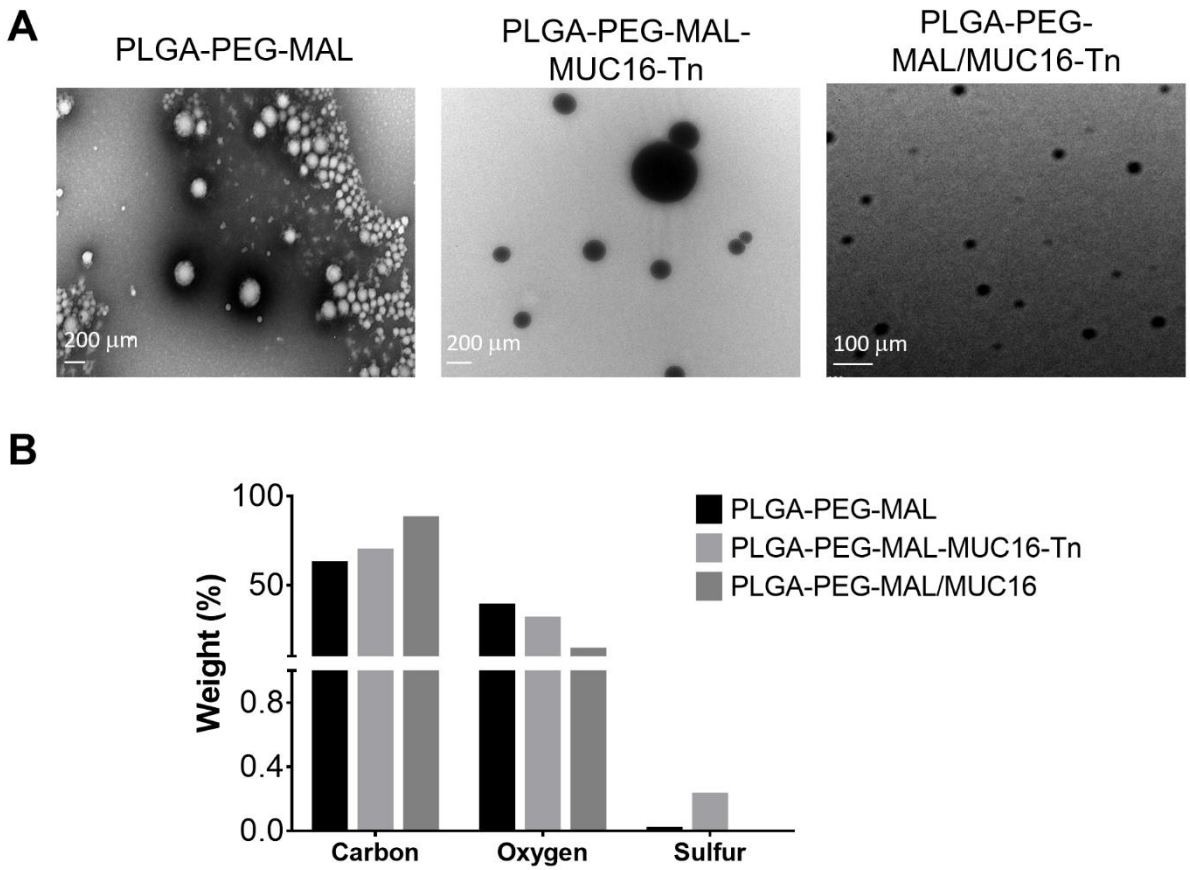

Figure 10. A) Transmission Electron Microscopy (TEM) analysis of PLGA-PEG-MAL, MUC16-Tn functionalized (PLGA-PEG-MAL-MUC16-Tn) and MUC16-Tn adsorbed (PLGA-PEG-MAL/MUC16-Tn) nanoparticles. TEM analysis demonstrating the spherical nature and nanodimensions of PLGA-PEG-MAL-NPs containing either covalently immobilized or adsorbed MUC16-Tn. Notably, nanoformulations presenting MUC16-Tn exhibited a dark nature under TEM analysis, which contrasted with the bright nature of the void nanoparticles, suggesting the presence of MUC16-Tn. **B) Element analysis (carbon, proton, sulfur) for each formulation expressed in terms of relative weight percentage.** An increase in the percentage of carbon for formulations containing MUC16-Tn in comparison to the void PLGA-PEG-MAL nanoparticles was shown. Sulfur from the cysteine tag in the formulations containing MUC16-Tn glycopeptides immobilized by covalent linkage was also detected. Collectively these observations support the presence of MUC16-Tn in the nanoparticles.

Complementary studies by proton NMR were performed to confirm the presence of MUC16-Tn in the nanoconstructs (**Figure 11**). The controls, corresponding to PLGA,

present typical signals between δ4.8-5.3 ppm and a spectral fingerprint in accordance with previous publications[68]. The PLGA-PEG-MAL presented an additional intense signal at δ3.5 ppm characteristic of PEG[69] and at δ1.5 corresponding to MAL[69]. The presence of these signals in the PEG-MAL spectra confirmed the previous assignment. The formulations containing MUC16-Tn glycopeptides presented additional broad signals between δ5.0-5.3 ppm, most likely from the anomeric protons of the GalNAc residue that composes the Tn antigen in different electronic environments[70]. Detected signals between δ3.5-4.0 ppm corresponded to the H2-H6 ring protons of the GalNAc residue[70]. The MUC16-Tn constructs also exhibited a clear signal between δ1.0-1.5 ppm from the NHAc group in GalNAc[70]. Several signals detected between δ3.5-4.0 ppm most likely corresponded to H^{α} protons from amino acids composing the peptide moiety[70]; however, water suppression during spectral acquisition may have hindered some of these signals. Notably, signals between δ2.0-3.0 ppm may also derive from amino acids H^{β} protons[70]. Finally, the spectrum corresponding to the MUC16-adsorbed nanoconstuct showed the MAL signal at δ1.7-1.5 ppm, which disappeared in the functionalized nanoconjugate spectrum, suggesting conjugation. This was accompanied by the appearance of a signal at δ7.5 ppm indicative of maleimide functionalization[69].

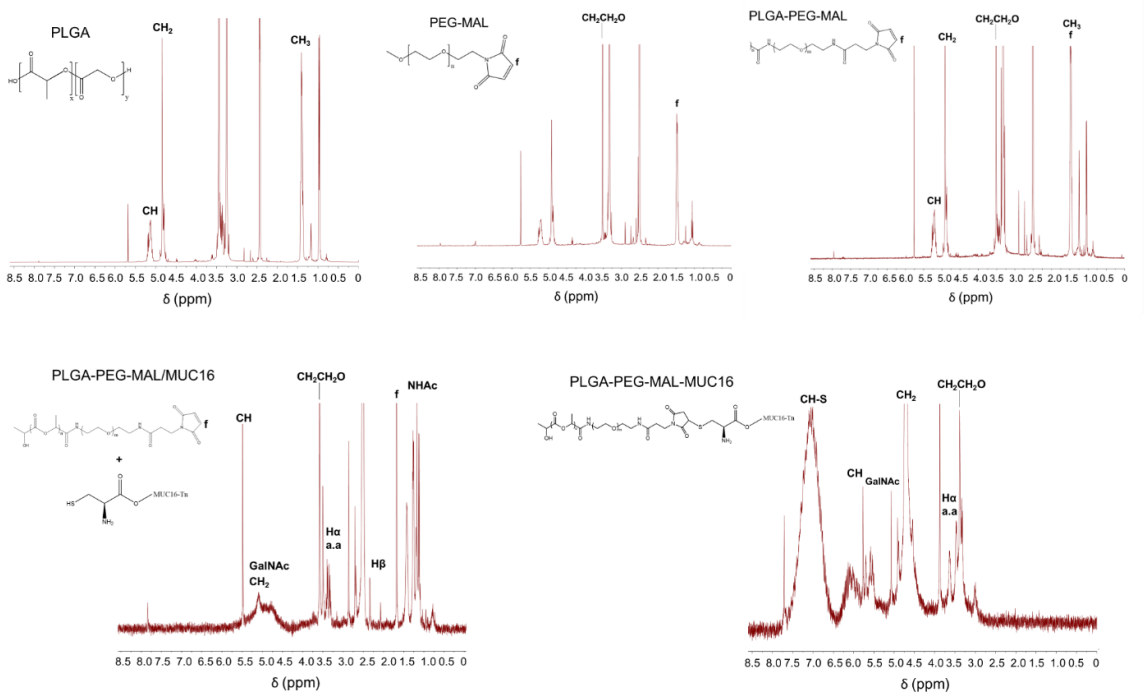

Figure 11. ^{1}H NMR spectra for PLGA, PEG-MAL, PLGA-PEG-MAL-MUC16 (covalent linkage to PLGA) and PLGA-PEG-MAL/MUC16 (adsorbed). The spectra highlight characteristic signals supporting the observed structures, with emphasis on the successful link of MUC16-Tn glycoepitopes to PLGA as well as adsorption to its surface.

4.4.2 Toxicity Profile and Uptake by Macrophages

The cytotoxicity of PLGA-PEG-MAL, PLGA-PEG-MAL-MUC16-Tn and PLGA-PEG-MAL/MUC16-Tn at different concentrations was determined using the metabolic MTT assay, a colorimetric assay assessing cell metabolic activity and reflecting the number of viable cells (**Figure *12*B and C**). The results were confirmed by fluorescence microscopy screening of cell density in the different conditions (**Figure *12*A**). PLGA-PEG-MAL nanoparticles were significantly toxic to THP-1 macrophage-like cells (approximately 70% of cell death), irrespectively of the used concentrations. MUC16-Tn glycopeptides also exhibited significant toxicity, inducing approximately 50% cell death (Figure 4). Our data suggests that MUC16-Tn glycopeptides may potentially have a deleterious effect towards APCs (**Figure *12*B**), which warrants evaluation in future studies. Notably, MUC16 is often subjected to proteolysis at the cell surface, which may potentially induce the release of many glycoforms into circulation[51,71]; nevertheless, the role of these molecules in immune modulation is not yet fully understood. On the other hand, the covalent immobilization of

MUC16 at the surface of nanoparticles or its adsorption induced a protective effect that significantly reduced the toxicity of both PLGA-PEG-MAL and MUC16-Tn for concentrations bellow 2.0 ng/μL of MUC16-Tn (**Figure *12*C**). We then evaluated the uptake of the two constructs (immobilized, adsorbed) by the macrophages at concentrations of 2.0 and 0.2 ng/μL, which was only observed at higher concentrations (**Figure *13***). In summary, we have defined important toxicity limits for the developed nanoformulations and ideal conditions to evaluate uptake by macrophages. The necessary rationale has been established to pursue the evaluation of the nanoformulations capacity to induce immune responses against MUC16-Tn expressing cells.

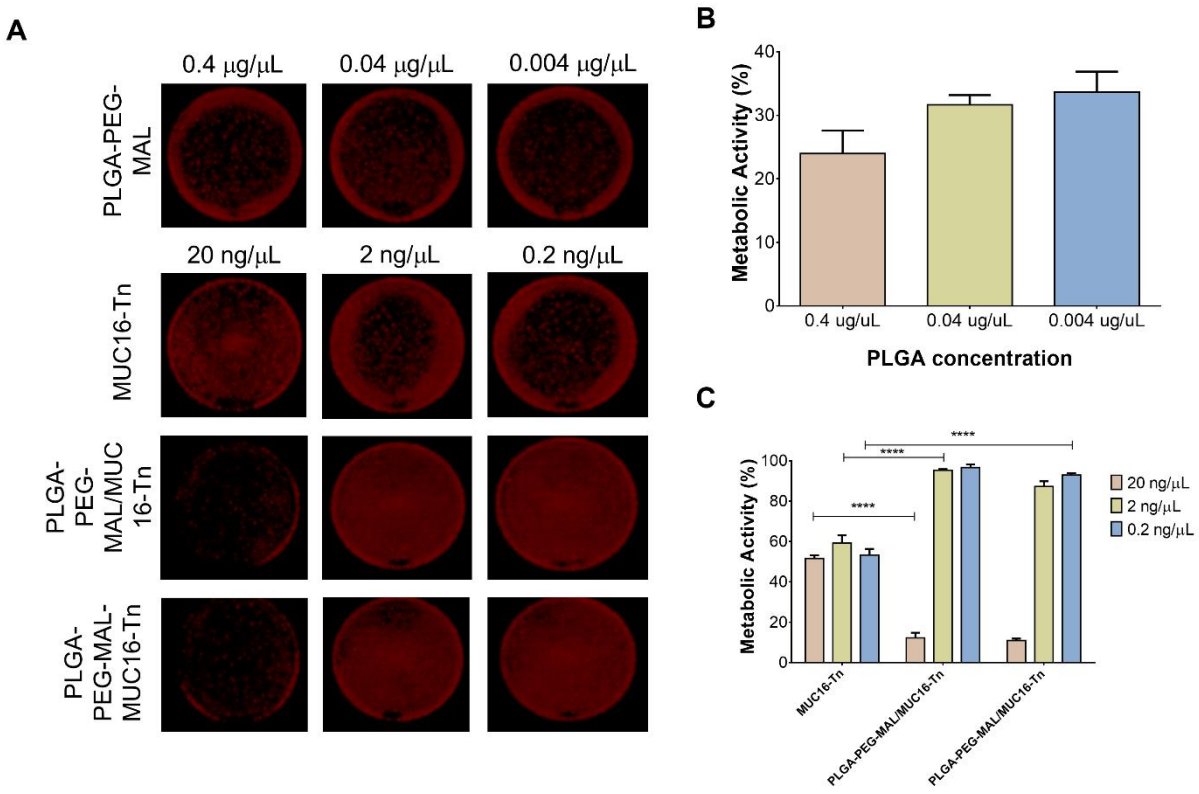

Figure 12. A) Fluorescence microscopy analysis of macrophages exposed to PLGA-PEG-MAL at different concentrations (0.4, 0.04 and 0.004 mg/mL) as well as MUC16-Tn, PLGA-PEG-MAL-MUC16-Tn (conjugation construct) and PLGA-PEG-MAL/MUC16-Tn (adsorption construct) at different MUC16-Tn concentrations (20, 2 and 0.2 ng/mL). B) MTT metabolic assay to assess cellular viability upon nanoconstructs exposure. PLGA-PEG-MAL as well as MUC16-Tn are toxic to TPH-1 cells at all studied concentrations. However, together they exert a co-protective effect that significantly diminishes cellular toxicity. No toxicity was observed for concentrations of 2

and 0.2 ng/μL of MUC16-Tn. Graphs represent the average value of three different replicates and ****p < 0.0001.

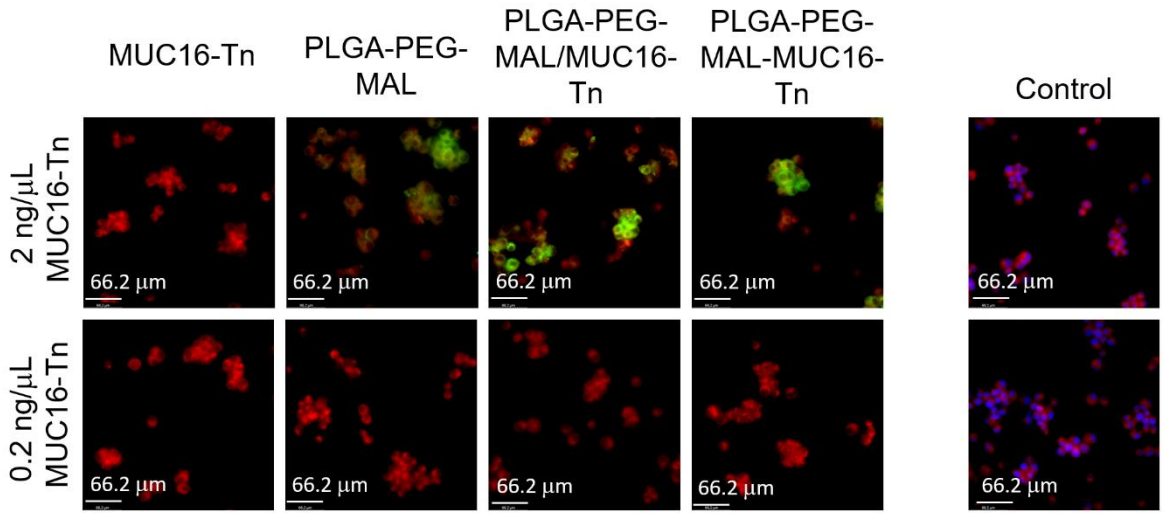

Figure 13. Nanoparticles uptake by macrophages at non-toxic concentrations (2.0 and 0.2ng/ml of MUC16-Tn) observed by immunofluorescence microscopy. Nanoparticles are observed in the green channel (coumarin-6 emission channel), whereas the cells are marked red (Orange CellMask). Control experiments involving non-treated cells were performed in parallel (nuclei stained with DAPI; cytoplasm stained with Orange CellMask). These experiments showed only detectable internalization of nanoparticles by macrophages at 2.0 ng/ml MUC16-Tn concentrations.

4.5 Concluding Remarks

Abnormally glycosylated peptides derived from clinically relevant cancer proteins such as MUC16 provide unique molecular signatures for precise cancer targeting and immunotherapy development[51,72]. Herein, we have explored MUC16-Tn glycopeptides present in more aggressive solid tumours but, to our knowledge, not in healthy tissues. These glycopeptides hold tremendous potential in the context of cancer vaccines once the limitations associated with their immunosuppressive nature are overcome[73,74]. Building on these observations, we have synthesized a wide array of glycoepitopes using as template a 20 amino acid variable tandem repeat sequence of MUC16 containing multiple glycosyation sites (Chapter III). This is expected to reflect the structural heterogeneity at the surface of cancer cells[75,76], enabling the construction of multivalent vaccine constructs.

We have then devoted to developing different PLGA nanovehicles to deliver these glycoepitopes to APCs. Although the exact molecular mechanisms supporting the superior performance of PLGA nanoparticles in comparison to conventional vaccine vehicles are yet to be fully elucidated, several reports demonstrate its potential in this context. Namely, PLGA nanoparticles have been demonstrated to induce enhanced DCs uptake of several active compounds with further T-cells responses activation[77]. Accordingly, we have successfully adsorbed and covalently immobilize MUC16-Tn glycoepitopes at the surface of PLGA-NPs. These constructs have been proven stable at physiological pH, suggesting potential to deliver glycopeptide cargo to APCs, which was reinforced by macrophage internalization assays. Moreover, we have identified important non-cytotoxic concentration thresholds for downstream system characterization *in vitro* as anti-cancer vaccines. Notably, we have attempted to encapsulate MUC16-Tn antigens, providing an alternative administration formulation; however, with limited success, most likely due to the high hydrophilic character of the glycopeptide. These observations support the need to explore alternative and more hydrophilic vehicles such as chitosan or liposomes, also widely used in nanovaccines development[60,61,64]. Also, further NPs functionalization towards more specific APC targeting is warranted. Namely, the use of TLR agonists and co-stimulatory molecules has been proven effective in enhancing APC uptake and subsequent cytotoxic T cells responses[42]. Nevertheless, to our knowledge, this is the first report describing MUC16-Tn-PLGA nanoassemblies, setting the grounds for further studies.

4.6 References

1 Stowell, S. R., Ju, T. & Cummings, R. D. Protein Glycosylation in Cancer. *Annu Rev Pathol* **10**, 473-510, (2016).

2 Ju, T., Wang, Y., Aryal, R. P., Lehoux, S. D., Ding, X., Kudelka, M. R., Cutler, C., Zeng, J., Wang, J., Sun, X., Heimburg-Molinaro, J., Smith, D. F. & Cummings, R. D. Tn and sialyl-Tn antigens, aberrant O-glycomics as human disease markers. *Proteomics - Clinical Applications* **7**, 618-631, (2013).

3 Granovsky, M., Fata, J., Pawling, J., Muller, W. J., Khokha, R. & Dennis, J. W. Suppression of tumor growth and metastasis in Mgat5-deficient mice. *Nat Med* **6**, 306-312, (2000).

4 Duarte, H. O., Balmana, M., Mereiter, S., Osorio, H., Gomes, J. & Reis, C. A. Gastric Cancer Cell Glycosylation as a Modulator of the ErbB2 Oncogenic Receptor. *Int J Mol Sci* **18**, (2017).

5 Pinho, S., Marcos, N. T., Ferreira, B., Carvalho, A. S., Oliveira, M. J., Santos-Silva, F., Harduin-Lepers, A. & Reis, C. A. Biological significance of cancer-associated sialyl-Tn antigen: modulation of malignant phenotype in gastric carcinoma cells. *Cancer Lett* **249**, 157-170, (2007).

6 Ferreira, J. A., Videira, P. A., Lima, L., Pereira, S., Silva, M., Carrascal, M., Severino, P. F., Fernandes, E., Almeida, A., Costa, C., Vitorino, R., Amaro, T., Oliveira, M. J., Reis, C. A., Dall'Olio, F., Amado, F. & Santos, L. L. Overexpression of tumour-associated carbohydrate antigen sialyl-Tn in advanced bladder tumours. *Mol Oncol* **7**, 719-731, (2013).

7 Davidson, B., Berner, A., Nesland, J. M., Risberg, B., Berner, H. S., Trope, C. G., Kristensen, G. B., Bryne, M. & Ann Florenes, V. E-cadherin and alpha-, beta-, and gamma-catenin protein expression is up-regulated in ovarian carcinoma cells in serous effusions. *J Pathol* **192**, 460-469, (2000).

8 Magalhaes, A., Duarte, H. O. & Reis, C. A. Aberrant Glycosylation in Cancer: A Novel Molecular Mechanism Controlling Metastasis. *Cancer Cell* **31**, 733-735, (2017).

9 Hakomori, S. Glycosylation defining cancer malignancy: New wine in an old bottle. *Proceedings of the National Academy of Sciences* **99**, 10231-10233, (2002).

10 Handerson, T., Camp, R., Harigopal, M., Rimm, D. & Pawelek, J. Beta1,6-branched oligosaccharides are increased in lymph node metastases and predict poor outcome in breast carcinoma. *Clin Cancer Res* **11**, 2969-2973, (2005).

11 Kudelka, M. R., Ju, T., Heimburg-Molinaro, J. & Cummings, R. D. *Simple sugars to complex disease-mucin-type O-glycans in cancer*. 1 edn, Vol. 126 (Elsevier Inc., 2015).

12 Giuntoli, R. L., Rodriguez, G. C., Whitaker, R. S., Dodge, R. & Voynow, J. A. Mucin Gene Expression in Ovarian Cancers. *Cancer Research* **58**, 5546-5550, (1998).

13 Reis, C. A., Osorio, H., Silva, L., Gomes, C. & David, L. Alterations in glycosylation as biomarkers for cancer detection. *Journal of Clinical Pathology* **63**, 322-329, (2010).

14 Steentoft, C., Vakhrushev, S. Y., Joshi, H. J., Kong, Y., Vester-Christensen, M. B., Schjoldager, K. T., Lavrsen, K., Dabelsteen, S., Pedersen, N. B., Marcos-Silva, L., Gupta, R., Bennett, E. P., Mandel, U., Brunak, S., Wandall, H. H., Levery, S. B. & Clausen, H. Precision mapping of the human O-GalNAc glycoproteome through SimpleCell technology. *EMBO J* **32**, 1478-1488, (2013).

15 Julien, S., Videira, P. A. & Delannoy, P. Sialyl-Tn in cancer: (How) did we miss the target? *Biomolecules* **2**, 435-466, (2012).

16 Hollingsworth, R. E. & Jansen, K. Turning the corner on therapeutic cancer vaccines. *npj Vaccines* **4**, 7, (2019).

17 Tagliamonte, M., Petrizzo, A., Tornesello, M. L., Buonaguro, F. M. & Buonaguro, L. Antigen-specific vaccines for cancer treatment. *Hum Vaccin Immunother* **10**, 3332-3346, (2014).

18 Guo, C., Manjili, M. H., Subjeck, J. R., Sarkar, D., Fisher, P. B. & Wang, X. Y. Therapeutic cancer vaccines: past, present, and future. *Adv Cancer Res* **119**, 421-475, (2013).

19 Kumai, T., Kobayashi, H., Harabuchi, Y. & Celis, E. Peptide vaccines in cancer-old concept revisited. *Curr Opin Immunol* **45**, 1-7, (2017).

20 Zhang, Y., Lin, S., Wang, X. Y. & Zhu, G. Nanovaccines for cancer immunotherapy. *Wiley Interdiscip Rev Nanomed Nanobiotechnol* **11**, e1559, (2019).

21 Moingeon, P. Cancer vaccines. *Vaccine* **19**, 1305-1326, (2001).

22 Ibrahim, N. K., Murray, J. L., Zhou, D., Mittendorf, E. A., Sample, D., Tautchin, M. & Miles, D. Survival Advantage in Patients with Metastatic Breast Cancer Receiving

Endocrine Therapy plus Sialyl Tn-KLH Vaccine: Post Hoc Analysis of a Large Randomized Trial. *J Cancer* **4**, 577-584, (2013).

23 O'Cearbhaill, R. E., Ragupathi, G., Zhu, J., Wan, Q., Mironov, S., Yang, G., Spassova, M. K., Iasonos, A., Kravetz, S., Ouerfelli, O., Spriggs, D. R., Danishefsky, S. J. & Sabbatini, P. J. A Phase I Study of Unimolecular Pentavalent (Globo-H-GM2-sTn-TF-Tn) Immunization of Patients with Epithelial Ovarian, Fallopian Tube, or Peritoneal Cancer in First Remission. *Cancers (Basel)* **8**, (2016).

24 Miles, D. W. & Taylor-Papadimitriou, J. Mucin based breast cancer vaccines. *Expert Opin Investig Drugs* **7**, 1865-1877, (1998).

25 RodrIguez, E., Schetters, S. T. T. & van Kooyk, Y. The tumour glyco-code as a novel immune checkpoint for immunotherapy. *Nat Rev Immunol* **18**, 204-211, (2018).

26 Perdicchio, M., Ilarregui, J. M., Verstege, M. I., Cornelissen, L. A., Schetters, S. T., Engels, S., Ambrosini, M., Kalay, H., Veninga, H., den Haan, J. M., van Berkel, L. A., Samsom, J. N., Crocker, P. R., Sparwasser, T., Berod, L., Garcia-Vallejo, J. J., van Kooyk, Y. & Unger, W. W. Sialic acid-modified antigens impose tolerance via inhibition of T-cell proliferation and de novo induction of regulatory T cells. *Proc Natl Acad Sci U S A* **113**, 3329-3334, (2016).

27 van Kooyk, Y. & Rabinovich, G. A. Protein-glycan interactions in the control of innate and adaptive immune responses. *Nat Immunol* **9**, 593-601, (2008).

28 Aarnoudse, C. A., Garcia Vallejo, J. J., Saeland, E. & van Kooyk, Y. Recognition of tumor glycans by antigen-presenting cells. *Curr Opin Immunol* **18**, 105-111, (2006).

29 Carrascal, M. A., Severino, P. F., Guadalupe Cabral, M., Silva, M., Ferreira, J. A., Calais, F., Quinto, H., Pen, C., Ligeiro, D., Santos, L. L., Dall'Olio, F. & Videira, P. A. Sialyl Tn-expressing bladder cancer cells induce a tolerogenic phenotype in innate and adaptive immune cells. *Mol Oncol* **8**, 753-765, (2014).

30 Takamiya, R., Ohtsubo, K., Takamatsu, S., Taniguchi, N. & Angata, T. The interaction between Siglec-15 and tumor-associated sialyl-Tn antigen enhances TGF-beta secretion from monocytes/macrophages through the DAP12-Syk pathway. *Glycobiology* **23**, 178-187, (2013).

31 Shao, K., Singha, S., Clemente-Casares, X., Tsai, S., Yang, Y. & Santamaria, P. Nanoparticle-based immunotherapy for cancer. *ACS Nano* **9**, 16-30, (2015).

32 Zhang, R., Billingsley, M. M. & Mitchell, M. J. Biomaterials for vaccine-based cancer immunotherapy. *J Control Release* **292**, 256-276, (2018).

33 Zhu, G., Zhang, F., Ni, Q., Niu, G. & Chen, X. Efficient Nanovaccine Delivery in Cancer Immunotherapy. *ACS Nano* **11**, 2387-2392, (2017).

34 Fontana, F., Liu, D., Hirvonen, J. & Santos, H. A. Delivery of therapeutics with nanoparticles: what's new in cancer immunotherapy? *Wiley Interdisciplinary Reviews: Nanomedicine and Nanobiotechnology* **9**, 1-26, (2017).

35 Joshi, M. D., Unger, W. J., Storm, G., Van Kooyk, Y. & Mastrobattista, E. Targeting tumor antigens to dendritic cells using particulate carriers. *Journal of Controlled Release* **161**, 25-37, (2012).

36 Krishnamachari, Y., Geary, S. M., Lemke, C. D. & Salem, A. K. Nanoparticle delivery systems in cancer vaccines. *Pharmaceutical Research* **28**, 215-236, (2011).

37 Rosalia, R. A., Cruz, L. J., van Duikeren, S., Tromp, A. T., Silva, A. L., Jiskoot, W., de Gruijl, T., Lowik, C., Oostendorp, J., van der Burg, S. H. & Ossendorp, F. CD40-targeted dendritic cell delivery of PLGA-nanoparticle vaccines induce potent anti-tumor responses. *Biomaterials* **40**, 88-97, (2015).

38 Ma, W., Chen, M., Kaushal, S., McElroy, M., Zhang, Y., Ozkan, C., Bouvet, M., Kruse, C., Grotjahn, D., Ichim, T. & Minev, B. PLGA nanoparticle-mediated delivery of tumor antigenic peptides elicits effective immune responses. *International Journal of Nanomedicine* **7**, 1475-1487, (2012).
39 Zhang, Z., Tongchusak, S., Mizukami, Y., Kang, Y. J., Ioji, T., Touma, M., Reinhold, B., Keskin, D. B., Reinherz, E. L. & Sasada, T. Induction of anti-tumor cytotoxic T cell responses through PLGA-nanoparticle mediated antigen delivery. *Biomaterials* **32**, 3666-3678, (2011).
40 Silva, A. L., Soema, P. C., Slütter, B., Ossendorp, F. & Jiskoot, W. PLGA particulate delivery systems for subunit vaccines: Linking particle properties to immunogenicity. *Human Vaccines and Immunotherapeutics* **12**, 1056-1069, (2016).
41 Allahyari, M. & Mohit, E. Peptide/protein vaccine delivery system based on PLGA particles. *Human Vaccines and Immunotherapeutics* **12**, 806-828, (2016).
42 Cruz, L. J., Tacken, P. J., Eich, C., Rueda, F., Torensma, R. & Figdor, C. G. Controlled release of antigen and Toll-like receptor ligands from PLGA nanoparticles enhances immunogenicity. *Nanomedicine (Lond)* **12**, 491-510, (2017).
43 Hamdy, S., Molavi, O., Ma, Z., Haddadi, A., Alshamsan, A., Gobti, Z., Elhasi, S., Samuel, J. & Lavasanifar, A. Co-delivery of cancer-associated antigen and Toll-like receptor 4 ligand in PLGA nanoparticles induces potent CD8+ T cell-mediated anti-tumor immunity. *Vaccine* **26**, 5046-5057, (2008).
44 Schmid, D., Park, C. G., Hartl, C. A., Subedi, N., Cartwright, A. N., Puerto, R. B., Zheng, Y., Maiarana, J., Freeman, G. J., Wucherpfennig, K. W., Irvine, D. J. & Goldberg, M. S. T cell-targeting nanoparticles focus delivery of immunotherapy to improve antitumor immunity. *Nat Commun* **8**, 1747, (2017).
45 Chesson, C. B. & Zloza, A. Nanoparticles: augmenting tumor antigen presentation for vaccine and immunotherapy treatments of cancer. *Nanomedicine (Lond)* **12**, 2693-2706, (2017).
46 Cotton, S., Azevedo, R., Gaiteiro, C., Ferreira, D., Lima, L., Peixoto, A., Fernandes, E., Neves, M., Neves, D., Amaro, T., Cruz, R., Tavares, A., Rangel, M., Silva, A. M. N., Santos, L. L. & Ferreira, J. A. Targeted O-glycoproteomics explored increased sialylation and identified MUC16 as a poor prognosis biomarker in advanced-stage bladder tumours. *Mol Oncol* **11**, 895-912, (2017).
47 Theriault, C., Pinard, M., Comamala, M., Migneault, M., Beaudin, J., Matte, I., Boivin, M., Piche, A. & Rancourt, C. MUC16 (CA125) regulates epithelial ovarian cancer cell growth, tumorigenesis and metastasis. *Gynecol Oncol* **121**, 434-443, (2011).
48 Shen, H., Guo, M., Wang, L. & Cui, X. MUC16 facilitates cervical cancer progression via JAK2/STAT3 phosphorylation-mediated cyclooxygenase-2 expression. *Genes Genomics*, (2019).
49 Kanwal, M., Ding, X. J., Song, X., Zhou, G. B. & Cao, Y. MUC16 overexpression induced by gene mutations promotes lung cancer cell growth and invasion. *Oncotarget* **9**, 12226-12239, (2018).
50 Duffy, M. J., Bonfrer, J. M., Kulpa, J., Rustin, G. J., Soletormos, G., Torre, G. C., Tuxen, M. K. & Zwirner, M. CA125 in ovarian cancer: European Group on Tumor Markers guidelines for clinical use. *Int J Gynecol Cancer* **15**, 679-691, (2005).
51 Felder, M., Kapur, A., Gonzalez-Bosquet, J., Horibata, S., Heintz, J., Albrecht, R., Fass, L., Kaur, J., Hu, K., Shojaei, H., Whelan, R. J. & Patankar, M. S. MUC16

(CA125): tumor biomarker to cancer therapy, a work in progress. *Mol Cancer* **13**, 129, (2014).

52 Vasudev, N. S., Trigonis, I., Cairns, D. A., Hall, G. D., Jackson, D. P., Broadhead, T., Buxton, J., Hutson, R., Nugent, D. & Perren, T. J. The prognostic and predictive value of CA-125 regression during neoadjuvant chemotherapy for advanced ovarian or primary peritoneal carcinoma. *Arch Gynecol Obstet* **284**, 221-227, (2011).

53 Gomes, M. J., Kennedy, P. J., Martins, S. & Sarmento, B. Delivery of siRNA silencing P-gp in peptide-functionalized nanoparticles causes efflux modulation at the blood-brain barrier. *Nanomedicine (Lond)* **12**, 1385-1399, (2017).

54 Sousa, F., Cruz, A., Fonte, P., Pinto, I. M., Neves-Petersen, M. T. & Sarmento, B. A new paradigm for antiangiogenic therapy through controlled release of bevacizumab from PLGA nanoparticles. *Sci Rep* **7**, 3736, (2017).

55 Fernandes, E., Ferreira, D., Peixoto, A., Freitas, R., Relvas-Santos, M., Palmeira, C., Martins, G., Barros, A., Santos, L. L., Sarmento, B. & Ferreira, J. A. Glycoengineered nanoparticles enhance the delivery of 5-fluoroucil and paclitaxel to gastric cancer cells of high metastatic potential. *Int J Pharm* **570**, 118646, (2019).

56 Esfandyari-Manesh, M., Mostafavi, S. H., Majidi, R. F., Koopaei, M. N., Ravari, N. S., Amini, M., Darvishi, B., Ostad, S. N., Atyabi, F. & Dinarvand, R. Improved anticancer delivery of paclitaxel by albumin surface modification of PLGA nanoparticles. *Daru* **23**, 28, (2015).

57 Zimmermann, J. L., Nicolaus, T., Neuert, G. & Blank, K. Thiol-based, site-specific and covalent immobilization of biomolecules for single-molecule experiments. *Nat Protoc* **5**, 975-985, (2010).

58 Fessi, H., Puisieux, F., Devissaguet, J. P., Ammoury, N. & Benita, S. Nanocapsule formation by interfacial polymer deposition following solvent displacement. *International Journal of Pharmaceutics* **55**, R1-R4, (1989).

59 Cohen-Sela, E., Chorny, M., Koroukhov, N., Danenberg, H. D. & Golomb, G. A new double emulsion solvent diffusion technique for encapsulating hydrophilic molecules in PLGA nanoparticles. *J Control Release* **133**, 90-95, (2009).

60 Banerjee, T., Mitra, S., Kumar Singh, A., Kumar Sharma, R. & Maitra, A. Preparation, characterization and biodistribution of ultrafine chitosan nanoparticles. *International Journal of Pharmaceutics* **243**, 93-105, (2002).

61 Calvo, P., Remuñán-López, C., Vila-Jato, J. L. & Alonso, M. J. Novel hydrophilic chitosan-polyethylene oxide nanoparticles as protein carriers. *Journal of Applied Polymer Science* **63**, 125-132, (1997).

62 Martins, S., Sarmento, B., Ferreira, D. C. & Souto, E. B. Lipid-based colloidal carriers for peptide and protein delivery--liposomes versus lipid nanoparticles. *Int J Nanomedicine* **2**, 595-607, (2007).

63 Ma, L., Kohli, M. & Smith, A. Nanoparticles for combination drug therapy. *ACS Nano* **7**, 9518-9525, (2013).

64 Fernandes, E., Ferreira, J. A., Andreia, P., Luis, L., Barroso, S., Sarmento, B. & Santos, L. L. New trends in guided nanotherapies for digestive cancers: A systematic review. *J Control Release* **209**, 288-307, (2015).

65 Kennedy, P. J., Perreira, I., Ferreira, D., Nestor, M., Oliveira, C., Granja, P. L. & Sarmento, B. Impact of surfactants on the target recognition of Fab-conjugated PLGA nanoparticles. *Eur J Pharm Biopharm* **127**, 366-370, (2018).

66 Gupta, V. & Trivedi, P. in *Lipid Nanocarriers for Drug Targeting* (ed Alexandru Mihai Grumezescu) 563-627 (William Andrew Publishing, 2018).

67 Levin, B. D., Zachman, M. J., Werner, J. G., Sahore, R., Nguyen, K. X., Han, Y., Xie, B., Ma, L., Archer, L. A., Giannelis, E. P., Wiesner, U., Kourkoutis, L. F. & Muller, D. A. Characterization of Sulfur and Nanostructured Sulfur Battery Cathodes in Electron Microscopy Without Sublimation Artifacts. *Microsc Microanal* **23**, 155-162, (2017).

68 Pereira, E. D., Cerruti, R., Fernandes, E., Peña, L., Saez, V., Pinto, J. C., Ramón, J. A., Oliveira, G. E. & Souza Júnior, F. G. d. Influence of PLGA and PLGA-PEG on the dissolution profile of oxaliplatin. *Polímeros* **26**, 137-143, (2016).

69 Ji, S., Zhu, Z., Hoye, T. R. & Macosko, C. W. Maleimide Functionalized Poly(epsilon-caprolactone)-b-poly(ethylene glycol) (PCL-PEG-MAL): Synthesis, Nanoparticle Formation, and Thiol Conjugation. *Macromol Chem Phys* **210**, 823, (2009).

70 Mortezai, N., Behnken, H. N., Kurze, A. K., Ludewig, P., Buck, F., Meyer, B. & Wagener, C. Tumor-associated Neu5Ac-Tn and Neu5Gc-Tn antigens bind to C-type lectin CLEC10A (CD301, MGL). *Glycobiology* **23**, 844-852, (2013).

71 Das, S., Majhi, P. D., Al-Mugotir, M. H., Rachagani, S., Sorgen, P. & Batra, S. K. Membrane proximal ectodomain cleavage of MUC16 occurs in the acidifying Golgi/post-Golgi compartments. *Sci Rep* **5**, 9759, (2015).

72 Aithal, A., Rauth, S., Kshirsagar, P., Shah, A., Lakshmanan, I., Junker, W. M., Jain, M., Ponnusamy, M. P. & Batra, S. K. MUC16 as a novel target for cancer therapy. *Expert Opin Ther Targets* **22**, 675-686, (2018).

73 McDonald, D. M., Byrne, S. N. & Payne, R. J. Synthetic self-adjuvanting glycopeptide cancer vaccines. *Front Chem* **3**, 60, (2015).

74 Rao Koganty, R., Reddish, M. A. & Michael Longenecker, B. Glycopeptide-and carbohydratebased synthetic vaccines for the immunotherapy of cancer. *Drug Discovery Today* **1**, 190-198, (1996).

75 Christiansen, M. N., Chik, J., Lee, L., Anugraham, M., Abrahams, J. L. & Packer, N. H. Cell surface protein glycosylation in cancer. *Proteomics* **14**, 525-546, (2014).

76 Hakomori, S. Glycosylation defining cancer malignancy: new wine in an old bottle. *Pnas* **99**, 10231-10233, (2002).

77 Jia, J., Zhang, Y., Xin, Y., Jiang, C., Yan, B. & Zhai, S. Interactions Between Nanoparticles and Dendritic Cells: From the Perspective of Cancer Immunotherapy. *Front Oncol* **8**, 404, (2018).

CHAPTER V

Glycoengineered cell model overexpressing Tn antigen for functional assays and potentially immunotherapy development

Glycoengineered cell model overexpressing Tn antigen for functional assays and potentially immunotherapy development

Rui Freitas[a,b,*], Andreia Peixoto[a,c,d,e,*], Elisabete Fernandes[a,c,d,] , Dylan Ferreira[a,c,d], Marta Relvas-Santos[a,c,d,e,f], Carlos Palmeira[a,h,i], Flávia Castro[c,d,e], Maria José Oliveira[c,d,g], Andre M. N.Silva[f], Lúcio Lara Santos[a ,e,i,j,k], Bruno Sarmento[c,d], José Alexandre Ferreira[a,e,k]

[a]Experimental Pathology and Therapeutics Group, Portuguese Institute of Oncology, 4200-162 Porto, Portugal; [b]QOPNA & LAQV-REQUIMTE, Department of Chemistry, University of Aveiro, Aveiro, Portugal; [c]Institute for Research and Innovation in Health (i3s), University of Porto, 4200-135 Porto, Portugal; [d]Institute for Biomedical Engineering (INEB), Porto, Portugal, 4200-135 Porto, Portugal; [e]Institute of Biomedical Sciences Abel Salazar (ICBAS), University of Porto, 4050-013 Porto, Portugal; [f]REQUIMTE-LAQV, Department of Chemistry and Biochemistry, Faculty of Sciences of the University of Porto, 4069-007 Porto, Portugal; [g]Department of Oncology and Pathology, Faculty of Medicine, University of Porto,4200-319 Porto, Portugal; [h]Immunology Department, Portuguese Institute of Oncology of Porto, 4200-162 Porto, Portugal; [i]Health Science Faculty, University of Fernando Pessoa, 4249-004 Porto, Portugal; [j]Department of Surgical Oncology, Portuguese Institute of Oncology of Porto, 4200-162 Porto, Portugal; [k]Porto Comprehensive Cancer Centre (P.ccc), 4200-162 Porto, Portugal;

*Equal Contribution

Corresponding author:

José Alexandre Ferreira (jose.a.ferreira@ipoporto.min-saude.pt)

Experimental Pathology and Therapeutics Group, Research Centre, Portuguese Oncology Institute of Porto, R. Dr. António Bernardino de Almeida 62, 4200-162 Porto, Portugal; Tel. +351 225084000 (ext. 5111).

Keywords: Tn antigen, glycoengineering, dendritic cells, cancer glycosylation, short glycans

5.1 Abstract

Cancer cells overexpress at the cell surface glycoproteins yielding short-chain *O*-glycans such as the Tn antigen, which result from a premature stop in protein glycosylation. These alterations are frequently found in more advanced solid tumours of different natures and associated with worst prognosis. Moreover, these glycans are not found or just residually expressed in healthy tissues, holding enormous potential for targeted therapeutics and immunotherapy. However, the functional implications of Tn antigen expression in cancer cells, including its relevance in the context of immune modulation, remains poorly understood. Envisaging the clarification of Tn antigen functional impact and to provide a cell model supporting the development of innovative glycan-based therapeutics, we have glycoengineered the T24 urothelial cell line using CRISPR/Cas9 technology for *C1GALT1* knockout (T24 C1GALT1 KO), precluding *O*-glycan elongation beyond Tn and sialyl-Tn antigens. Immunofluorescence microscopy and flow cytometry analysis using VVA lectin demonstrated high levels of Tn antigen at the cell surface. Notably, this antigen was only residually detected in T24 wild type cells (T24 WT). Complementary glycomics analysis confirmed the loss of more extended glycans in T24 C1GALT1 KO cells. Tn antigen expression had no impact on cell proliferation, migration or invasion. Moreover, it did not change the expression of HLA-ABC, CD47 and PD-L1 immunomodulators, which constitute key promotors of cancer cell immune escape. Furthermore, Tn overexpressing cells co-culture with dendritic cells (DC) could have induced DC dedifferentiation, translated by the loss of CD11c lineage marker, while downregulating CD86 and HLA-DR responsible for antigen presentation. Collectively, our data also supports that these effects cannot be fully rescued by stimulation with LPS, which warrants confirmation in future studies. These observations suggest that the Tn antigen may contribute to dampen anti-cancer immune responses and provide a critical model to develop innovative immunotherapies targeting this antigen.

5.2 Introduction

Most advanced stage solid tumours overexpress short-chain glycans such as the Tn and sialyl-Tn (STn) antigens, as result of a premature stop in protein *O*-glycosylation. In

cancer, these events have been mainly associated to the following events: i) miss-localization of different glycosyltransferases across the endoplasmic reticulum and Golgi apparatus[1,2]; ii) changes in the expression of glycogenes encoding enzymes involved in glycan biosynthesis[3,4]; iii) Fluctuations in nucleotide sugar donors abundance in response to microenvironmental stimuli such as oxygen and nutrient levels[5,6]; iv) *ST6GALNAC1* overexpression, leading to Tn antigen sialylation and abrogation of further extension[2,7]; v) mutation or promoter hypermethylation of *COSMC* gene, encoding a highly relevant T synthase chaperone; thereby, compromising T antigen biosynthesis and consequently exacerbating Tn and STn precursors [8,9]. Increased levels of short-chain *O*-glycans in solid tumours are generally associated with higher metastatic potential and decreased survival[10-12]. Moreover, even though abundantly expressed in cancer tissues of different origins, the presence of short chain glycans is rarely detected in healthy tissues, making them attractive targets for cancer therapy[13]. Of note, short *O*-GalNAc glycans are also absent from most cancer cell models, suggesting a dependence on specific microenvironmental cues. In line with this, several studies support the pivotal role of cross-talks between the immune and cancer cells under inflammatory conditions[14,15]. Moreover, hypoxia, a common feature of advanced stage tumours, is also amongst the events suggested to antagonize *O*-glycan extension by downregulating key enzymes involved in glycan elongation[6]. While much effort has been put in understanding the microenvironmental promoters of altered glycosylation, glycoengineered cell lines remain an important tool to gain insights on the functional relevance of glycans in cancer[16,17]. In fact, distinct cell models (gastric, colorectal, bladder, prostate) engineered to overexpress *ST6GALNAC1* consensually highlighted an increase in migration, invasion and activation of relevant oncogenic pathways[18-21], decisively demonstrating the key role played by altered glycosylation in cancer. Moreover, STn-expressing cancer cells impaired DC maturation, while promoting a more tolerogenic phenotype and limiting their capacity to trigger protective anti-tumour T cell responses[19]. As such, the STn antigen and, in particular, STn (+) glycoproteins are regarded as potential targets for circumventing tumour-induced tolerogenic mechanisms. On the other hand, the functional role of Tn antigen is much less understood. The Tn antigen has been regarded as promoter of metastasis via H-Ras mediated epithelial-mesenchymal transition in colorectal cancer[22]. In addition, MUC1-Tn glycoforms may be recognized by Galectin-3, contributing to metastatic extravasation[23]. The Tn antigen may also be recognized by the C-type

macrophage galactose binding lectin (MGL) expressed in DC and macrophages, leading to immunosuppressive effects that enable tumour cells to escape immunosurveillance[24-26]; however, the role of Tn in immunological responses against cancer cells remains poorly understood. As such, more studies are required to fully characterize its functional implications in different models, including a more precise characterization of Tn antigen immunological relevance towards more effective cancer immunotherapies.

Based on these observations, the present work concerns the development of a CRISPR-Cas9 glycoengineered cell model overexpressing the Tn antigen. Emphasis is set on exploiting the aggressive T24 cancer cell model envisaging more insights on Tn functional role in advanced bladder cancer, where it is widely expressed [27]. We also aim to provide bases for understanding DC immune response to Tn (+) cancer cells, while providing a model for novel immunotherapies testing.

5.3 Material and Methods

5.3.1 Cell lines and culture conditions

The T24 bladder cancer cell line was acquired from DSMZ (Düsseldorf, Germany) and recently characterized and authenticated by our group[28]. T24 CIGALT1 knock-out (KO) cells were glycoengineered in-house by CRISPR Cas-9 modification of T24 cells. Both cell lines were cultured in RPMI 1640 + GlutaMAX™ medium (Gibco™, Thermo Fisher Sientific) supplemented with 10% heat-inactivated FBS (GibcoTM, Thermo Fisher Sientific) and 1% penicillin-streptomycin (10,000 Units/mL penicillin; 10,000 µg/mL streptomycin; Gibco™, Thermo Fisher Sientific). Cell lines were cultured as a monolayer at 37°C in a 5% CO2 humidified atmosphere.

5.3.2 CRISPR Cas-9 glycoengineered cell models

T24 cells were plated onto 24-well plates to be 70% confluent at the time of transfection. A recombinant *Streptococcus pyogenes* Cas9 (GeneArt™ Platinum Cas9 Nuclease, Thermo Fisher Scientific) together with a single-guided RNA (GTAAAGCAGGGCTACATGAG sgRNA) were used to generate site-specific DSBs in the *C1GALT1* gene *in vitro*. Lipofectamine™ CRISPRMAX™ Transfection Reagent (Thermo Fisher Scientific) was used according to the manufacturer's instructions. Complexes were

made in serum-free medium (Opti-MEM™ I Reduced Serum Medium), added directly to cells in culture medium and incubated for 24h.

5.3.3 *C1GALT1* mutation analysis

Genomic DNA from wild-type T24 and T24 C1GALT1 KO cells was purified using the GRS Genomic DNA Kit (GRISP Research Solutions), according to the manufacturer's instructions. Mutation screening of the *C1GALT1* gene was performed by Sanger sequencing. For this purpose, primers (**Table 1**) were designed using the Primer-BLAST design tool from the National Center for Biotechnology Information (NCBI)[29]. For PCR product amplification, a PCR reaction setup was prepared according to **Table 2** and a thermocycler was used for an initial denaturation step at 95°C for 15 min, followed by 35 cycles with denaturation at 95°C for 30s, annealing at appropriate temperature (59°C) for 30s and extension at 72°C for 45s. A final extension step at 72°C for 9 min was included. The amplification was confirmed by electrophoresis in a 2% (w/v) agarose gel stained with SYBR safe DNA gel stain (Thermo Fisher Scientific). The PCR product was purified using a exonuclease I (20µg/µl) (Thermo Fisher Scientific) and Fast Thermosensitive Alkaline Phosphatase (1µg/µl) (Thermo Fisher Scientific) mix, in a proportion of 1:2. The purification was carried out in a thermocycler at 37ºC for 50 min for proper enzyme activity, followed by 15 minutes at 85ºC for enzymes inactivation. For this reaction, 2µl of ExoSap mix was added to 5µl of PCR product, allowing the degradation of unincorporated primers and nucleotides. The DNA amplicons were sequenced using the BigDye® Terminator v3.1 Cycle Sequencing Kit from AppliedBiosystems® (Life Technologies), according to **Table 3**. The thermocycler PCR program consisted on an initial denaturation step at 96ºC for 10 min, followed by 35 cycles of denaturation at 96ºC for 10 sec, annealing at 52ºC for 5 sec and extension at 60ºC for 6 min. In order to reduce possible contaminants, the sequencing product was purified with IIlustra Sephadex® G-50 fine columns (GE Healthcare, Life Sciences, Cleveland, USA), according to the manufacturer 's instructions. Finally, to stabilize the DNA, samples were eluted in 15µl of deionized formamide (Applied Biosystems). The sequencing was performed on a 3500 Genetic Analyzer (Thermo Fisher Scientific) and CRISPR editing results were analysed with ICE from Synthego[30].

Table 5. Primer sequences used for sequencing C1GALT1 gene

	Primer sequence
Primer Forward	5'-CCGGCCCTCAAAACCTAGAG-3'
Primer Reverse	5'-TGCATCTCCCCAGTGCTAAG-3'

Table 6. Amplification PCR reaction setup

Component	**20 µl -rxn**
ddH_2O	To 20µl
10X PCR Buffer	2 µl
10 mM dNTP Mix	1 µl
25 mM $MgCl_2$	2 µl
10 µM forward primer	1 µl
10 µM reverse primer	1 µl
Template DNA	0.5µl
AmpliTaq Gold DNA Polymerase (5U/µl)	0.2µl

Table 7. BigDye™ Terminator v3.1 Cycle Sequencing reaction

Component	**10 µl -rxn**
BigDye® Mix	0.5µl
5X Sequencing Buffer	3.4µl
Primer	0.5µl
ddH_2O	4.78µl
PCR product	1µl (75 ng)

5.3.4 *O*-glycomics

T24 WT and C1GALT1 KO cells *O*-glycome was characterized using Cellular *O*-glycome Reporter/Amplification method, as previously described[31]. Briefly, benzyl 2-acetamido-2-deoxy-α-D-galactopyranoside (Sigma-Aldrich) was peracetylated and administered to semi-confluent cells to a final concentration of 150 µM. Following 24h incubation, glycans were isolated from the conditioned media by filtration using 10 kDa centrifugal filter (Amicon Ultra-4, Merck Millipore) followed by reversed-phase chromatography in Sep-Pak 3 cc C18 cartridges (Waters). Finally, Bn-*O*-glycans were permethylated and analyzed by nanoLC-ESI-MS/MS using a nanoLC system (Dionex, 3000 Ultimate nano-LC) coupled online to an LTQ-Orbitrap XL mass spectrometer (Thermo Scientific) equipped with a nano-electrospray ion source (Thermo Scientific, EASY-Spray source). Eluent A was aqueous formic acid (0.2%) and eluent B was formic acid (0.2%) in

acetonitrile. Samples (20 µl) were injected directly into a trapping column (C18 PepMap 100, 5 µm particle size) and washed with an isocratic flux of 90% eluent A and 10% eluent B at a flow rate of 30 µl/min. After 3 minutes, the flux was redirected to the analytical column (EASY-Spray C18 PepMap, 100 Å, 150 mm × 75µm ID and 3 µm particle size) at a flow rate of 0.3 µl/min. Column temperature was set at 35°C. Permethylated glycan separation occurred using a multistep linear gradient to obtain 10% eluent B at 10 min, 38% eluent B at 20 min, 50% eluent B at 55 min and 90% eluent B at 65 min. The column was maintained at90% eluent B for 10 min before re-equilibration at 10% eluent B. The mass spectrometer was operated in the positive ion mode, with a spray voltage of 1.9 kV and a transfer capillary temperature of 250°C. Tube lens voltage was set to 120 V and the capillary voltage to 9 V. MS survey scans were acquired at an Orbitrap resolution of 60,000 for an *m/z* range from 300 to 2000. Tandem MS (MS/MS) data was acquired in the linear ion trap using a data dependent method with dynamic exclusion. The top 6 most intense ions were selected for collision induced dissociation (CID). CID settings were 35% normalized collision energy, 2 Da isolation window 30 ms activation time and an activation Q of 0.250. A window of 90 s was used for dynamic exclusion. Automatic Gain Control (AGC) was enabled and target values were 1.00e+6 for the Orbitrap and 1.00e+4 for LTQ MS analysis. Data were recorded with Xcalibur software version 2.1. Glycan structures were assigned based on characteristic product ion spectra and previous knowledge about *O*-glycosylation pathways [31]. Glycans were expressed in terms of relative abundance in comparison to the sum of all individual contributions to the glycome.

5.3.5 Glycoproteomics

Proteins were extracted from the cells using $20x10^6$ cells by scrapping with fractionation buffer (20mM HEPES buffer (pH=7.4), 10mM KCl, 2mM $MgCl_2$, 1mM EDTA and 1mM EGTA) on ice. Cell suspension was then passed through a 27G needle and left on ice for 20 min. Samples were then centrifuged at 720 x g for 5 min at 4ºC to remove nuclei, transferred to a fresh tube and recentrifuged at 10.000 x g for 5 min at 4ºC to remove mitochondria. Samples were transferred to polycarbonate centrifuge bottles with cap assemblies and centrifuged for 1h at 100.000g at 4ºC in a Beckman Coulter Optima L-XP series ultracentrifuge. Pellets were resuspended in fractioning buffer and passed through a 25G needle before centrifugation for 45 min at 100.000g at 4ºC. Finally, pellets were resuspended in an appropriate volume of TBS/0.1% SDS. MUC16 was isolated from plasma

membrane enriched extracts (200 μg) by immunoprecipitation using the anti-CA125 (MUC16) monoclonal antibody [sc-365002] (Santa Cruz Biotechnology) immobilized at the surface of magnetic beads using the Pierce™ Direct IP Kit (26148, ThermoFisher Scientific) according to the manufacturer's instructions. Glycoproteins were reduced with 5 mM DTT (Sigma-Aldrich) for 40 minutes at 60ºC, alkylated with 10 mM iodocetamide for 45 minutes in the dark (Sigma-Aldrich) and digested with trypsin as previously described by us[32]. NanoLC-nES-MS/MS analysis and protein identifications were carried out according to the conditions previously described by us[27]. Data was analyzed automatically using the SequestHT search engine with the Percolator algorithm for validation of protein identifications (Proteome Discoverer 2.3.0.523, Thermo Scientific). Data was searched against the human proteome obtained from the SwissProt database in 10/25/2019, selecting trypsin as the enzyme and allowing up to 2 missed cleavage sites and a precursor ion mass tolerance of 10 ppm and 0.6 Da for product ions. Carbamidomethylcysteine was selected as a fixed modification while oxidation of methionine (+15.99491) was defined as variable modification. An ultra-tolerant database search was then applied for glycosites annotation also comprehending substitutions of serine and threonine with HexNAc (+203.079; Tn antigen). In this case, protein grouping filters were set to consider peptide-to-spectrum matches (PSMs) with low confidence and ΔCn better than 0.05 to accommodate limitations associated with glycopeptides annotation based on CID fragmentation[27,33]. At least two PSMs per protein were required and the strict maximum parsimony principle was applied for positive protein annotation. Accordingly, the glycopeptide annotations list included high and medium/low confidence identifications. For definitive confirmation, all low scoring glycopeptides were subjected to additional manual confirmation.

5.3.6 Cell proliferation assay

Cell proliferation was evaluated using the colorimetric Cell Proliferation ELISA, BrdU kit (Roche, Sigma-Aldrich) based on the measurement of the incorporation of bromodeoxyuridine (BrdU, a synthetic nucleoside analogue of thymidine) into newly synthesized DNA of proliferative cells. Procedure steps were followed according to the manufacturer's instructions and results were monitored at 450 nm using a microplate reader (iMARK™, Bio-Rad). All experiments were performed in triplicates.

5.3.7 Invasion assay

Invasion assays were performed using BD Biocoat Matrigel^{TM} invasion chambers as described in Peixoto *et al.(2016)*[6]. Prior to each experiment, invasion chambers were re-hydrated in RPMI 1640 + GlutaMAX^{TM} medium for 2 h at 37 ºC. After detachment of subconfluent cells with trypsin/EDTA, cells were resuspended in culture medium and seeded on the upper side of the matrigel-coated filter at a density of 5 x 10^4 cells/well. After 24 h at 37 ºC, filters were fixed in 4% paraformaldehyde and non-invading cells were completely removed by washing and scrubbing to facilitate analysis. The Matrigel coated filters were mounted with VECTASHIELD® mounting medium with DAPI (Vector Laboratories, CA, USA) and visualized through a Zeiss Axiovert 200M fluorescence microscope (Carl Zeiss, Germany). Invasive cells were scored in at least 12 microscopic fields (20x objective). Results are presented as mean ± SD. Triplicate experiments were performed for each cell line.

5.3.8 Migration assay

Wound healing assays were performed using specific wound assay chambers (Ibidi) containing silicone inserts delimiting a fixed gap of 500 µm. Cells were seeded to confluence within the silicone inserts, which were removed after cell attachment to allow cell migration towards the gap. Cells were monitored until gap closure under an inverted microscope (Motic, AE2000). Images were captured with a Moticam 5 camera (Motic, CMOS). Triplicate experiments were performed for each cell line.

5.3.9 Immunofluorescence for Tn and MUC16-Tn expression detection

In order to evaluate Tn antigen and MUC16 expressions, T24 and T24 C1GALT1 KO cell lines were cultured at low density and fixed with 4% paraformaldehyde (PFA; Sigma-Aldrich), following immunofluorescent staining. Namely, cells were stained with FITC – label *Vicia Villosa Lectin* (VVA; FL-1231 Vector Laboratories) 0,01 µg/µL in PBS 2% FBS or anti-MUC16 antibody (1:20; HPA065600; Sigma-Aldrich) for 1 hour at room temperature. The goat anti-rabbit IgG (H+L), Alexa Fluor 594 (1:300; A11012; Thermo Fisher Scientific) was used as a secondary antibody for MUC16 detection and incubated 30 minutes at room temperature in obscurity. After antigen staining, cells were marked with 2,3x10^{-3} µg/µL 4',6-Diamidino-2-Phenylindole, Dihydrochloride (DAPI, Thermo Fisher

Scientific) for 10 minutes at room temperature in the dark. All images were acquired on a Leica DMI6000 FFW microscope using Las X software (Leica).

5.3.10 Human monocyte isolation and DC differentiation

Human monocytes were isolated from buffy coats from healthy blood donors, as described in *Cardoso et al. (2014)*[34]. Briefly, peripheral blood mononuclear cells (PBMC) were collected from centrifuged buffy coats (30 min, 1200xg, RT, without brake) and incubated with RosetteSep human monocyte enrichment kit (StemCell Technologies), according to manufacturer's instructions. The mixture was diluted 1:1 with PBS supplemented with 2% FBS, layered over Histopaque-1077 (Sigma-Aldrich) and centrifuged in the same conditions. The enriched monocyte layer was collected and washed with PBS. For monocyte-DC differentiation, $2.0x10^6$ monocytes/9.6 cm2 (6-wells plate) were differentiated for 5 days in complete RPMI 1640 medium further supplemented with 50 ng/mL IL-4 and GM-CSF (Immunotools).

5.3.11 Co-culture of DC and bladder cancer cell lines

Co-cultures of DC with bladder cancer cell lines were established as described in *Carrascal et al.(2014)*[19]. Briefly, $1x10^5$ bladder cancer cells were plated in 24-well plates and co-cultured with DC in the proportion of 1:5 (cancer cell: DCs) in adhesion buffer (20 mmol/l of trizma-HCl, 150 mmol/l of sodium chloride, 1 mmol/l calcium chloride, 1 mmol/l magnesium chloride and 0.5% BSA, pH 8.0) and culture medium (1:2) for 2h or 24h. After washing, DC were detached with PBS on ice for 10 minutes.

5.3.12 Flow cytometry

DCs activation was assessed by immunostaining with Allophycocyanin (APC)-labelled antibody against CD11c (21487116, Immunotools), fluorescein isothiocyanate (FITC) – labelled antibody against CD86 (21480863, Immunotools) and Phycoerythrin (PE) – labelled antibody against HLA-DR (21278994, Immunotools), all in a 1:25 dilution in PBS 2% FBS 0.01% sodium azide (FACS buffer). Cells were incubated with appropriate conjugated antibodies in the dark for 40 minutes at 4°C. To define background staining isotype-matched antibodies were used as negative controls. Cells were analysed on a FACS

Canto Flow Cytometer and data was mined using ImageJ 1.43u software. For Tn, CD47, HLA-ABC and PDL1 expression evaluation, T24 and T24 C1GALT1 KO cells were detached using Versene 1X solution (Thermo Fisher, Waltham, MA,USA), fixed with 2% paraformaldehyde (PFA; Sigma-Aldrich) and stained. FITC – label *Vicia Villosa Lectin* (VVA; FL-1231 Vector Laboratories) 0,01 μg/μL in PBS 2% FBS was used for Tn detection for 1 hour at room temperature. FITC – labelled antibody against CD47 (21270473, Immunotools), FITC – labelled antibody against PDL1 (558065, Immunotools) and PE – labelled antibody against HLA-ABC (21159034, Immunotools) were used for immunoregulatory molecules measurements for 45 minutes at 4°C at 1:25 dilution in FACS buffer. Cells were analysed on a FC500 Flow Cytometer (Beckman Coulter) and data was mined using CXP Software.

5.3.13 Statistical analysis

Statistical analysis and data mining Statistical analysis was performed using the Student's T-test for unpaired samples. Differences were considered to be significant when $p < 0.05$.

5.4 Results and discussion

The main objective of this work was to develop a cell model expressing the Tn antigen that could be used to gain more insights on the functional implications of Tn expression in cancer and ultimately support the development of innovative glycan-based immunotherapies. As such, we have stably glycoengineered the T24 urothelial cancer cell line using CRISPR/Cas9 technology towards Tn antigen overexpression. The T24 cell line is amongst the most explored models of bladder cancer aggressiveness, reflecting the FGFR3/CCND1 carcinogenesis pathway, while having mutated HRAS. Preliminary studies did not identify the Tn antigen in this cell line using different anti-Tn monoclonal antibodies (clone 5F4 and IE3 data not shown). Nevertheless, Tn antigen is significantly overexpressed in more aggressive bladder tumours, reinforcing the relevance of inducing Tn expression in cancer cell models. Tn-expressing cell models were then explored to understand the contribution of short-chain *O*-glycans to cell proliferation, migration and invasion, which are critical aspects underlying disease development and poor outcomes. The stablished model was also used to define the Tn antigen contribution to the immunological profile of

cells, namely concerning the expression of relevant molecules for immune escape (HLA-ABC, CD47, PDL1) and dendritic cells activation. These findings are expected to provide the necessary rationale for testing *in vitro* the anti-Tn vaccine constructs developed in previous chapters.

5.4.1 CRISPR/Cas 9 Glycoengineering

The genome of T24 cells was glycoengineered by gene edition with CRISPR/Cas 9 using a single guide RNA targeting the *C1GALT1* gene, which encodes the main glycosyltransferase responsible by Tn elongation towards more complex glycan structures. After transfection, *C1GALT1* CRISPR/Cas 9 knockouts were screened for specific mutations in this gene. Preliminary analysis by agarose gel electrophoresis after genomic DNA probing with specific *C1GALT1* oligonucleotides has revealed a complete 400bp amplicon for T24 wild type cells (T24 WT), while a significant percentage of T24 C1GALT1 KO cells displays a considerably smaller amplicon, suggesting successful editing (**Figure 14A**). Subsequentially, genomic sequencing and data mining through ICE analysis retrieved a knock-out score of 83%, confirming successful genome editing (**Figure 14B**).

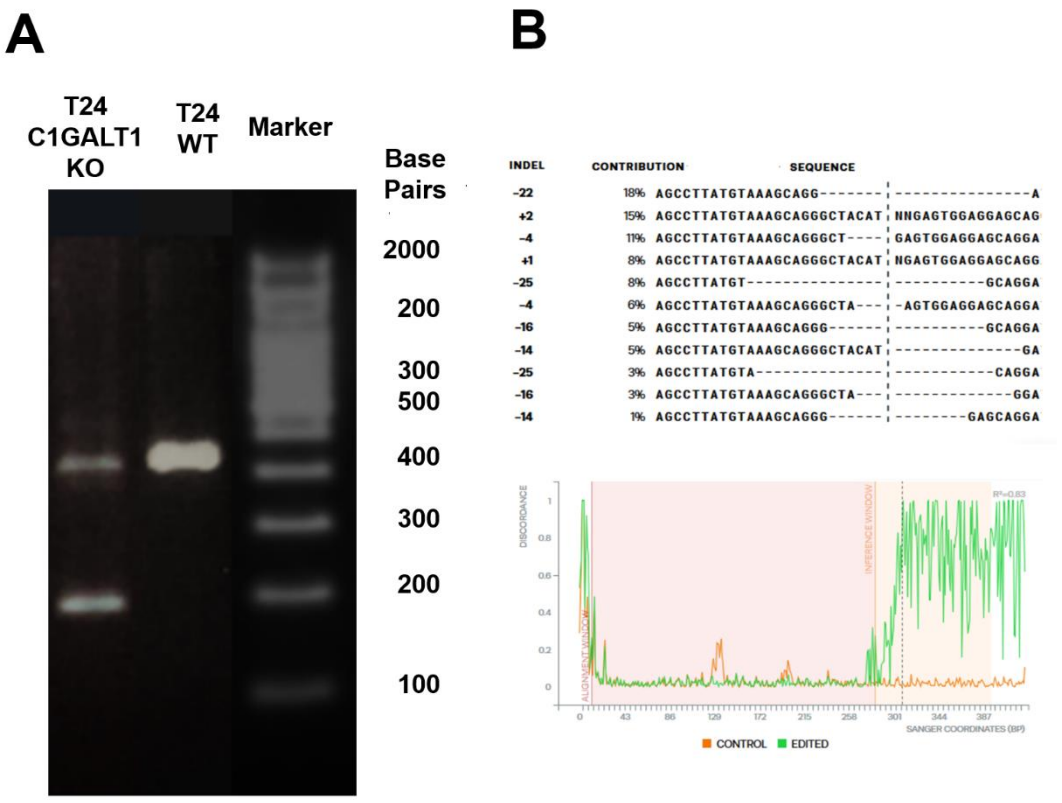

Figure 14. A) Agarose gel electrophoresis for C1GALT1 amplified amplicons in T24 WT and C1GALT1 KO cells. Specific primer selection led to the amplification of a pure 456bp PCR product in both cell lines. Moreover, a significant decrease in product length was observed for T24 C1GALT1 KO, suggesting considerable genome editing. **B) C1GALT1 gene sequencing for T24 WT and C1GALT1 KO cells highlighting gene edited areas**. The cut sites are represented by black vertical dotted lines in the top panel. The lower panel corresponds to a discordance plot, detailing the level of alignment per base between T24 WT (control) and the T24 C1GALT1 KO (edited) cell lines for the inference window (the region around the cute site). The green and orange lines are close together before the cut site. CRISPR editing led to an increase in discordance near the cut site and beyond, confirming successful editing.

5.4.2 Glycomics

T24 WT and T24 C1GALT1 KO cells were first screened for Tn expression by VVA lectin immunofluorescence microscopy. As highlighted by **Figure 15A**, T24 WT cells did not express detectable Tn antigen levels, reinforcing previous preliminary data from our

group (data not shown). Flow cytometry analysis showed very residual Tn expressions in approximately 40% of T24 WT cells, confirming these observations (**Figure 15B**). Contrastingly, all T24 C1GALT1 cells exhibited the Tn antigen at the cell membrane and, to some extent, in the cytoplasm, most likely in proteins being processed across the secretory pathways. Flow cytometry analysis confirmed a tremendous increase in Tn expression (300 times higher that T24 WT) in all analysed cells.

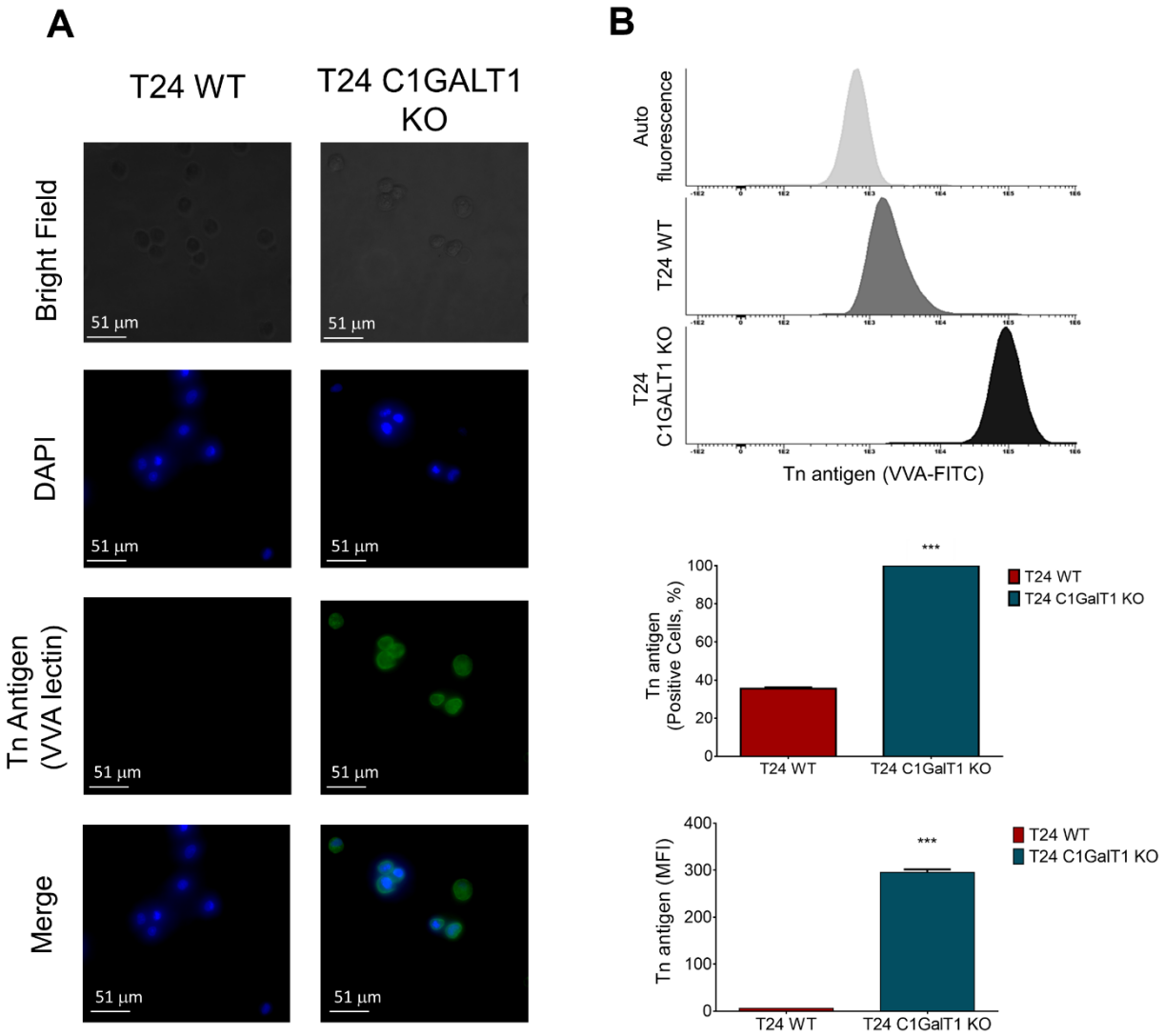

Figure 15. **A) Tn antigen expression in T24 WT and T24 C1GALT1 KO cells by immunofluorescence microscopy using the VVA lectin.** The image confirms the lack of detectable Tn antigen in T24 WT and its expression in T24 C1GALT1 KO at the cell surface. **B) Flow cytometry analysis for the Tn antigen in T24 WT and T24 C1GALT1 KO cells using the VVA lectin.** Flow cytometry analysis supports the massive increase in Tn expression in T24 C1GALT1 KO cells suggested by fluorescence microscopy. Graphs represent average value of three independent experiments, *p < 0.05; **p < 0.01; ***p < 0.001 (Student's T-test).

T24 WT and C1GALT1 KO cells were then characterized in relation to the capacity to extend *O*-glycosylation by glycomics analysis. Briefly, a Tn glycan mimetic capable of being processed by the glycosylation machinery along the secretory pathways and

subsequently secreted into the cell medium was used towards this end. The glycans were then recovered from the culture medium, permethylated and analyzed by ESI-MS/MS. According to Figure 16, T24 cells mainly express T antigen (m/z 572.3) and to less extent its fucosylated (m/z 746.4), mono (m/z 933.5) and disialylated (m/z 1294.7) forms. Residual amounts of more elongated core 2 glycans were also detected (m/z 991.5; 1021.5; 1195.6; 1369.7; 1382.7; 1470.8; 1556.8; 1644.8; 1743.9). In addition, this cell line also expressed significant amounts of the core 3 antigen (m/z 613.3) and residual amounts of the STn antigen (m/z 729.4), implicated in an onset of malignant features in bladder cancer[6,35,36]. On the other hand, T24 C1GALT1 KO cells significantly decreased the total amount of complex sugars, losing the capacity to produce core 2 glycans such as the T antigen, significantly reducing core 3 glycans expression as well as more extended structures. Taken together with immunofluorescence microscopy and flow cytometry analysis, these findings support the successful induction of a simple cell glycosidic phenotype in T24 cells, characterized by a profound remodeling of the cell-surface glycome towards Tn expression.

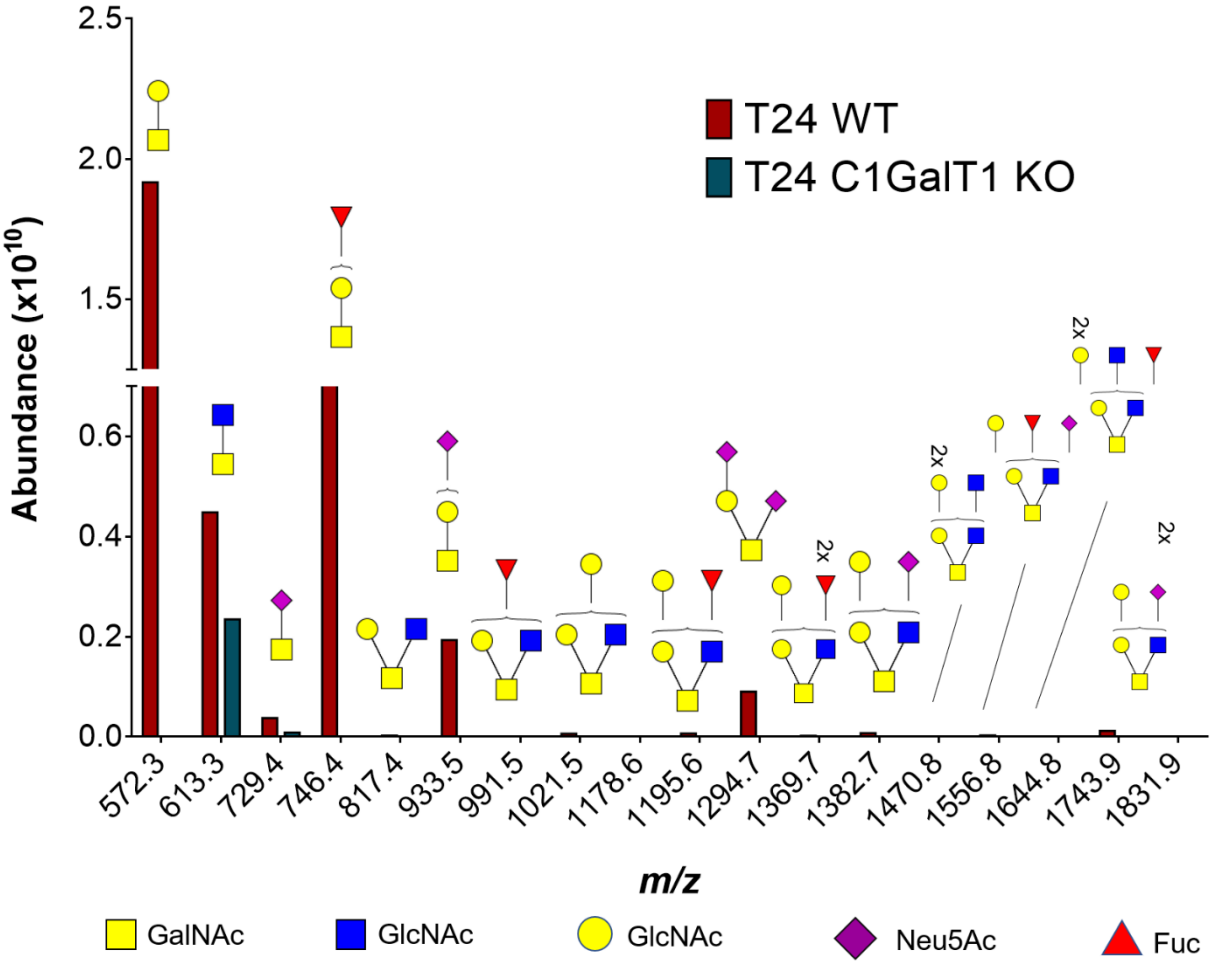

Figure 16. Glycomics analysis for T24 WT and C1GALT1 KO cells. C1GALT1 KO cells almost completely obliterated *O*-glycans extension, with the exception of residual expression of STn (m/z 729.4) and core 3 (m/z 613.3) glycans, which were extend by an alternative biosynthesis route.

5.4.3 MUC16 expression in T24 C1GALT1 KO cells

Previous studies have shown that MUC16 is a major carrier of abnormal short-chain glycosylation in T24 cells, in more aggressive bladder tumours[27] and several other solid tumors[37-39]. As such, in Chapters III and IV we have developed different potential vaccine constructs based on cancer-associated MUC16 glycoepitopes (KLH-MUC16 glycoconjugates, MUC16-Tn grafted and MUC16-Tn adsorbed PLGA nanoconstructs). As such, we have devoted to confirming the expression of these glycoforms in the T24 C1GALT1 KO model foreseeing its future exploitation in the establishment of innovative glycan-based vaccines. Fluorescence microscopy screening of both T24 WT and T24 C1GALT1 KO cells demonstrated the presence of MUC16 in more than 40% of analyzed

cells (**Figure 17A**). The glycoprotein was mainly detected in the cytoplasm and at the cell membrane; however, without clear membrane definition (**Figure 17A**). Notably, MUC16 co-localized with Tn antigen expression in the T24 C1GALT1 KO model (**Figure 17A**). The presence of MUC16 in the cytoplasm may be associated with the detection of the glycoprotein in traffic to the cell membrane, as described in previous reports[40,41]. However, the lack of clear membrane reinforcement may also suggest that the glycoprotein may be experience proteolysis at the cell membrane, also as previously described[42]. Notably, in this study we have used an antibody targeting the CA125 antigen, a MUC16 glycoform associated with cancer[43,44]; however, the exact nature of the glycoepitope targeted by the antibody has not been disclosed. Nevertheless, MUC16 may present a wide array of distinct proteoforms resulting from different processing events associated to significant glycosylation density and glycan diversity, which makes its detection based on antibodies a challenging task[2,45]. As such, complementary immunoassays involving a wider panel of well characterized monoclonal antibodies targeting different regions of the protein should be performed in the future. Therefore, to confirm the existence of MUC16-Tn membrane glycopeptides, MUC16 was isolated by immunoprecipitation from T24 C1GALT1 KO membrane protein enriched extracts and then reduced, alkylated, digested with trypsin and analyzed by nanoLC-ESI-MS/MS. This enabled the identification of MUC16-Tn glycopeptides, confirming the expression of MUC16 short-chain proteoglycoforms, as translated by the MS/MS spectra presented in Figure 17B. These observations suggest that T24 C1GALT1 KO cells may be a good model to test formulations targeting the MUC16-Tn antigen.

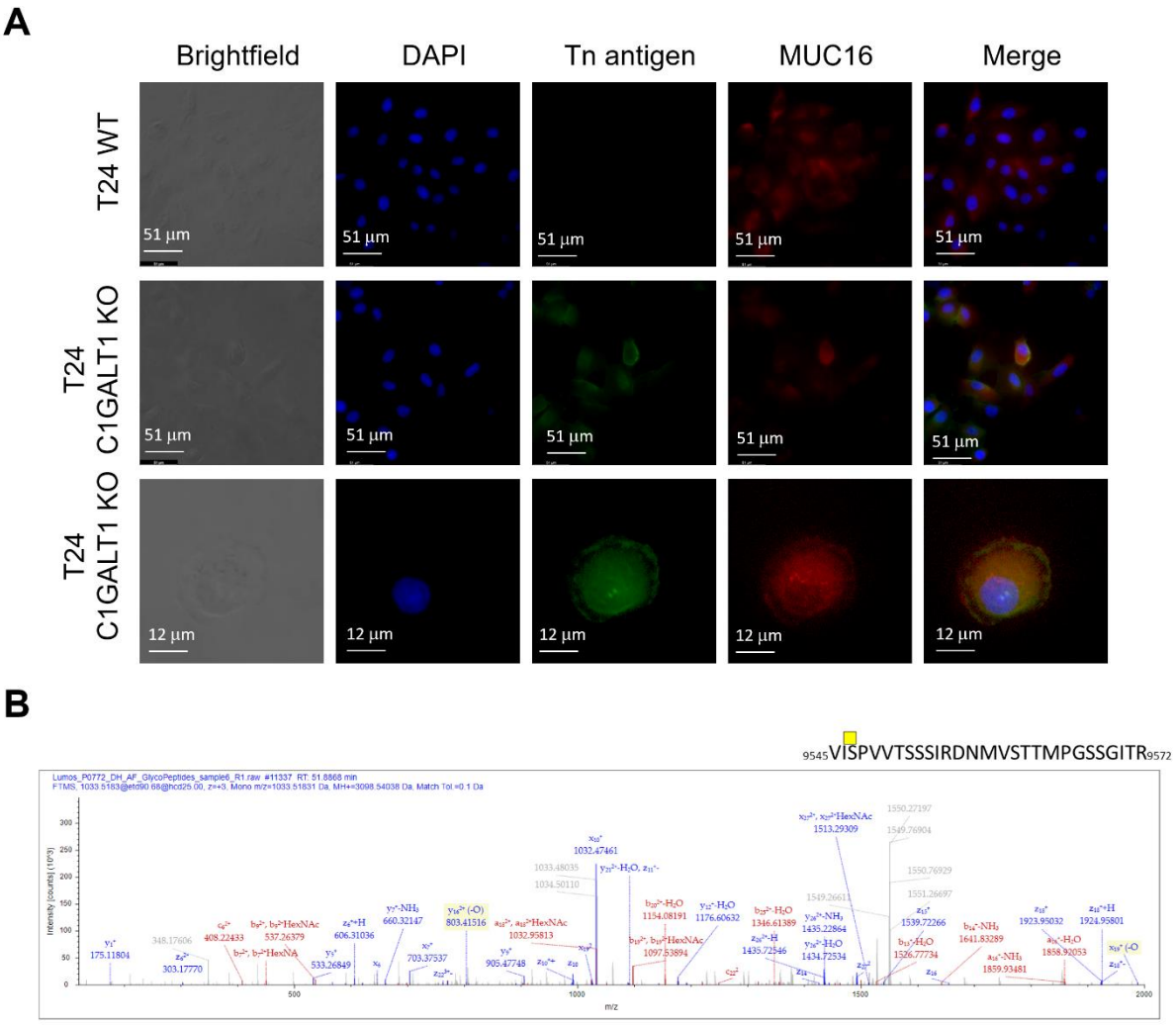

Figure 17. A) Tn antigen and MUC16 expressions in T24 WT and C1GALT1 KO cells by immunofluorescence microscopy. The Tn antigen was only detected in T24 C1GALT1 KO cells whereas MUC16 was detected in the cytoplasm and the membrane of both T24 WT and C1GALT1 cells, co-localizing with the Tn antigen. **B) nanoLC-MS/MS spectrum of a MUC16-Tn glycopeptide fragment of MUC16 isolated from T24 C1GALT1 KO cells.** The identification of MUC16-Tn glycopeptides supports that T24 C1GALT1 KO cells express abnormal MUC16 glycoforms, as suggested by microscopy analysis.

5.4.4 Proliferation, Migration and Invasion

Increased proliferation, migration and invasion are key aspects of malignancy; however, the impact of severe reductions in *O*-glycans complexity translated by Tn expression is not well understood. Proliferation was evaluated based on the capacity of cells to incorporate BrdU, a synthetic nucleoside analog of thymidine that can be incorporated

into newly synthesized DNA during cell division. According to **Figure 18A**, Tn expression did not influence proliferation. We then evaluated the capacity of cells to migrate/invade Matrigel, a polymeric protein mixture mimicking the extracellular matrix as well as the capacity of cells to migrate into a defined cleared space. Notably, both T24 WT and C1GALT1 KO cells presented similar invasion and migration profiles, demonstrating little impact of Tn expression at this level for this specific cell model (**Figure 18A and B**).

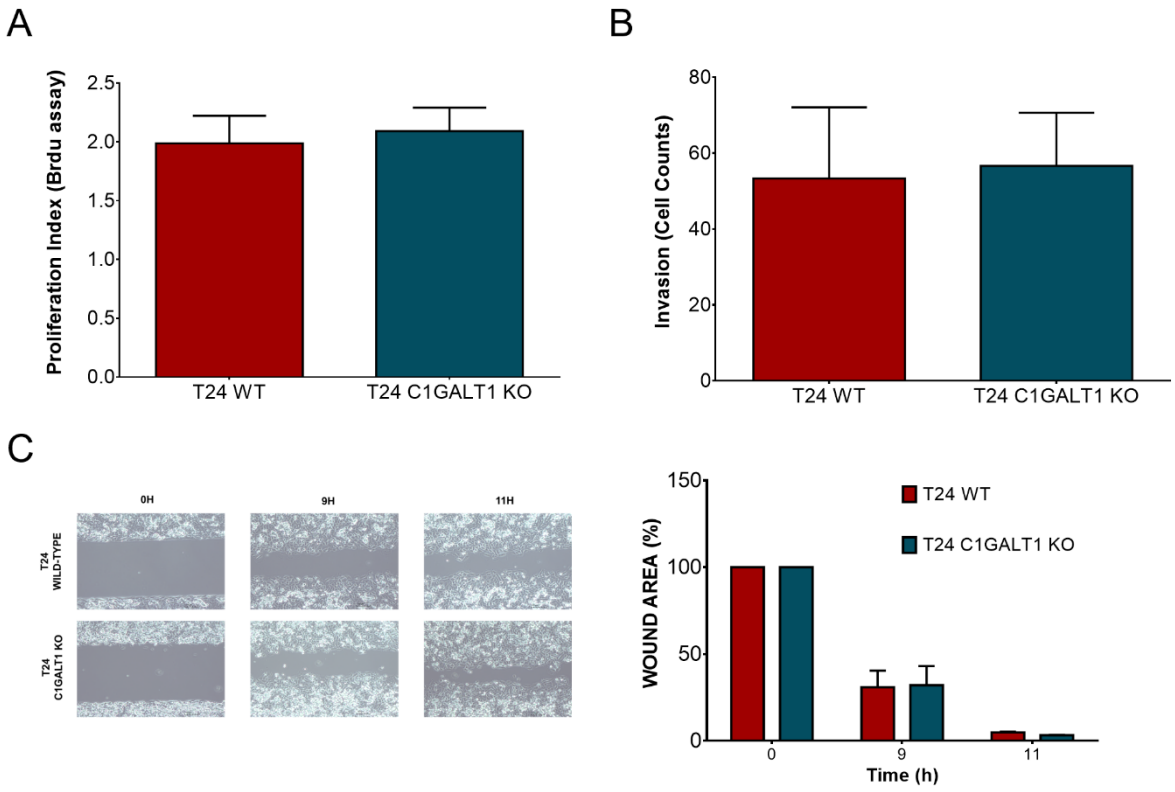

Figure 18. A) Proliferation, B) invasion and C) migration assays of T24 WT and C1GALT1 KO cells. Tn overexpression, translated by the C1GALT1 KO model, did not affect cell proliferation, invasion or migration in this particular experimental setting.

5.4.5 Immune check point molecules

Cancer cells are well known for developing molecular strategies of immune evasion. Namely, it is well described that cancer cells may downregulate the expression of HLA-ABC (MHC-I) receptors, reducing their capacity to present antigens to the immune system[46]. Cancer cells also frequently overexpress CD47, a transmembrane integrin associated protein (IAP) that acts as an inhibitory receptor. CD47 interacts with signal receptor protein-alpha (SIPR-α, also named CD172a or SHPS-1) in macrophages and T cells, enabling immune

escape[47]. In addition, cancer cells may overexpress Programmed death-ligand 1 (PD-L1), which interacts with the immune checkpoint inhibitor protein PD-1 to negatively regulate T-cell mediated immune responses. As highlighted in **Figure 19**, all T24 WT and *C1GALT1* KO cells express high levels of HLA-ABC, which is not influenced by the induction of Tn expression. In addition, 20-30% of cells express low amounts of CD47 and PD-L1 and no statistically relevant differences were observed upon *C1GALT1* knock-out. These observations support that glycome remodeling had little impact on the immunosuppressive nature of T24 cells, as translated by HLA-ABC, CD47 and PD-L1.

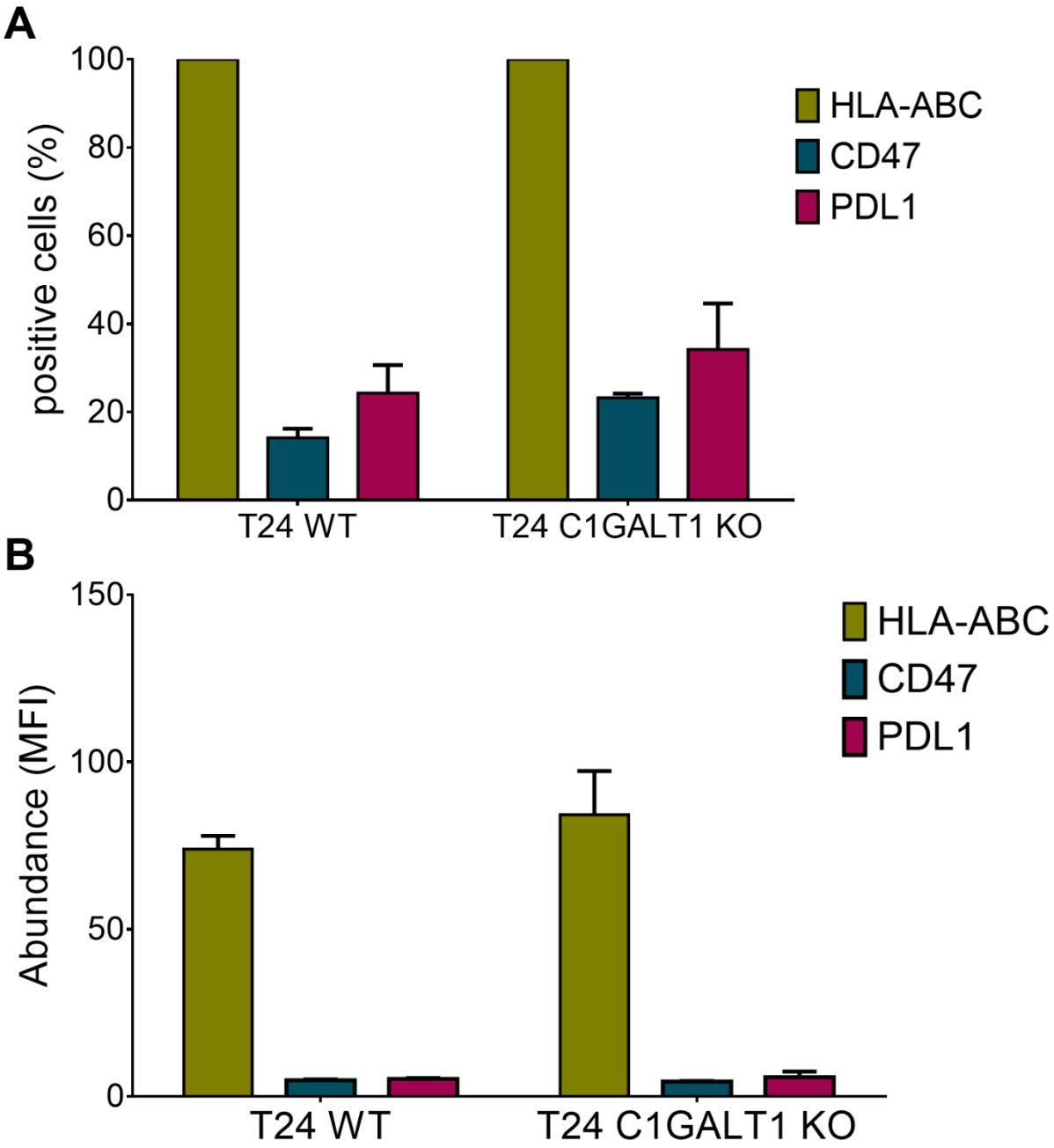

Figure 19. A) Percentage of positive cells and B) protein abundance expressed in terms of mean fluorescence intensity (MFI) for HLA-ABC, CD47 and PDL-1 in T24 WT and C1GALT1 KO cells analyzed by flow cytometry. C1GALT1 KO and consequent Tn overexpression did not affect the expression of HLA-ABC, CD47 and PDL-1.

5.4.6 Co-culture with Dendritic Cells

T24 WT and C1GALT1 KO cells were co-cultured with DCs differentiated from monocytes from three different healthy blood donors to disclose the potential influence of Tn antigen on DC activation. Despite significant donor variability, DCs exposed to T24 C1GALT1 KO cells lost the expression of the lineage marker CD11c in comparison to DCs alone or exposed to T24 WT cells (**Figure 20**). Although not statistically significant, similar observations were made for cells exposed to LPS. The levels of CD86, a protein expressed on APCs that produces costimulatory signals necessary for T cells activation and survival were similar between DCs alone or in the presence of the different cell lines. However, upon activation with LPS, the levels of this marker were significantly decreased in DCs exposed to T24 C1GALT1 KO cells in comparison to DCs alone or in the presence of T24 WT cells. In addition, HLA-DR, an MHC class II cell surface receptor necessary for antigens presentation to T cells, was significantly decreased in DCs exposed to Tn-expressing cells in comparison to DCs alone or exposed to T24 WT. Analysis in the presence of LPs suggested a similar trend. Collectively, these findings suggest that the Tn antigen might be inducing DC dedifferentiation together with impaired antigen presentation, which cannot be rescued by LPS stimulation.

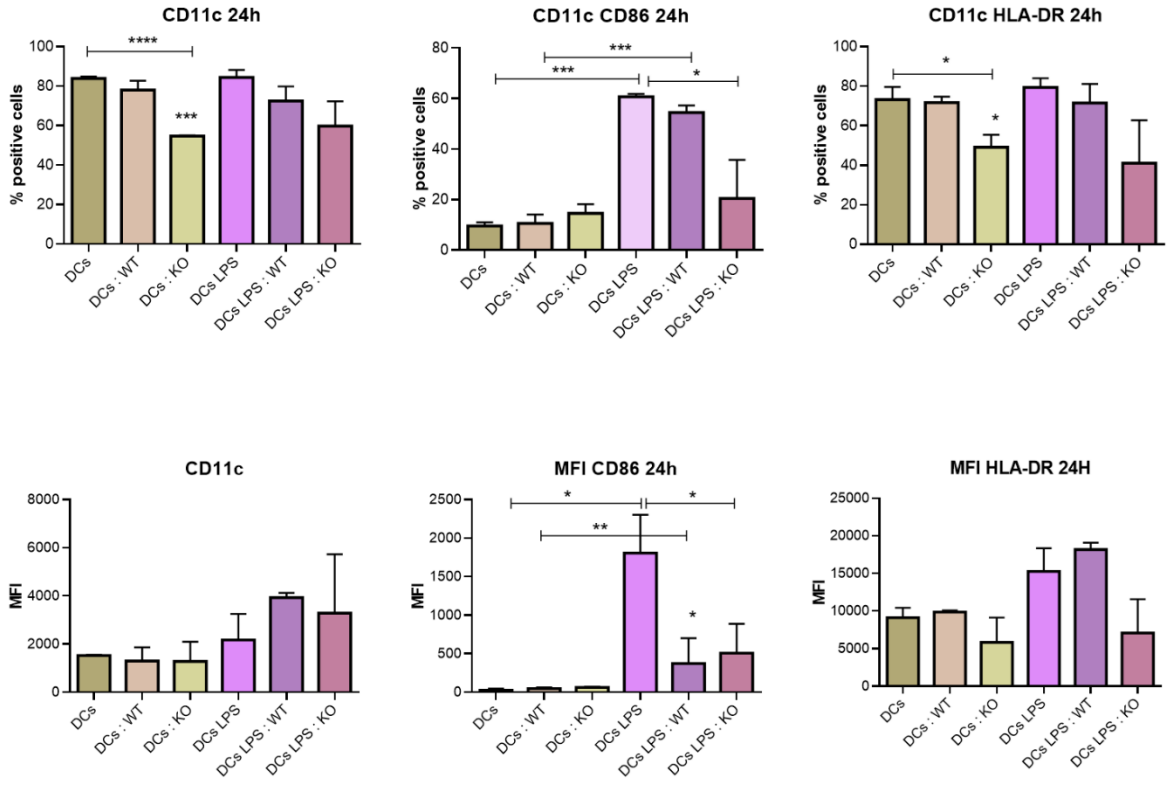

Figure 20. Evaluation of CD11, CD86 and HLA-DR in dendritic cells exposed to T24 WT and C1GALT1 KO cells with and without LPS stimulation. CD11, CD86 and HLA-DR expression was evaluated by flow cytometry. The upper panel corresponds to the percentage of positive cells, whereas the lower panel refers to protein levels expressed in terms of mean fluorescence intensity (MFI). These analyses support that Tn antigen expressing cells may induce a decrease in the number of CD11c in DC cells. It also reduced the expression of CD86 in CD11c-DCs upon LPS stimuli, suggesting decrease capacity for presenting antigens. Moreover, it reduced HLA-DR expression, reinforcing low capacity to promote antigen presentation. Collectively, these findings suggest that T24 C1GALT1 KO cells may negatively influence DCs function against cancer cells, inducing an immunosuppressive response most likely mediated by the Tn antigen. Graphs represent average value of three independent experiments, *p < 0.05; **p < 0.01; ***p < 0.001 (Student's T-test).

5.5 Concluding Remarks

Cancer cells cell-surface glycoproteome often experiences significant remodeling translated by the overexpression of short-chain *O*-glycans such as the Tn and STn antigens instead of more extended structures[2,7,48]. These glycans are rarely observed in healthy human cells, originating unique molecular fingerprints that may be explored in the context of targeted therapeutics and immunotherapy[49,50]. However, most known cancer cell models do not express these antigens, suggesting that microenvironmental aspects play a key role at this level[6,36]. In order to surpass these limitations, different cell models have been glycoengineered to overexpress the STn antigen, mostly by inducing *ST6GALNAC1* overexpression, which encodes the enzyme responsible by Tn antigen *O*-6 sialylation[6,21,51,52]. STn-overexpressing cells of different origins, including bladder cancer, have demonstrated that this antigen is a promoter of cell migration and invasion[18-21]. These functional studies have been supported by clinical data demonstrating clear associations between STn overexpression, advanced stage and grade, poor prognosis and the presence of metastasis of different types of tumours (bladder, gastric, colorectal, breast)[21,50,53,54]. It is also consensual that STn favors immune evasion by interacting with siglecs at the surface of APCs, inducing relevant inhibitory signals that dampen immune responses[55-57]. Supporting these observations, we have recently reported that STn increased binding of DCs to bladder cancer cells, inducing a more immature phenotype[19]. Moreover, T cells primed by DCs pulsed with antigens derived from STn-expressing cancer cells were not activated, limiting their capacity to trigger protective anti-tumour T cell responses[19]. This rationale has prompted significant research towards novel anti-STn antibodies[58] and STn-based vaccine constructs that hold great potential for innovative cancer therapeutics[19].

Contrasting with the clear rational concerning the STn antigen, little is known about the role of Tn antigen in cancer development. Nevertheless, clinical data from different tumours also supports an association between Tn expression and more aggressive forms of disease[59,60]. In bladder cancer, which has been our research focus over the last ten years, the Tn antigen has been associated with muscle invasion and, consequently, poor prognosis[58]. Finally, few reports suggest that MUC1-Tn glycoforms may be internalized by DCs and presented at the cell surface, promoting T-cell inhibition[61], also supporting an immunosuppressive character for the Tn antigen, which warrants future validation. With the objective of gaining more insights on the functional implications of Tn antigen in cancer, we

have successfully glycoengineered the T24 urothelial cancer cell line to overexpress this antigen. Notably, we have not observed any impact on proliferation, migration and invasion, which clearly contrasted with the observations for the STn antigen across different models. These observations suggest that distinct short-chain *O*-glycans may play different biological roles and that sialylation may act as promoter of more motile phenotypes, as previously described[6,62,63]. Nevertheless, future studies involving the induction of STn expression in this cell line are required to confirm this hypothesis. In addition, the T24 C1GALT1 KO model conserved HLA-ABC, CD47 and PD-L1 expressions comparable to wild type cells. However, co-culture experiments strongly suggested that Tn overexpression might induce DC dedifferentiation translated by the loss of the lineage marker CD11c, which warrants confirmation in future studies potentially involving the evaluation of a broader panel of biomarkers such as CD14 and CD80. Our data also suggests that Tn expression may reduce CD86 and HLA-DR levels that cannot be rescued by LPS stimulation, a bacterial polysaccharide commonly used for DC activation. Although preliminary, these observations support the importance of future validation involving a higher number of blood donors. The evaluation of other markers such as IL-12, TNF-α, IL-23 and IL-10 as well as the impact of Tn expression on macrophages, T cells and other relevant immune cells will also be critical for characterizing the immunological response associated to this glycan. The diversification of cell models will be required to disclose possible influence of cell-specific glycoproteomes on immune response.

In summary, this chapter describes an innovative cell model expressing the Tn antigen in mimicry of advanced bladder tumors. Moreover, it supports the immune suppressive role of this glycan suggested by other authors[24-26]. Finally, it highlights that this cell line express MUC16-Tn glycoforms often associated with more aggressive forms of the disease[27,64,65]. As such, the cellular models and molecular foundations are set for future studies concerning the potential of the multivalent vaccine constructs developed in Chapters III (KLH-MUC16-Tn) and IV (MUC16-Tn-PLGA grafted and adsorbed nanoformulations) as innovative cancer immunotherapies. Given that MUC16-Tn is widely observed across different types of tumors, applications beyond bladder cancer can be envisaged.

5.6 References

1 Brockhausen, I. Mucin-type O-glycans in human colon and breast cancer: Glycodynamics and functions. *EMBO Reports* **7**, 599-604, (2006).

2 Marcos, N. T., Pinho, S., Grandela, C., Cruz, A., Samyn-Petit, B., Harduin-Lepers, A., Almeida, R., Silva, F., Morais, V., Costa, J., Kihlberg, J., Clausen, H. & Reis, C. A. Role of the human ST6GalNAc-I and ST6GalNAc-II in the synthesis of the cancer-associated sialyl-Tn antigen. *Cancer Res* **64**, 7050-7057, (2004).

3 Kannagi, R., Yin, J., Miyazaki, K. & Izawa, M. Current relevance of incomplete synthesis and neo-synthesis for cancer-associated alteration of carbohydrate determinants--Hakomori's concepts revisited. *Biochim Biophys Acta* **1780**, 525-531, (2008).

4 Pinho, S. S., Oliveira, P., Cabral, J., Carvalho, S., Huntsman, D., Gartner, F., Seruca, R., Reis, C. A. & Oliveira, C. Loss and recovery of Mgat3 and GnT-III Mediated E-cadherin N-glycosylation is a mechanism involved in epithelial-mesenchymal-epithelial transitions. *PLoS One* **7**, e33191, (2012).

5 Silsirivanit, A. Glycosylation markers in cancer. *Adv Clin Chem* **89**, 189-213, (2019).

6 Peixoto, A., Fernandes, E., Gaiteiro, C., Lima, L., Azevedo, R., Soares, J., Cotton, S., Parreira, B., Neves, M., Amaro, T., Tavares, A., Teixeira, F., Palmeira, C., Rangel, M., Silva, A. M., Reis, C. A., Santos, L. L., Oliveira, M. J. & Ferreira, J. A. Hypoxia enhances the malignant nature of bladder cancer cells and concomitantly antagonizes protein O-glycosylation extension. *Oncotarget* **7**, 63138-63157, (2016).

7 Sewell, R., Backstrom, M., Dalziel, M., Gschmeissner, S., Karlsson, H., Noll, T., Gatgens, J., Clausen, H., Hansson, G. C., Burchell, J. & Taylor-Papadimitriou, J. The ST6GalNAc-I sialyltransferase localizes throughout the Golgi and is responsible for the synthesis of the tumor-associated sialyl-Tn O-glycan in human breast cancer. *J Biol Chem* **281**, 3586-3594, (2006).

8 Radhakrishnan, P., Dabelsteen, S., Madsen, F. B., Francavilla, C., Kopp, K. L., Steentoft, C., Vakhrushev, S. Y., Olsen, J. V., Hansen, L., Bennett, E. P., Woetmann, A., Yin, G., Chen, L., Song, H., Bak, M., Hlady, R. A., Peters, S. L., Opavsky, R., Thode, C., Qvortrup, K., Schjoldager, K. T., Clausen, H., Hollingsworth, M. A. & Wandall, H. H. Immature truncated O-glycophenotype of cancer directly induces oncogenic features. *Proc Natl Acad Sci U S A* **111**, E4066-4075, (2014).

9 Schultz, M. J., Swindall, A. F. & Bellis, S. L. Regulation of the metastatic cell phenotype by sialylated glycans. *Cancer metastasis reviews* **31**, 501-518, (2012).

10 Oliveira-Ferrer, L., Legler, K. & Milde-Langosch, K. Role of protein glycosylation in cancer metastasis. *Seminars in Cancer Biology* **44**, 141-152, (2017).

11 Ferrer, C. M., Lu, T. Y., Bacigalupa, Z. A., Katsetos, C. D., Sinclair, D. A. & Reginato, M. J. O-GlcNAcylation regulates breast cancer metastasis via SIRT1 modulation of FOXM1 pathway. *Oncogene* **36**, 559-569, (2017).

12 Nguyen, A. T., Chia, J., Ros, M., Hui, K. M., Saltel, F. & Bard, F. Organelle Specific O-Glycosylation Drives MMP14 Activation, Tumor Growth, and Metastasis. *Cancer Cell* **32**, 639-653 e636, (2017).

13 Cao, Y., Stosiek, P., Springer, G. F. & Karsten, U. Thomsen-Friedenreich-related carbohydrate antigens in normal adult human tissues: a systematic and comparative study. *Histochem Cell Biol* **106**, 197-207, (1996).

14 Cascio, S., Kvorjak, M., Ahmed, Y., Miller, M., Al Hashash, J., Hartman, D., Miskov-Zivanov, N., Telmer, C. & Finn, O. J. The cross-talk between infiltrating macrophages and inflamed or malignant colonic epithelium promotes overexpression of ST6GALNAC1 and epithelial MUC1 tumor form MUC1-sTn. *The Journal of Immunology* **202**, 135.135-135.135, (2019).

15 Cascio, S., Faylo, J. L., Sciurba, J. C., Xue, J., Ranganathan, S., Lohmueller, J. J., Beatty, P. L. & Finn, O. J. Abnormally glycosylated MUC1 establishes a positive feedback circuit of inflammatory cytokines, mediated by NF-kappaB p65 and EzH2, in colitis-associated cancer. *Oncotarget* **8**, 105284-105298, (2017).

16 Posey, A. D., Jr., Schwab, R. D., Boesteanu, A. C., Steentoft, C., Mandel, U., Engels, B., Stone, J. D., Madsen, T. D., Schreiber, K., Haines, K. M., Cogdill, A. P., Chen, T. J., Song, D., Scholler, J., Kranz, D. M., Feldman, M. D., Young, R., Keith, B., Schreiber, H., Clausen, H., Johnson, L. A. & June, C. H. Engineered CAR T Cells Targeting the Cancer-Associated Tn-Glycoform of the Membrane Mucin MUC1 Control Adenocarcinoma. *Immunity* **44**, 1444-1454, (2016).

17 Wang, W. Y., Cao, Y. X., Zhou, X., Wei, B., Zhan, L. & Sun, S. Y. Stimulative role of ST6GALNAC1 in proliferation, migration and invasion of ovarian cancer stem cells via the Akt signaling pathway. *Cancer Cell Int* **19**, 86, (2019).

18 Freitas, D., Campos, D., Gomes, J., Pinto, F., Macedo, J. A., Matos, R., Mereiter, S., Pinto, M. T., Polonia, A., Gartner, F., Magalhaes, A. & Reis, C. A. O-glycans truncation modulates gastric cancer cell signaling and transcription leading to a more aggressive phenotype. *EBioMedicine* **40**, 349-362, (2019).

19 Carrascal, M. A., Severino, P. F., Guadalupe Cabral, M., Silva, M., Ferreira, J. A., Calais, F., Quinto, H., Pen, C., Ligeiro, D., Santos, L. L., Dall'Olio, F. & Videira, P. A. Sialyl Tn-expressing bladder cancer cells induce a tolerogenic phenotype in innate and adaptive immune cells. *Mol Oncol* **8**, 753-765, (2014).

20 Munkley, J., Oltean, S., Vodak, D., Wilson, B. T., Livermore, K. E., Zhou, Y., Star, E., Floros, V. I., Johannessen, B., Knight, B., McCullagh, P., McGrath, J., Crundwell, M., Skotheim, R. I., Robson, C. N., Leung, H. Y., Harries, L. W., Rajan, P., Mills, I. G. & Elliott, D. J. The androgen receptor controls expression of the cancer-associated sTn antigen and cell adhesion through induction of ST6GalNAc1 in prostate cancer. *Oncotarget* **6**, 34358-34374, (2015).

21 Ogawa, T., Hirohashi, Y., Murai, A., Nishidate, T., Okita, K., Wang, L., Ikehara, Y., Satoyoshi, T., Usui, A., Kubo, T., Nakastugawa, M., Kanaseki, T., Tsukahara, T., Kutomi, G., Furuhata, T., Hirata, K., Sato, N., Mizuguchi, T., Takemasa, I. & Torigoe, T. ST6GALNAC1 plays important roles in enhancing cancer stem phenotypes of colorectal cancer via the Akt pathway. *Oncotarget* **8**, 112550-112564, (2017).

22 Liu, Z., Liu, J., Dong, X., Hu, X., Jiang, Y., Li, L., Du, T., Yang, L., Wen, T., An, G. & Feng, G. Tn antigen promotes human colorectal cancer metastasis via H-Ras mediated epithelial-mesenchymal transition activation. *J Cell Mol Med* **23**, 2083-2092, (2019).

23 Kolbl, A. C., Jeschke, U., Friese, K. & Andergassen, U. The role of TF- and Tn-antigens in breast cancer metastasis. *Histol Histopathol* **31**, 613-621, (2016).

24 Ju, T., Wang, Y., Aryal, R. P., Lehoux, S. D., Ding, X., Kudelka, M. R., Cutler, C., Zeng, J., Wang, J., Sun, X., Heimburg-Molinaro, J., Smith, D. F. & Cummings, R. D. Tn and sialyl-Tn antigens, aberrant O-glycomics as human disease markers. *Proteomics - Clinical Applications* **7**, 618-631, (2013).

25 Saeland, E., van Vliet, S. J., Backstrom, M., van den Berg, V. C., Geijtenbeek, T. B., Meijer, G. A. & van Kooyk, Y. The C-type lectin MGL expressed by dendritic cells detects glycan changes on MUC1 in colon carcinoma. *Cancer Immunol Immunother* **56**, 1225-1236, (2007).

26 Napoletano, C., Rughetti, A., Agervig Tarp, M. P., Coleman, J., Bennett, E. P., Picco, G., Sale, P., Denda-Nagai, K., Irimura, T., Mandel, U., Clausen, H., Frati, L., Taylor-Papadimitriou, J., Burchell, J. & Nuti, M. Tumor-associated Tn-MUC1 glycoform is internalized through the macrophage galactose-type C-type lectin and delivered to the HLA class I and II compartments in dendritic cells. *Cancer Res* **67**, 8358-8367, (2007).

27 Cotton, S., Azevedo, R., Gaiteiro, C., Ferreira, D., Lima, L., Peixoto, A., Fernandes, E., Neves, M., Neves, D., Amaro, T., Cruz, R., Tavares, A., Rangel, M., Silva, A. M. N., Santos, L. L. & Ferreira, J. A. Targeted O-glycoproteomics explored increased sialylation and identified MUC16 as a poor prognosis biomarker in advanced-stage bladder tumours. *Mol Oncol* **11**, 895-912, (2017).

28 Pinto-Leite, R., Carreira, I., Melo, J., Ferreira, S. I., Ribeiro, I., Ferreira, J., Filipe, M., Bernardo, C., Arantes-Rodrigues, R., Oliveira, P. & Santos, L. Genomic characterization of three urinary bladder cancer cell lines: understanding genomic types of urinary bladder cancer. *Tumour Biol* **35**, 4599-4617, (2014).

29 Ye, J., Coulouris, G., Zaretskaya, I., Cutcutache, I., Rozen, S. & Madden, T. L. Primer-BLAST: a tool to design target-specific primers for polymerase chain reaction. *BMC Bioinformatics* **13**, 134, (2012).

30 Hsiau, T., Conant, D., Rossi, N., Maures, T., Waite, K., Yang, J., Joshi, S., Kelso, R., Holden, K., Enzmann, B. L. & Stoner, R. Inference of CRISPR Edits from Sanger Trace Data. *bioRxiv*, 251082, (2019).

31 Kudelka, M. R., Antonopoulos, A., Wang, Y., Duong, D. M., Song, X., Seyfried, N. T., Dell, A., Haslam, S. M., Cummings, R. D. & Ju, T. Cellular O-Glycome Reporter/Amplification to explore O-glycans of living cells. *Nat Methods* **13**, 81-86, (2016).

32 Cova, M., Oliveira-Silva, R., Ferreira, J. A., Ferreira, R., Amado, F., Daniel-da-Silva, A. L. & Vitorino, R. Glycoprotein enrichment method using a selective magnetic nano-probe platform (MNP) functionalized with lectins. *Methods Mol Biol* **1243**, 83-100, (2015).

33 Chick, J. M., Kolippakkam, D., Nusinow, D. P., Zhai, B., Rad, R., Huttlin, E. L. & Gygi, S. P. A mass-tolerant database search identifies a large proportion of unassigned spectra in shotgun proteomics as modified peptides. *Nat Biotechnol* **33**, 743-749, (2015).

34 Cardoso, A. P., Pinto, M. L., Pinto, A. T., Oliveira, M. I., Pinto, M. T., Goncalves, R., Relvas, J. B., Figueiredo, C., Seruca, R., Mantovani, A., Mareel, M., Barbosa, M. A. & Oliveira, M. J. Macrophages stimulate gastric and colorectal cancer invasion through EGFR

Y(1086), c-Src, Erk1/2 and Akt phosphorylation and smallGTPase activity. *Oncogene* **33**, 2123-2133, (2014).

35 Costa, C., Pereira, S., Lima, L., Peixoto, A., Fernandes, E., Neves, D., Neves, M., Gaiteiro, C., Tavares, A., Gil da Costa, R. M., Cruz, R., Amaro, T., Oliveira, P. A., Ferreira, J. A. & Santos, L. L. Abnormal Protein Glycosylation and Activated PI3K/Akt/mTOR Pathway: Role in Bladder Cancer Prognosis and Targeted Therapeutics. *PLoS One* **10**, e0141253, (2015).

36 Azevedo, R., Peixoto, A., Gaiteiro, C., Fernandes, E., Neves, M., Lima, L., Santos, L. L. & Ferreira, J. A. *Over forty years of bladder cancer glycobiology: Where do glycans stand facing precision oncology?* , Vol. 8 (2017).

37 Felder, M., Kapur, A., Gonzalez-Bosquet, J., Horibata, S., Heintz, J., Albrecht, R., Fass, L., Kaur, J., Hu, K., Shojaei, H., Whelan, R. J. & Patankar, M. S. MUC16 (CA125): tumor biomarker to cancer therapy, a work in progress. *Mol Cancer* **13**, 129, (2014).

38 Kanwal, M., Ding, X. J., Song, X., Zhou, G. B. & Cao, Y. MUC16 overexpression induced by gene mutations promotes lung cancer cell growth and invasion. *Oncotarget* **9**, 12226-12239, (2018).

39 Lakshmanan, I., Ponnusamy, M. P., Das, S., Chakraborty, S., Haridas, D., Mukhopadhyay, P., Lele, S. M. & Batra, S. K. MUC16 induced rapid G2/M transition via interactions with JAK2 for increased proliferation and anti-apoptosis in breast cancer cells. *Oncogene* **31**, 805-817, (2012).

40 Das, S., Rachagani, S., Torres-Gonzalez, M. P., Lakshmanan, I., Majhi, P. D., Smith, L. M., Wagner, K. U. & Batra, S. K. Carboxyl-terminal domain of MUC16 imparts tumorigenic and metastatic functions through nuclear translocation of JAK2 to pancreatic cancer cells. *Oncotarget* **6**, 5772-5787, (2015).

41 Chen, X., Li, X., Wang, X., Zhu, Q., Wu, X. & Wang, X. MUC16 impacts tumor proliferation and migration through cytoplasmic translocation of P120-catenin in epithelial ovarian cancer cells: an original research. *BMC Cancer* **19**, 171, (2019).

42 Das, S. & Batra, S. K. Understanding the Unique Attributes of MUC16 (CA125): Potential Implications in Targeted Therapy. *Cancer Res* **75**, 4669-4674, (2015).

43 Aithal, A., Junker, W. M., Kshirsagar, P., Das, S., Kaur, S., Orzechowski, C., Gautam, S. K., Jahan, R., Sheinin, Y. M., Lakshmanan, I., Ponnusamy, M. P., Batra, S. K. & Jain, M. Development and characterization of carboxy-terminus specific monoclonal antibodies for understanding MUC16 cleavage in human ovarian cancer. *PLoS One* 13, e0193907, (2018).

44 Scholler, N. & Urban, N. CA125 in ovarian cancer. Biomark Med 1, 513-523, (2007).

45 Hattrup, C. L. & Gendler, S. J. Structure and function of the cell surface (tethered) mucins. Annu Rev Physiol 70, 431-457, (2008).

46 Lisiecka, U. & Kostro, K. Mechanisms of tumour escape from immune surveillance. 60, 453, (2016).

47 Chao, M. P., Weissman, I. L. & Majeti, R. The CD47-SIRPalpha pathway in cancer immune evasion and potential therapeutic implications. Curr Opin Immunol 24, 225-232, (2012).

48 Pinho, S. S. & Reis, C. A. Glycosylation in cancer : mechanisms and clinical implications. Nature Publishing Group 16, 540-550, (2015).

49 Pearce, O. M. T. Cancer glycan epitopes: biosynthesis, structure and function. Glycobiology 28, 670-696, (2018).

50 Lima, L., Neves, M., Oliveira, M. I., Dieguez, L., Freitas, R., Azevedo, R., Gaiteiro, C., Soares, J., Ferreira, D., Peixoto, A., Fernandes, E., Montezuma, D., Tavares, A., Ribeiro, R., Castro, A., Oliveira, M., Fraga, A., Reis, C. A., Santos, L. L. & Ferreira, J. A. Sialyl-Tn identifies muscle-invasive bladder cancer basal and luminal subtypes facing decreased survival, being expressed by circulating tumor cells and metastases. Urol Oncol 35, 675 e671-675 e678, (2017).

51 Lo, C. Y., Antonopoulos, A., Gupta, R., Qu, J., Dell, A., Haslam, S. M. & Neelamegham, S. Competition between core-2 GlcNAc-transferase and ST6GalNAc-transferase regulates the synthesis of the leukocyte selectin ligand on human P-selectin glycoprotein ligand-1. J Biol Chem 288, 13974-13987, (2013).

52 Munkley, J. The role of sialyl-Tn in cancer. International Journal of Molecular Sciences 17, 1-9, (2016).

53 Miles, D. W., Happerfield, L. C., Smith, P., Gillibrand, R., Bobrow, L. G., Gregory, W. M. & Rubens, R. D. Expression of sialyl-Tn predicts the effect of adjuvant chemotherapy in node-positive breast cancer. Br J Cancer 70, 1272-1275, (1994).

54 Victorzon, M., Nordling, S., Nilsson, O., Roberts, P. J. & Haglund, C. Sialyl Tn antigen is an independent predictor of outcome in patients with gastric cancer. Int J Cancer 65, 295-300, (1996).

55 Nardy, A. F. F. R., Freire-de-Lima, L., Freire-de-Lima, C. G. & Morrot, A. The Sweet Side of Immune Evasion: Role of Glycans in the Mechanisms of Cancer Progression. Frontiers in Oncology 6, 1-7, (2016).

56 van Kooyk, Y. & Rabinovich, G. A. Protein-glycan interactions in the control of innate and adaptive immune responses. Nat Immunol 9, 593-601, (2008).

57 Takamiya, R., Ohtsubo, K., Takamatsu, S., Taniguchi, N. & Angata, T. The interaction between Siglec-15 and tumor-associated sialyl-Tn antigen enhances TGF-beta secretion from monocytes/macrophages through the DAP12-Syk pathway. Glycobiology 23, 178-187, (2013).

58 Ferreira, J. A., Videira, P. A., Lima, L., Pereira, S., Silva, M., Carrascal, M., Severino, P. F., Fernandes, E., Almeida, A., Costa, C., Vitorino, R., Amaro, T., Oliveira, M. J., Reis, C. A., Dall'Olio, F., Amado, F. & Santos, L. L. Overexpression of tumour-associated carbohydrate antigen sialyl-Tn in advanced bladder tumours. Mol Oncol 7, 719-731, (2013).

59 Ju, T., Aryal, R. P., Kudelka, M. R., Wang, Y. & Cummings, R. D. The Cosmc connection to the Tn antigen in cancer. Cancer Biomark 14, 63-81, (2014).

60 Springer, G. F. Immunoreactive T and Tn epitopes in cancer diagnosis, prognosis, and immunotherapy. J Mol Med (Berl) 75, 594-602, (1997).

61 van Kooyk, Y. & Rabinovich, G. A. Protein-glycan interactions in the control of innate and adaptive immune responses. Nature Immunology 9, 593-601, (2008).

62 Vajaria, B. N., Patel, K. R., Begum, R. & Patel, P. S. Sialylation: an Avenue to Target Cancer Cells. Pathology and Oncology Research 22, 443-447, (2016).

63 Bresalier, R. S., Ho, S. B., Schoeppner, H. L., Kim, Y. S., Sleisenger, M. H., Brodt, P. & Byrd, J. C. Enhanced sialylation of mucin-associated carbohydrate structures in human colon cancer metastasis. Gastroenterology 110, 1354-1367, (1996).

64 Aithal, A., Rauth, S., Kshirsagar, P., Shah, A., Lakshmanan, I., Junker, W. M., Jain, M., Ponnusamy, M. P. & Batra, S. K. MUC16 as a novel target for cancer therapy. Expert Opin Ther Targets 22, 675-686, (2018).

65 Rao, T. D., Tian, H., Ma, X., Yan, X., Thapi, S., Schultz, N., Rosales, N., Monette, S., Wang, A., Hyman, D. M., Levine, D. A., Solit, D. & Spriggs, D. R. Expression of the Carboxy-Terminal Portion of MUC16/CA125 Induces Transformation and Tumor Invasion. PLoS One 10, e0126633, (2015).

CHAPTER VI

Concluding Remarks and Future Perspectives

6.1 Concluding Remarks

The shortening of protein glycosylation that accompanies malignant transformation and disease progression is often responsible by generating cancer-specific molecular signatures at the cell-surface. These glycans are directly implicated in disease progression and dissemination, holding great potential for targeted therapeutics and immunotherapy. Namely, these glycans may be explored in the context of cancer vaccines once difficulties related with their low immunogenicity and immunosuppressive roles are overcome.

Building on this rationale, this work described a single pot chemoenzymatic strategy to produce libraries of glycopeptides carrying different types of short-chain *O*-glycans (Tn, STn, S3T and S6T). We have used as template a 20 amino acid variable tandem repeat peptide from MUC16 containing multiple glycosites, however, the stablished methodology may now be applied to the production of different types of glycoepitopes. Moreover, we have successfully coupled MUC16-Tn and MUC16-STn to protein immunogens such as Keyhole limpet hemocyanin (KLH), which is commonly used as immunogenic for vaccine development[1,2] . KLH is a high-molecular-weight glycoprotein of marine origin capable of inducing both cell-mediated and humoral responses. KLH allies potent immunogenicity and low toxicity to availability at clinical grade quality. Therefore, we anticipate that this may constitute a good approach to foster the development of glycan-based vaccines and a good benchmark to test other formulations, such as the nanovaccine constructs also developed in this work. Notably, this is the first vaccine formulation exploiting abnormally glycosylated MUC16 glycoepitopes. We anticipate that MUC16-based glycovaccines may serve a wide number of solid tumours such as bladder, lung, cervical and ovarian[3-6], where these molecules play a key role in disease progression as well as immunosuppression by modulation of APCs function.

Facing the objective of innovative and more effective glycan-based vaccines, we have then devoted to the development of MUC16-Tn nanoconstructs exploiting PLGA, a biocompatible polymer widely used for drug formulations in clinical settings. Emphasis was set on formulations yielding the Tn antigen, the simplest form of cancer-associated *O*-glycosylation, which is mostly absent from healthy tissues. Accordingly, we have covalently immobilized and adsorbed MUC16-Tn presenting a diversified array of glycosylation patterns at the surface of PLGA nanoconstructs envisaging multivalent formulations that better reflect the structural diversity at the cancer cells surface. We have characterized these

formulations from the physicochemical point of view, demonstrating their nanodimensions, stability, molecular homogeneity and low polydispersion, supporting ideal premices for vaccine development[7,8]. Toxicity and uptake thresholds were defined using macrophages as model cells. This has created the necessary molecular foundations for future studies concerning the establishment of more effective cancer vaccines, which includes estimating the capacity of the nanoformulations to elicit both humoral and cellular responses against cancer cells *in vitro* and *in vivo* in comparison to conventional vaccine constructs based on glycoepitope-protein conjugates.

Notably, a thorough assessment of the efficacy of MUC16-Tn vaccines depends critically on the existence of well characterized cellular models reflecting these glycoepitopes. However, despite its widespread nature in cancer, the Tn antigen is not expressed by cancer cells grown *in vitro*, suggesting dependence from microenvironmental cues that are yet to be disclose. To overcome this limitation, we have edited the genome of T24 bladder cancer cells using CRISPR/Cas9 technology to produce a stable *C1GALT1* knock-out. This cell line expressed significantly high levels of the Tn antigen at the cell surface and completely obliterated the expression of extended glycoforms. Moreover, we found that this model expressed MUC16-Tn and may be potentially useful to test the developed vaccine constructs. Interestingly, this had not impact on cell proliferation, migration and invasion as well as in the expression of important molecules related with cancer immune escape (HLA-ABC, CD47 and PD-L1). Nevertheless, our data suggests that Tn expressing cancer cells my negatively influence dendritic cells differentiation and downregulate relevant molecules involved in antigen presentation that cannot be completely rescued by stimulation with LPS (HLA-DR, CD11c, CD86). Such findings agree with previous reports concerning the role of short-chain *O*-glycans in immune responses, potentially highlighting a novel class of immune check point inhibitors contributing to cancer immune escape. However, more studies are warranted to confirm these preliminary observations, including their impact on T-cell response. Ultimately, it highlights the importance of pursuing effective strategies to overcome the immunosuppressive nature of glycans.

In summary, a rationale has been created to support the development and improvement of glycan-based vaccines for cancer foreseeing studies *in vivo*. Given the

pancarcinomic nature of these glycoepitopes, the generalization of more efficient vaccines to different cell models may be envisaged.

6.2 References

1 Kantele, A., Hakkinen, M. P., Zivny, J., Elson, C. O., Mestecky, J. & Kantele, J. M. Humoral immune response to keyhole limpet haemocyanin, the protein carrier in cancer vaccines. *Clin Dev Immunol* **2011**, 614383, (2011).

2 Wimmers, F., de Haas, N., Scholzen, A., Schreibelt, G., Simonetti, E., Eleveld, M. J., Brouwers, H. M., Beldhuis-Valkis, M., Joosten, I., de Jonge, M. I., Gerritsen, W. R., de Vries, I. J., Diavatopoulos, D. A. & Jacobs, J. F. Monitoring of dynamic changes in Keyhole Limpet Hemocyanin (KLH)-specific B cells in KLH-vaccinated cancer patients. *Sci Rep* **7**, 43486, (2017).

3 Freitas, D., Campos, D., Gomes, J., Pinto, F., Macedo, J. A., Matos, R., Mereiter, S., Pinto, M. T., Polonia, A., Gartner, F., Magalhaes, A. & Reis, C. A. O-glycans truncation modulates gastric cancer cell signaling and transcription leading to a more aggressive phenotype. *EBioMedicine* **40**, 349-362, (2019).

4 Carrascal, M. A., Severino, P. F., Guadalupe Cabral, M., Silva, M., Ferreira, J. A., Calais, F., Quinto, H., Pen, C., Ligeiro, D., Santos, L. L., Dall'Olio, F. & Videira, P. A. Sialyl Tn-expressing bladder cancer cells induce a tolerogenic phenotype in innate and adaptive immune cells. *Mol Oncol* **8**, 753-765, (2014).

5 Munkley, J., Oltean, S., Vodak, D., Wilson, B. T., Livermore, K. E., Zhou, Y., Star, E., Floros, V. I., Johannessen, B., Knight, B., McCullagh, P., McGrath, J., Crundwell, M., Skotheim, R. I., Robson, C. N., Leung, H. Y., Harries, L. W., Rajan, P., Mills, I. G. & Elliott, D. J. The androgen receptor controls expression of the cancer-associated sTn antigen and cell adhesion through induction of ST6GalNAc1 in prostate cancer. *Oncotarget* **6**, 34358-34374, (2015).

6 Ogawa, T., Hirohashi, Y., Murai, A., Nishidate, T., Okita, K., Wang, L., Ikehara, Y., Satoyoshi, T., Usui, A., Kubo, T., Nakastugawa, M., Kanaseki, T., Tsukahara, T., Kutomi, G., Furuhata, T., Hirata, K., Sato, N., Mizuguchi, T., Takemasa, I. & Torigoe, T. ST6GALNAC1 plays important roles in enhancing cancer stem phenotypes of colorectal cancer via the Akt pathway. *Oncotarget* **8**, 112550-112564, (2017).

7 Allahyari, M. & Mohit, E. Peptide/protein vaccine delivery system based on PLGA particles. *Human Vaccines and Immunotherapeutics* **12**, 806-828, (2016).

8 Zhao, L., Seth, A., Wibowo, N., Zhao, C. X., Mitter, N., Yu, C. & Middelberg, A. P. Nanoparticle vaccines. *Vaccine* **32**, 327-337, (2014).